TM X-71522

NASA-TM-X-71522)   EXTENSION OF CASE'S
METHOD TO THE TWO-REGION CRITICAL
CYLINDER AND ITS APPLICATION AS AN
ANALYTIC STANDARD   Ph.D. Thesis -
Virginia (NASA)   130 p HC $9.50 CSCL 20H

N74-17424

/33

G3/24   Unclas
         29456

EXTENSION OF CASE'S METHOD TO THE TWO-REGION CRITICAL CYLINDER

AND ITS APPLICATION AS AN ANALYTIC STANDARD

A Dissertation

Presented to

the Faculty of the School of Engineering and Applied Science

University of Virginia

In Partial Fulfillment

of the Requirement for the Degree

Doctor of Philosophy (Nuclear Engineering)

by

Robert Michael Westfall

May, 1974

/

ACKNOWLEDGMENTS

Preceding page blank

v

TABLE OF CONTENTS

CHAPTER

LIST OF TABLES

viii

LIST OF FIGURES

LIST OF SYMBOLS

a_o discrete expansion coefficient

$A(\nu)$ continuum expansion coefficient

b_o discrete expansion coefficient

$B(\nu)$ continuum expansion coefficient

$c(\ )$ mean number of neutron secondaries per collision, a capital "C" is used for subscripted values in Chapter IV

d_o discrete expansion coefficient

$D(\nu)$ continuum expansion coefficient

E energy

$f(\ )$ frequency function

$F(\ )$ function

$H(\ )$ function

I_z integral term on variable z

$I(\ )$ modified Bessel function of the first kind

$J(\ )$ Bessel function of the first kind

k_{eff} effective multiplication factor

$K(\ )$ modified Bessel function of the second kind

$M(\ )$ function

N normalization integral

$N(\ )$ normalization function, also "N" function - Appendix B

p variable

P Cauchy Principal Value

$q(\ )$ function

r radial position

$\underline{r}$ position vector

R radial boundary

R( )   function

s   displacement

S_n discrete-ordinates approximation

t   time - Chapter II, radial variable - elsewhere

u   transform variable

v   neutron speed - Chapter II, variable - elsewhere

w   weight factor

x   variable

Y( )   Bessel function of the second kind

Y   variable

z   variable

α constant

β constant

γ Euler's Constant

δ( )   Dirac Delta Function

ϵ belongs to

η direction cosine - Chapter VI

η( )   pseudo eigenfunction

λ( )   Case's Function

Λ( )   dispersion function

μ direction cosine - Chapters II and VI
          transform variable - elsewhere

ν mean number of neutrons per fission - Chapter VI
          eigenvalue - elsewhere

ξ direction cosine

ρ( )   neutron density

σ( )   macroscopic neutron cross section

Σ macroscopic neutron cross section - Chapter VI

τ optical length - Chapter II
        reflector thickness - elsewhere

$\varphi(\ )$ singular eigenfunction of Case

$\Phi(\ )$ neutron distribution function - Chapter II
        pseudo neutron distribution function - elsewhere

$\chi(\ )$ function

$\underline{\Omega}$ neutron direction

SUBSCRIPTS

a	absorption
f	fission
i, j, k, M, m, n	integers
$\ell=1,\ 2$	region number
$n=0,\ 1$	Bessel function order (where appropriate)
s	scattering
t	total
ν	continuum (eigenfunctions, etc.)
o	discrete (eigenvalues, eigenfunctions, etc.)
—	vector

SUPERSCRIPTS

| + | boundary value of the function approaching the cut from above |
| - | boundary value of the function approaching the cut from below |

xiii

ABSTRACT

The normal mode expansion technique is applied to the transformed monoenergetic integral transport equation to develop a solution for the rotationally invariant and axially infinite, critical, two-region cylinder with a finite outer reflector boundary. The model assumes isotropic scattering and identical neutron mean free paths in the core and reflector regions. The solution in terms of singular integral equations is obtained by applying a completeness theorem found for the singular eigenfunctions. Numerical results for a variety of core and reflector multiplying properties and reflector thicknesses are presented and compared with the results of other methods. The completeness inherent in this solution and the high precision in the numerical calculations provide results which may be used as analytic standards for this problem. An example of this type of application is given in a study of approximations inherent in the neutronic design analysis of a small, fast-neutron-spectrum reactor concept proposed as a space power source. Using the highly precise critical dimensions for the case which most closely approximates this reactor, investigations were made of the reactivity effects of angular quadrature type and order and two-dimensional geometrical models used in the discrete-ordinates transport analysis of this concept.

CHAPTER I

INTRODUCTION

1.1 Purpose and Scope

The purpose of this dissertation is to present in detail the development of a highly precise transport solution for the radially reflected critical cylinder and to demonstrate how the results from this solution can be used as analytic standards in evaluating approximations inherent in numerical transport treatments employed in reactor design analysis.

A complete solution for the rotationally invariant and axially infinite two-region critical cylinder with a finite outer reflector boundary is obtained by applying the singular eigenfunction expansion technique to the transformed monoenergetic integral transport equation. The model assumes isotropic scattering and identical neutron mean free paths in the core and reflector regions. Numerical results for a variety of core and reflector multiplying properties and reflector thicknesses are presented and compared with the results of other methods. The critical dimensions and the neutron density distribution for one of these cases are then used as analytic standards in evaluating discrete angular segmentation transport programs used in reactor design.

Three aspects of the numerical programs were studied.

1. Angular quadrature order (number of segmentations in the angular variable)

2. Type of angular quadrature (direction cosines and weights chosen by various prescriptions)

3. The step-boundary approximation inherent in X-Y geometrical representations of circular boundaries.

1.2 Background and Dissertation Organization

Neutron transport as a function of position, energy, angle and time is generally assumed to be described by the Boltzmann equation. In Chapter II this equation is reduced to the time-independent, one-dimensional, monoenergetic form. In 1960, Case[1] obtained a complete solution to the reduced Boltzmann equation in one-dimensional plane geometry in terms of singular eigenfunctions. This solution is briefly described in Chapter II. Concluding Chapter II is a demonstration of the equivalence between the integral form of the transport equation and the Boltzmann equation.

In 1963 Mitsis[2] obtained exact solutions for the critical sphere and for the critical infinite cylinder by transforming the monoenergetic integral transport equation and applying the singular eigenfunction expansion method of Case. Case and Zweifel[3] have shown a more general treatment of the same problems by demonstrating a replication property of the kernel of the integral transport equation. The replication method has been extended by Gibbs[4] to obtain solutions in arbitrary convex geometry. For the critical sphere and cylinder, Gibbs specialized his general solution to duplicate the results of Mitsis.

Lathrop and Leonard[5] have suggested that numerical results from the Mitsis solution for the critical cylinder could be used to investigate the accuracy of two-dimensional discrete-ordinates angular quadrature sets. However, a recent bibliography[6] of neutral particle transport

theory does not contain any reference to such results and initial
investigation under the present study was directed towards determining
the efficacy of the Mitsis solution for the bare critical cylinder.
This investigation found that the solution as formulated by Mitsis
is not convergent. However, a converging solution could be obtained
by reformulating a function used in separating the outer boundary
condition into singular and nonsingular parts and by redefining the
continuum expansion coefficient. Another variation of the solution
for the bare critical cylinder presented in Chapter III from that of
Mitsis is a more straightforward, though equivalent, treatment of the
singular eigenfunctions. The advantages of this new singular eigen-
function treatment are discussed below.

The development of the solution for the radially reflected critical
cylinder is presented in Chapter IV. The solution is based upon the
integral transform approach developed for the bare core solution by
Mitsis. The same approach has been taken by Smith and Siewert[7] and
by Leuthäuser[8] in developing solutions for the reflected critical
sphere. Both of these solutions assume identical neutron mean free
paths in the core and reflector regions. Smith[9] has demonstrated the
complicated form of the transformed integral equation when this assump-
tion is not made. To reduce the complexity of the problem, the same
assumption is imposed on this solution for the reflected critical
cylinder. However, the multiplying properties of the two media are
allowed to differ. In the context of the monoenergetic model, the
identical mean free path assumption is not a severe restriction,

especially for fast energy spectrum reactors where total neutron cross
sections are of the same order of magnitude.

Transformation of the integral transport equation in two-region
cylindrical geometry results in integral equations for the neutron
density in each region. Contained in these expressions are kernels
made up of sums of integrals of modified Bessel functions over the
spatial variable. These kernels are separated out and defined as
pseudo neutron distribution functions. The pseudo neutron distribution
functions are shown to satisfy the same integro-differential equation
as arises in the bare core case with the same centerline and outer
boundary conditions. Additional boundary conditions are continuity
of the pseudo neutron distribution function and its spatial derivative
at the core-reflector interface.

Solutions in terms of modified Bessel functions and singular
eigenfunctions (called pseudo eigenfunctions because they are functions
of the transformed variable) are found for the integro-differential
equation by the separation of variables technique. When Mitsis[2]
introduced these pseudo eigenfunctions, he initially considered the
full range on the eigenvalues. Then he observed that the pseudo
eigenfunctions correspond to the sum of the Case plane geometry eigen-
functions and showed completeness by the theorem proven by Case.[1]
In the present solutions for both the bare and reflected systems,
advantage is taken of the evenness of the pseudo eigenfunctions and
of the dispersion function for the eigenvalues to consider only those
eigenvalues in the positive half-range. A full-range completeness
theorem for the pseudo eigenfunctions is proven in Appendix B and its

easy extension to the half-range is shown. This procedure provides a basis for developing the solution entirely in terms of the eigenfunctions found, without using a decomposition into the Case plane geometry eigenfunctions as done by Mitsis in obtaining the bare core solution. A particular advantage of the present approach is the lack of dependence on the half-range plane geometry eigenfunction completeness theory which requires the calculation of X-functions.[3] Also inherent in the proof of completeness are several very useful orthogonality and normalization relations for the pseudo eigenfunctions. These relations are developed in Appendix A.

Substitution of the pseudo eigenfunctions into the boundary conditions and application of the orthogonality-normalization relations results in two coupled iterative sequences with which the expansion coefficients can be calculated to any desired degree of accuracy. The critical condition arises from the reduction of the outer boundary condition to a Fredholm integral equation for one of the reflector expansion coefficients. It corresponds directly to an auxiliary condition required in the proof of completeness.

Chapter V contains a description of the numerical techniques used to obtain the various functions and parameters appearing in the solutions developed in Chapters III and IV. The accuracy of these techniques is drawn from comparison with tabulated values. Then follows a demonstration of how the precision of the results varies with the order of numerical quadrature used in evaluating the integral terms appearing in the solutions. Finally the numerical results for a wide variety of cases are presented and compared with the results of other

methods. The bare core results are compared with the results of other analytic solutions found in the literature. The reflected core results are compared with the results of high order numerical calculations.

Chapter VI contains a demonstration of how the results from the highly precise solution for the reflected cylinder can be used as analytic standards. A case is chosen which, in the context of the model, most closely approximates the Advanced Power Reactor[10] concept being studied at the Lewis Research Center. Then, using the exact critical dimensions, the discrete angular segmentation programs used in the design of this concept are employed to study the three effects listed under the Purpose and Scope of this study (1.1).

Chapter VII contains the conclusions and recommendations drawn from this study. The conclusions pertain both to the analytic solutions found and to the accuracies of the various numerical design approximations studied. Based on these conclusions, recommendations are made as to order of approximation required for desired design accuracies and as to where indicated sources of error might be reduced.

CHAPTER II

MONOENERGETIC TRANSPORT THEORY

2.1 The Boltzmann Equation

The assumptions under which the Boltzmann equation describes neutron transport in a medium free of independent sources are listed.

1. The neutron acts as a point particle which travels in a straight line with constant speed between neutron-nuclei interactions.

2. The probability of neutron-neutron interactions is much less than the probability of neutron-nuclei interactions and is, therefore, ignored.

3. The neutron population is sufficiently large so that statistical fluctuations may be ignored.

4. Secondary neutrons are produced at the time and position of the primary neutrons.

5. The total cross section, $\sigma(\underline{r},E)$, describing the probability of a neutron-nucleus interaction per unit path length, is a function of energy and position only.

With these assumptions, the Boltzmann equation for a medium free of independent sources is written as[11]

$$\frac{1}{v}\frac{\partial \Phi}{\partial t}(\underline{r},\underline{\Omega},E,t) + \underline{\Omega}\cdot\nabla\Phi(\underline{r},\underline{\Omega},E,t) + \sigma(\underline{r},E)\ \Phi(\underline{r},\underline{\Omega},E,t)$$

$$= \int_{E'}\int_{\underline{\Omega}'}\sigma(\underline{r},E')\ f(\underline{r};\underline{\Omega}',E'\rightarrow\underline{\Omega},E)\ \Phi(\underline{r},\underline{\Omega}',E',t)d\underline{\Omega}'dE' \qquad (2.1)$$

where the neutron angular flux, $\Phi(\underline{r},\underline{\Omega},E,t)$, is a function of position, angle, energy and time; v is the neutron speed; and $\sigma(\underline{r},E)$ x $f(\underline{r};\underline{\Omega}',E'\to\underline{\Omega},E)$ gives the total probability of neutron transfer from $\underline{\Omega}',E'$ to $\underline{\Omega},E$.

The present study is restricted to the greatly simplified, mono-energetic, stationary form of the Boltzmann equation. Elimination of the energy and time dependence in Eq. (2.1) yields

$$\underline{\Omega}\cdot\nabla\Phi(\underline{r},\underline{\Omega}) + \sigma(\underline{r})\,\Phi(\underline{r},\underline{\Omega}) = \sigma(\underline{r})c(\underline{r})\int_{\underline{\Omega}'} f(\underline{r};\underline{\Omega}'\to\underline{\Omega})\,\Phi(\underline{r},\underline{\Omega}')d\underline{\Omega}' \qquad (2.2)$$

where $c(\underline{r})$ is defined as the mean number of neutron secondaries per collision and enters from the operation

$$\int_{E'} f(\underline{r};\underline{\Omega}',E'\to\underline{\Omega},E)dE' = c(\underline{r})\,f(\underline{r};\underline{\Omega}'\to\underline{\Omega})$$

where $c(\underline{r})$, $\sigma(\underline{r})$ and $f(\underline{r};\underline{\Omega}'\to\underline{\Omega})$ are one group, spectrum averaged values.

In order to demonstrate Case's singular eigenfunction technique, Eq. (2.2) is written for infinite plane geometry with dependence on one coordinate only. In planar geometry we have the relations

$$\underline{\Omega}\cdot\nabla\Phi = \mu\,\frac{\partial\Phi}{\partial z}\,, \quad \text{where } \mu = \underline{\Omega}\cdot\hat{z},$$

and also $d\underline{\Omega}' = 2\pi d\mu'$, $-1 \leq \mu \leq 1$.

With these substitutions, Eq. (2.2) becomes

$$\mu\,\frac{\partial\Phi}{\partial z}\,(z,\mu) + \sigma(z)\Phi(z,\mu) = \sigma(z)c(z)2\pi\int_{-1}^{1} f(z;\underline{\Omega}'\to\underline{\Omega})\Phi(z,\mu')d\mu'. \qquad (2.3)$$

Eq. (2.3) is further simplified by the restriction to isotropic scatterings in the laboratory system. In this instance,

$$f(z;\underline{\Omega}'\rightarrow\underline{\Omega}) = 1/4\ \pi.$$

Finally, the spatial variation is expressed in neutron mean free paths through the definition:

$$x = \int_0^z \sigma(z')dz'$$

from which follows $\frac{\partial}{\partial z} = \sigma(z)\frac{\partial}{\partial x}$.

With the above substitutions, Eq. (2.3) becomes

$$\mu\frac{\partial\Phi}{\partial x}(x,\mu) + \Phi(x,\mu) = \frac{c}{2}\int_{-1}^{1}\Phi(x,\mu')d\mu' \ . \tag{2.4}$$

Eq. (2.4) is the stationary, monoenergetic, one-dimensional, Boltzmann equation for a source-free, isotropic, homogeneous medium in plane geometry for which Case[1] developed the singular eigenfunction solution.

2.2 Case's Singular Eigenfunction Method

The solution to Eq. (2.4) is sought through the separation of variables technique. Thus we assume a general solution of the form

$$\Phi(x,\mu) = X(x)\varphi(\mu) \tag{2.5}$$

Substitution of Eq. (2.5) into Eq. (2.4) yields

$$\mu\varphi(\mu)\frac{dX(x)}{dx} + X(x)\varphi(\mu) = \frac{c}{2}X(x)\int_{-1}^{1}\varphi(\mu')d\mu'. \tag{2.6}$$

After collecting like variables in Eq. (2.6) we obtain

$$\frac{1}{X(x)}\frac{dX(x)}{dx} = \frac{c}{2\mu\varphi(\mu)}\int_{-1}^{1}\varphi(\mu')d\mu' - \frac{1}{\mu} \ . \tag{2.7}$$

Next, each side of Eq. (2.7) is set equal to the separation constant, $-1/\upsilon$, to obtain the two equations:

$$\frac{dX(x)}{dx} + \frac{X(x)}{\upsilon} = 0 \qquad (2.8)$$

and

$$\left(\frac{1}{\mu} - \frac{1}{\upsilon}\right)\frac{2\mu\varphi(\mu)}{c} = \int_{-1}^{1} \varphi(\mu')d\mu'. \qquad (2.9)$$

The solution of Eq. (2.8) is immediately written as

$$X(x) = (\text{constant})e^{-x/\upsilon}. \qquad (2.10)$$

To obtain the solution for Eq. (2.9), we first normalize

$$\int_{-1}^{1} \varphi(\mu)d\mu = 1$$

after which Eq. (2.9) becomes

$$(\upsilon - \mu)\varphi(\mu) = \frac{c\upsilon}{2} \qquad (2.11)$$

Eq. (2.11) yields a family of nonsingular and singular solutions depending on the value of υ. For $\upsilon \notin [-1,1]$, we have two discrete solutions given by

$$\varphi_{0\pm}(\mu) = \frac{c}{2}\frac{\upsilon_0}{\upsilon_0 \mp \mu} \qquad (2.12)$$

where $\pm \upsilon_0$ are the roots of the dispersion function

$$\Lambda(\upsilon) = 1 - c\upsilon\tanh^{-1}(1/\upsilon) = 0. \qquad (2.13)$$

For $\upsilon \in [-1,1]$, we have a continuum of solutions

$$\varphi_{\upsilon}(\mu) = \frac{c}{2} P \frac{\upsilon}{\upsilon-\mu} + \lambda(\upsilon)\delta(\upsilon-\mu) \qquad (2.14)$$

where $\lambda(\upsilon)$ is the function of Case defined by

$$\lambda(\upsilon) = 1 - c\upsilon\tanh^{-1}(\upsilon), \qquad (2.15)$$

and P indicates that the Cauchy principal value is taken for integrals involving $\varphi_\upsilon(\mu)$. Collecting Eqs. (2.10, 2.12, 2.14), we write the general solution of Eq. (2.4) as

$$\Phi(x,\mu) = a_{0+}\varphi_{0+}(\mu)e^{-x/\upsilon_0} + a_{0-}\varphi_{0-}(\mu)e^{x/\upsilon_0} + \int_{-1}^{1} A(\upsilon)\varphi_\upsilon(\mu)e^{-x/\upsilon}d\upsilon.$$

(2.16)

$$-1 \leq \mu \leq 1$$

Case[1] proved a completeness theorem for the above expansion which is constructive in the sense that it provides a method for obtaining the expansion coefficients. He also proved a partial range completeness theorem. Since these proofs are rather involved and are well documented, we do not include them here. However, an analogous proof for the eigenfunctions developed in Chapter III is presented in Appendix B.

2.3 The Integral Transport Equation

Attempts by Mitsis to apply Case's method for solving the Boltzmann equation in other than plane geometry were unsuccessful. However, successful applications were obtained in spherical and cylindrical geometry after making suitable transformations of the integral form of the transport equation. Here we wish to show the equivalence of the Boltzmann equation and the integral transport equation. First the monoenergetic, stationary Boltzmann equation as it appears in Eq. (2.2) is rewritten as

$$\underline{\Omega} \cdot \nabla\Phi(\underline{r},\underline{\Omega}) + \sigma(\underline{r})\Phi(\underline{r},\underline{\Omega}) = q(\underline{r},\underline{\Omega})$$

(2.17)

where the source term, $q(\underline{r},\underline{\Omega})$, is given by

$$q(\underline{r},\underline{\Omega}) = \sigma(\underline{r})c(\underline{r})\int_{\underline{\Omega}'} f(\underline{r};\underline{\Omega}' \to \underline{\Omega})\Phi(\underline{r},\underline{\Omega}')d\underline{\Omega}'.$$

With the position vectors as shown below,
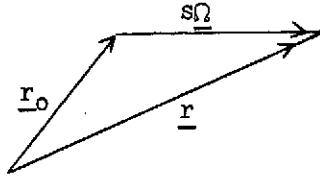
we define $\underline{r} = \underline{r}_0 + s\underline{\Omega}$ and write Eq. (2.17) as

$$\frac{\partial \Phi}{\partial s}(\underline{r}_0 + s\underline{\Omega}, \underline{\Omega}) + \sigma(\underline{r}_0 + s\underline{\Omega})\Phi(\underline{r}_0 + s\underline{\Omega}, \underline{\Omega}) = q(\underline{r}_0 + s\underline{\Omega}, \underline{\Omega}). \qquad (2.18)$$

Operation on Eq. (2.18) with the integrating factor

$$\exp\left[\int_{-\infty}^{s} \sigma(\underline{r}_0 + s'\underline{\Omega})ds'\right]$$

results in

$$\frac{\partial}{\partial s}\left\{\exp\left[\int_{-\infty}^{s}\sigma(\underline{r}_0 + s'\underline{\Omega})ds'\right]\Phi(\underline{r}_0 + s\underline{\Omega}, \underline{\Omega})\right\} = \exp\left[\int_{-\infty}^{s}\sigma(\underline{r}_0 + s'\underline{\Omega})ds'\right]q(r_0 + s\underline{\Omega}, \underline{\Omega})$$

$$(2.19)$$

as can be shown by applying Leibnitz's Rule. In Eq. (2.19) we replace s by s' and s' by s", then operate by the integral over s' from $-\infty$ to s obtaining

$$\left[\exp\left[\int_{-\infty}^{s'}\sigma(\underline{r}_0 + s"\underline{\Omega})ds"\right]\Phi(\underline{r}_0 + s'\underline{\Omega}, \underline{\Omega})\right]_{-\infty}^{s} = \int_{-\infty}^{s}\exp\left[\int_{-\infty}^{s'}\sigma(\underline{r}_0 + s"\underline{\Omega})ds"\right]q(r_0 + s'\underline{\Omega}, \underline{\Omega})ds'.$$

$$(2.20)$$

In evaluating the left hand side of Eq. (2.20) at the lower limit we assume that

$$\lim_{s' \to -\infty} \Phi(\underline{r}_0 + s'\underline{\Omega}, \underline{\Omega}) = 0.$$

Transposing the exponential term on the left hand side of Eq. (2.20), dividing the range on the integral in the transposed exponential from $-\infty$ to s' and from s' to s, and, after cancellation, we obtain

$$\Phi(\underline{r}_o + s\underline{\Omega},\underline{\Omega}) = \int_{-\infty}^{s} \exp -\left[\int_{s'}^{s} \sigma(\underline{r}_o + s''\underline{\Omega})ds''\right]q(\underline{r}_o + s'\underline{\Omega},\underline{\Omega})ds'. \quad (2.21)$$

Now recalling that $\underline{r} = \underline{r}_o + s\underline{\Omega}$, $\underline{r}_o = \underline{r} - s\underline{\Omega}$, we write Eq. (2.21) as

$$\Phi(\underline{r},\underline{\Omega}) = \int_{-\infty}^{s} \exp\left[-\int_{s'}^{s} \sigma(\underline{r} + [s'' - s]\underline{\Omega})ds''\right]q(\underline{r} + [s' - s]\underline{\Omega},\underline{\Omega})ds'. \quad (2.22)$$

Next, inserting new variables $p'' = s - s''$ and $p' = s - s'$, Eq. (2.22)

becomes

$$\Phi(\underline{r},\underline{\Omega}) = \int_{0}^{\infty} \exp\left[-\int_{0}^{p'} \sigma(\underline{r} - p''\underline{\Omega})dp''\right]q(\underline{r} - p'\underline{\Omega},\underline{\Omega})dp'. \quad (2.23)$$

Returning to the more conventional displacement variable, we let

$p' = s$ and $p'' = s'$ in Eq. (2.23) obtaining

$$\Phi(\underline{r},\underline{\Omega}) = \int_{0}^{\infty} \exp\left[-\int_{0}^{s} \sigma(\underline{r} - s'\underline{\Omega})ds'\right]q(\underline{r} - s\underline{\Omega},\underline{\Omega})ds. \quad (2.24)$$

Upon imposing isotropic scattering on the source term, thereby eliminating

its dependence on Ω' as it appears in Eq. (2.17), Eq. (2.24) becomes

$$\Phi(\underline{r},\underline{\Omega}) = \frac{1}{4\pi}\int_{0}^{\infty} \exp\left[-\int_{0}^{s} \sigma(\underline{r} - s'\underline{\Omega})ds'\right]\sigma(\underline{r} - s\underline{\Omega})c(\underline{r} - s\underline{\Omega})\Phi(\underline{r} - s\underline{\Omega})ds. \quad (2.25)$$

In order to eliminate the angular dependence, we operate on Eq. (2.25)

with the integral over $\underline{\Omega}$ as follows:

$$\int_{\underline{\Omega}} \Phi(\underline{r},\underline{\Omega})d\underline{\Omega} = \frac{1}{4\pi}\int\int_{\underline{\Omega}}\int_{0}^{\infty} \exp\left[-\int_{0}^{s} \sigma(\underline{r} - s'\underline{\Omega})ds'\right]\sigma(\underline{r} - s\underline{\Omega})c(\underline{r} - s\underline{\Omega})\Phi(\underline{r} - s\underline{\Omega})ds\,d\underline{\Omega}, \quad (2.26)$$

let $\underline{r}' = \underline{r} - s\underline{\Omega}$, and recognize that the volume element $ds\,d\underline{\Omega} = d\underline{r}'/|\underline{r}-\underline{r}'|^2$, and use the definition for optical length, $\tau(|\underline{r}'-\underline{r}|) = \int_{0}^{|\underline{r}'-\underline{r}|} \sigma(\underline{r}-s'\underline{\Omega})ds'$, to obtain

$$\Phi(\underline{r}) = \frac{1}{4\pi}\int_{\underline{r}'} \frac{\exp[-\tau(|\underline{r}' - \underline{r}|)]}{|\underline{r} - \underline{r}'|^2} \sigma(\underline{r}')c(\underline{r}')\Phi(\underline{r}')d\underline{r}'. \quad (2.27)$$

After expressing the volume element $d\underline{r}'$ as d^3r' and changing the spatial variable to mean free paths, Eq. (2.27) becomes

$$\Phi(\underline{r}) = \frac{1}{4\pi} \int_{\underline{r}'} \frac{e^{-|\underline{r}-\underline{r}'|}}{|\underline{r}-\underline{r}'|^2} c(\underline{r}')\Phi(\underline{r}')d^3r'. \qquad (2.28)$$

Finally we rewrite Eq. (2.28) in terms of the neutron density by multiplying through by the average speed, v, and using $\rho(\underline{r}) = v\Phi(\underline{r})$, to obtain

$$\rho(\underline{r}) = \frac{1}{4\pi} \int_{\underline{r}'} \frac{e^{-|\underline{r}-\underline{r}'|}}{|\underline{r}-\underline{r}'|^2} c(\underline{r}')\rho(\underline{r}')d^3r'. \qquad (2.29)$$

Eq. (2.29) is the stationary, monoenergetic, integral transport equation for the neutron density in a source free, homogeneous medium with isotropic scattering.

CHAPTER III

SOLUTION FOR THE BARE CRITICAL CYLINDER

3.1 Transformation of the Integral Equation in Cylindrical Geometry

The monoenergetic integral transport equation, Eq. (2.29), is written for a single region as follows:

$$\rho(\underline{r}) = \frac{c}{4\pi} \int_{\underline{r}'} \frac{\rho(\underline{r}')e^{-|\underline{r} - \underline{r}'|}}{|\underline{r} - \underline{r}'|^2} d^3r', \tag{3.1}$$

where c, the mean number of neutron secondaries per collision, is a constant. We wish to apply this equation to the bare cylindrical geometry shown in Fig. 1. In Fig. 1 we have represented the position $\underline{r}'$ by the cylindrical coordinates (t, α, z) and have located $\underline{r}$ at (r, o, o). We observe from Fig. 1 that

$$|\underline{r} - \underline{r}'|^2 = x^2 + z^2 = r^2 + t^2 - 2rt\cos(\alpha) + z^2. \tag{3.2}$$

Expressing the volume integral over $\underline{r}'$ in cylindrical coordinates, Eq. (3.1) becomes

$$\rho(r) = \frac{c}{4\pi} \int_0^R t\rho(t)dt \int_0^{2\pi} d\alpha \int_{-\infty}^{\infty} \frac{\exp\left[-\sqrt{x^2 + z^2}\right]}{x^2 + z^2} dz, \tag{3.3}$$

where R represents the radius of the outer boundary and the limits on z correspond to the axially infinite cylinder.

The integral over z is reduced by first defining I_z as

$$I_z = \frac{2}{x^2} \int_0^{\infty} \frac{\exp\left[-x\sqrt{1 + (z/x)^2}\right]}{1 + (z/x)^2} dz. \tag{3.4a}$$

Then I_z can be written as

$$I_z = \frac{2}{x^2} \int_0^{\infty} \frac{dz}{\sqrt{1 + (z/x)^2}} \int_x^{\infty} \exp\left[-u\sqrt{1 + (z/x)^2}\right] du. \tag{3.4b}$$
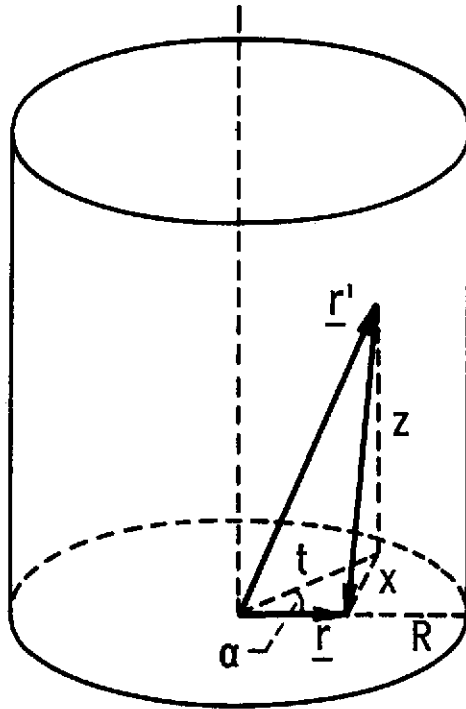
Figure 1. – One region cyl-
indrical geometry.

Substituting $v = z/x$, Eq. (3.4b) becomes

$$I_z = \frac{2}{x} \int_x^\infty du \int_0^\infty \frac{\exp\left[-u\sqrt{1+v^2}\right]}{\sqrt{1+v^2}} dv. \qquad (3.4c)$$

Now by defining $t' = \sqrt{1+v^2}$, we can express Eq. (3.4c) as

$$I_z = \frac{2}{x} \int_x^\infty du \int_1^\infty \frac{e^{-ut'} dt'}{\sqrt{t'^2-1}} . \qquad (3.4d)$$

The second integral in Eq. (3.4d) corresponds to the Laplace transform of $F(t') = (t'^2-1)^{-1/2}$, which is equal to $K_0(u)$, modified Bessel function of the second kind; therefore,

$$I_z = \frac{2}{x} \int_x^\infty K_0(u) du. \qquad (3.4e)$$

Finally, we make the substitution, $\mu = x/u$, into Eq. (3.4e) obtaining

$$I_z = 2 \int_0^1 \frac{K_0(x/\mu)}{\mu^2} d\mu. \qquad (3.4f)$$

Substitution of Eq. (3.4f) into Eq. (3.3) and expressing x as in Eq. (3.2) results in

$$\rho(r) = \frac{c}{2\pi} \int_0^R t\rho(t) dt \int_0^{2\pi} d\alpha \int_0^1 K_0\left(\frac{\sqrt{r^2+t^2-2rt\cos(\alpha)}}{\mu}\right) \frac{d\mu}{\mu^2} . \qquad (3.5)$$

The integral over α in Eq. (3.5) is performed by applying the addition theorem for the modified Bessel function of the second kind; namely,

$$K_0\left(\frac{\sqrt{r^2+t^2-2rt\cos(\alpha)}}{\mu}\right) = \sum_{-\infty}^\infty e^{in\alpha} \begin{cases} K_n(r/\mu)I_n(t/u), & r \geq t \\ K_n(t/\mu)I_n(r/\mu), & r \leq t \end{cases} \qquad (3.6a)$$

and noting that

$$\int_0^{2\pi} e^{in\alpha} d\alpha = \begin{matrix} 2\pi, & n = 0 \\ 0, & n \neq 0. \end{matrix} \qquad (3.6b)$$

The result of this procedure is an integral equation for the neutron density distribution with integrals over the radial variable, t, and the transformed variable, μ.

$$\rho(r) = c \int_0^1 \frac{d\mu}{\mu^2} \left[\int_0^r K_0(r/\mu) I_0(t/\mu) t\rho(t) dt \right.$$

$$\left. + \int_r^R K_0(t/\mu) I_0(r/\mu) t\rho(t) dt \right] \qquad (3.7)$$

3.2 The Pseudo Neutron Distribution Function

Adopting the nomenclature of Mitsis,[2] we define the kernel appearing in Eq. (3.7) as a pseudo neutron distribution function, $\Phi(r,\mu)$, related to the neutron density such that

$$\rho(r) = \int_0^1 \frac{\Phi(r,\mu)}{\mu^2} d\mu, \qquad (3.8)$$

where

$$\Phi(r,\mu) = c \left[\int_0^r K_0(r/\mu) I_0(t/\mu) t\rho(t) dt \right.$$

$$\left. + \int_r^R K_0(t/\mu) I_0(r/\mu) t\rho(t) dt \right]. \qquad (3.9)$$

Next, we wish to show that $\Phi(r,\mu)$ obeys an integrodifferential equation made up of first and second derivative terms. In taking the first derivative, we use the relations:

$$K_0'(z) = -K_1(z); I_0'(z) = I_1(z).$$

Use of Leibnitz's Rule and the above relations yields the first derivative of $\Phi(r,\mu)$ with respect to r as

$$\frac{\partial \Phi(r,\mu)}{\partial r} = \frac{c}{\mu} \left[-\int_0^r K_1(r/\mu) I_0(t/\mu) t\rho(t) dt + \int_r^R K_0(t/\mu) I_1(r/\mu) t\rho(t) dt \right]. \qquad (3.10a)$$

The second derivative is found by continuing the above procedure and using the additional relations:

$$I_1'(z) = I_0(z) - \frac{1}{z} I_1(z); K_1'(z) = -K_0(z) - \frac{1}{z} K_1(z);$$

and the Wronskian[12] for the modified Bessel functions:

$$K_0(z)I_1(z) + K_1(z)I_0(z) = 1/z.$$

Use of the above relations yields the second derivative of $\Phi(r,\mu)$ as

$$\frac{\partial^2 \Phi(r,\mu)}{\partial r^2} = \frac{c}{\mu^2} \int_0^r \left[K_0(r/\mu) + \frac{\mu}{r} K_1(r/\mu) \right] I_0(t/\mu) t\rho(t) dt$$

$$+ \frac{c}{\mu^2} \int_r^R K_0(t/\mu) \left[I_0(r/\mu) - \frac{\mu}{r} I_1(r/\mu) \right] t\rho(t) dt$$

$$- c\rho(r). \tag{3.10b}$$

Now substituting from Eqs. (3.9), (3.10a) and (3.10b), we form the equation:

$$\frac{\partial^2 \Phi(r,\mu)}{\partial r} + \frac{1}{r} \frac{\partial \Phi(r,\mu)}{\partial r} - \frac{1}{\mu^2} \Phi(r,\mu) =$$

$$\frac{c}{\mu^2} \int_0^r \left[K_0(r/\mu) + \frac{\mu}{r} K_1(r/\mu) \right] I_0(t/\mu) t\rho(t) dt +$$

$$\frac{c}{\mu^2} \int_r^R K_0(t/\mu) \left[I_0(r/\mu) - \frac{\mu}{r} I_1(r/\mu) \right] t\rho(t) dt - c\rho(r) +$$

$$\frac{c}{\mu r} \left[-\int_0^r K_1(r/\mu) I_0(t/\mu) t\rho(t) dt + \int_r^R K_0(t/\mu) I_1(r/\mu) t\rho(t) dt \right] -$$

$$\frac{c}{\mu^2} \left[\int_0^r K_0(r/\mu) I_0(t/\mu) t\rho(t) dt + \int_r^R K_0(t/\mu) I_0(r/\mu) t\rho(t) dt \right]. \tag{3.10c}$$

Canceling like terms on the right hand side of Eq. (3.10c) and substituting Eq. (3.8) for $\rho(r)$ we obtain

$$\frac{\partial^2 \Phi(r,\mu)}{\partial r^2} + \frac{1}{r}\frac{\partial \Phi(r,\mu)}{\partial r} - \frac{1}{\mu^2}\Phi(r,\mu) = -c\int_0^1 \frac{\Phi(r,\mu')}{\mu'^2}\,d\mu'. \qquad (3.10d)$$

Having shown the integro-differential equation that $\Phi(r,\mu)$ obeys, now we need to establish the boundary conditions satisfied by $\Phi(r,\mu)$. Inspection of $\Phi(r,\mu)$ as defined in Eq. (3.9) at the core centerline, $r = o$, with the consideration that $I_o(0) = 1$ and that the limit of $t\,K_o(t/\mu) = o$ as $t \to o$, establishes the boundary condition:

$$\Phi(o,\mu) \text{ finite.} \qquad (3.11a)$$

The outer boundary condition is constructed by first substituting $r = R$ into Eq. (3.9) to determine $\Phi(R,\mu)$ as

$$\Phi(R,\mu) = c\int_0^R K_o(R/\mu)I_o(t/\mu)t\rho(t)\,dt. \qquad (3.11b)$$

Next, substituting $r = R$ into Eq. (3.10a) yields for the first derivative term

$$\frac{\partial \Phi(r,\mu)}{\partial r}\Bigg|_{r=R} = -\frac{c}{\mu}\int_0^R K_1(R/\mu)I_o(t/\mu)t\rho(t)\,dt. \qquad (3.11c)$$

Inspection of Eqs. (3.11b and c) as combined below establishes the outer boundary condition as

$$K_o(R/\mu)\;\frac{\partial \Phi(r,\mu)}{\partial r}\Bigg|_{r=R} + \frac{K_1(R/\mu)}{\mu}\,\Phi(R,\mu) = 0. \qquad (3.11d)$$

3.3 Singular Eigenfunction Expansion and Solution

In developing the eigenfunctions, we assume a solution of Eq. (3.10d) of the form

$$\Phi_\nu(r,\mu) = R_\nu(r)M_\nu(\mu). \qquad (3.12)$$

Substitution of Eq. (3.12) into Eq. (3.10d) and using $1/\nu^2$ as the separation constant yields

$$\frac{d^2 R_\nu(r)}{dr^2} + \frac{1}{r}\frac{dR_\nu(r)}{dr} - \frac{1}{\nu^2} R_\nu(r) = 0 \qquad (3.13)$$

and

$$\left(\frac{1}{\mu^2} - \frac{1}{\nu^2}\right) M_\nu(\mu) = c \int_0^1 \frac{M_\nu(\mu')}{\mu'^2} d\mu'. \qquad (3.14)$$

The general solution of Eq. (3.13) is

$$R_\nu(r) = \alpha I_0(r/\nu) + \beta K_0(r/\nu). \qquad (3.15)$$

To find the eigenfunctions and eigenvalues of Eq. (3.14), we first normalize by setting

$$\int_0^1 \frac{M_\nu(\mu')}{\mu'^2} d\mu' = 1 \qquad (3.16)$$

after which we have

$$(\nu^2 - \mu^2) M_\nu(\mu) = c\nu^2\mu^2, \quad 0 \le \mu \le 1 \qquad (3.17)$$

Here we find it convenient to make the definition

$$\eta_\nu(\mu) = M_\nu(\mu)/\mu^2, \qquad (3.18)$$

where we call $\eta_\nu(\mu)$ our pseudo eigenfunction. Substitution of Eq. (3.18) into Eq. (3.17) yields one discrete solution as

$$\eta_0(\mu) = \frac{c\nu_0^2}{\nu_0^2 - \mu^2}, \quad \nu \notin [0,1] \qquad (3.19)$$

where ν_0 is obtained from the dispersion function, Eq. (2.13). For $\nu \epsilon [0,1]$, a continuum of solutions is obtained as

$$\eta_\nu(\mu) = cP \frac{\nu^2}{\nu^2 - \mu^2} + \lambda(\nu)\delta(\nu - \mu) \qquad (3.20)$$

where P denotes that the Cauchy principal value is taken for integrals

involving $\eta_\nu(\mu)$, and $\lambda(\nu)$ is the function of Case[1] given by Eq. (2.15).

When Mitsis[2] introduced these pseudo eigenfunctions, he initially

considered both positive and negative ranges on the eigenvalues, and

then observed that the pseudo eigenfunctions are related to the plane

geometry eigenfunctions of Case, Eqs. (2.12) and (2.14), in the following

manner:

$$\eta_o(\mu) = \varphi_{o+}(\mu) + \varphi_{o-}(\mu)$$

and

$$\eta_\nu(\mu) = \varphi_\nu(\mu) + \varphi_{-\nu}(\mu).$$

Mitsis went on to complete his bare core solution in terms of the plane

geometry eigenfunctions. Therefore, the Mitsis solution depends on

half-range plane geometry eigenfunction completeness theory which

involves the calculation of X-functions. Here we take advantage of

the evenness of the pseudo eigenfunctions and the dispersion function

to consider only those eigenvalues in the positive half range. In

Appendix B we prove a full-range completeness theorem for the pseudo

eigenfunctions and show its easy extension to the half range. This

procedure provides a basis for developing the solution entirely in

terms of the pseudo eigenfunctions. In addition to the theoretical

consistency of the present approach, the resulting solution provides

a simpler sequence for obtaining numerical results than the approach

taken by Mitsis. The numerical results from both approaches are

equivalent. Furthermore, the proof of completeness for the pseudo

eigenfunctions involves orthogonality and normalization relations

developed in Appendix A which are very useful in obtaining the solution

for the two-region problem. Efforts to obtain a two-region solution with the Mitsis approach, that is, using the plane geometry eigenfunctions, were unsuccessful.

Proceeding with the bare core solution, the general solution for $\Phi(r,\mu)$ is obtained by substituting Eqs. (3.15), (3.19) and (3.20) into Eq. (3.12) yielding

$$0 \leq r \leq R \quad \Phi(r,\mu) = [a_0 I_0(r/\nu_0) + b_0 K_0(r/\nu_0)]\mu^2 \eta_0(\mu)$$
$$0 \leq \mu \leq 1$$

$$+ \int_0^1 [A(\nu)I_0(r/\nu) + B(\nu)K_0(r/\nu)]\mu^2 \eta_\nu(\mu)d\nu. \tag{3.21}$$

For a critical system, c, the mean number of neutron secondaries per collision, must be greater than unity. In this instance, ν_0 as given by Eq. (2.13) will be purely imaginary. Thus, in Eq. (3.21), $I_0(r/\nu_0)$ becomes $J_0(r/|\nu_0|)$ and $K_0(r/\nu_0)$ is equal to $\frac{\pi}{2} i[J_0(r/|\nu_0|) + iY(r/|\nu_0|)]$. With the singular nature of $Y_0(r/|\nu_0|)$ and $K_0(r/\nu)$ at $r = 0$, b_0 and $B(\nu)$ must be zero to satisfy the boundary condition, Eq. (3.11a). Eq. (3.21) for the pseudo distribution function is now rewritten as

$$\Phi(r,\mu) = a_0 J_0(r/|\nu_0|)\mu^2 \eta_0(\mu) + \int_0^1 A(\nu)I_0(r/\nu)\mu^2 \eta_\nu(\mu)d\nu. \tag{3.22}$$

The next step in the solution is to substitute $\Phi(r,\mu)$ as defined in Eq. (3.22) into the outer boundary condition, Eq. (3.11d), yielding

$$\left\{ \frac{K_1(R/\mu)J_0(R/|\nu_0|)}{\mu} - \frac{K_0(R/\mu)J_1(R/|\nu_0|)}{|\nu_0|} \right\} a_0 \mu^2 \eta_0(\mu)$$

$$+ \int_0^1 \left\{ \frac{K_1(R/\mu)I_0(R/\nu)}{\mu} + \frac{K_0(R/\mu)I_1(R/\nu)}{\nu} \right\} A(\nu)\mu^2 \eta_\nu(\mu)d\nu = 0. \tag{3.23}$$

Multiplying Eq. (3.23) by R/μ^2, we obtain

$$\left\{\frac{K_1(R/\mu)J_0(R/|\nu_0|)}{\mu} - \frac{K_0(R/\mu)J_1(R/|\nu_0|)}{|\nu_0|}\right\}Ra_0\eta_0(\nu)$$

$$+\int_0^1 A(\nu)q(\nu,\mu)\eta_\nu(\mu)d\nu = 0, \qquad (3.24)$$

where

$$q(\nu,\mu) = \frac{R}{\mu}K_1(R/\mu)I_0(R/\nu) + \frac{R}{\nu}K_0(R/\mu)I_1(R/\nu).$$

At this point we wish to separate Eq. (3.24) into singular and nonsingular parts. This is effected by defining the function:

$$H(\nu,\mu) = \frac{1}{\nu-\mu}\left\{\frac{I_0(R/\mu)}{I_0(R/\nu)}\,q(\nu,\mu) - 1\right\} \qquad (3.25a)$$

or

$$H(\nu,\mu) = \frac{1}{\nu-\mu}\left\{\frac{R}{\mu}K_1(R/\mu)I_0(R/\mu) + \frac{R}{\nu}K_0(R/\mu)I_0(R/\mu)\frac{I_1(R/\nu)}{I_0(R/\nu)} - 1\right\}. \qquad (3.25b)$$

Considering the behavior of the modified Bessel functions as shown in Fig. 2 and the asymptotic expressions, Eqs. (5.10) and (5.11), pg. 55, it can be seen that $H(\nu,\mu)$ is a bounded function. This procedure closely parallels the work of Mitsis.[2] However, the function of Mitsis which corresponds to $H(\nu,\mu)$ is unbounded. The reformulation of $H(\nu,\mu)$ as presented here is suggested in the general solution of Gibbs[4] for arbitrary convex bodies.

Since ν and μ range over the same values, it can be shown with the use of the Wronskian that $H(\nu,\mu)$, as defined in Eq. (3.25b), is indeterminate. Use of L'Hospital's rule yields $H(\nu,\nu)$ as

$$H(\nu,\nu) = \frac{R^2}{\nu^3}K_0(R/\nu)\left\{I_1^2(R/\nu)/I_0(R/\nu) - I_0(R/\nu)\right\} \qquad (3.25c)$$

which is also a bounded function.

$I_0(x)$, $K_0(x)$, $I_1(x)$, and $K_1(x)$
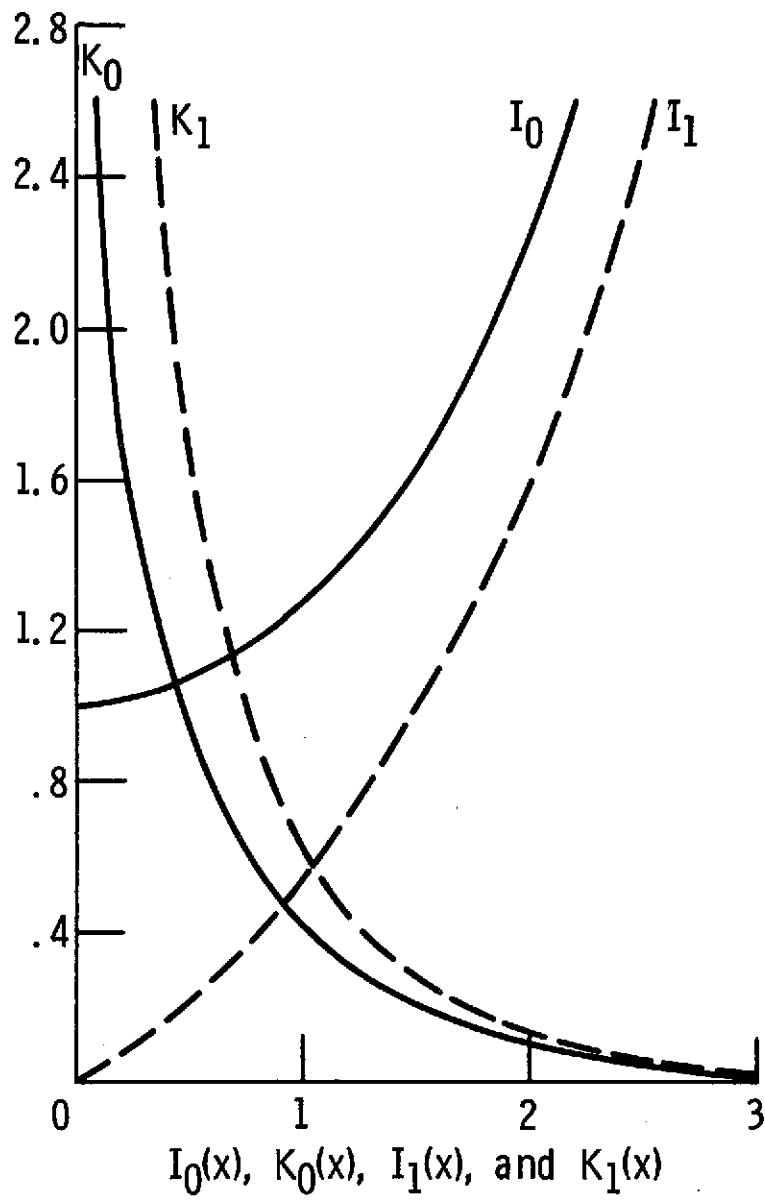
Figure 2. - Modified Bessel functions.

Next we rewrite Eq. (3.25a) as

$$q(\nu,\mu) = \frac{I_0(R/\nu)}{I_0(R/\mu)}\left\{1 + (\nu-\mu)H(\nu,\mu)\right\} \qquad (3.25d)$$

and substitute for $q(\nu,\mu)$ in Eq. (3.24) obtaining

$$\int_0^1 A(\nu)\,\frac{I_0(R/\nu)}{I_0(R/\mu)}\left\{1 + (\nu-\mu)H(\nu,\mu)\right\}\eta_\nu(\mu)d\nu$$

$$= -\left\{\frac{K_1(R/\mu)J_0(R/|\nu_0|)}{\mu} - \frac{K_0(R/\mu)J_1(R/|\nu_0|)}{|\nu_0|}\right\}Ra_0\eta_0(\mu). \qquad (3.26a)$$

Now returning to the pseudo eigenfunction as defined in Eq. (3.20) we note that

$$\int_0^1 (\nu-\mu)\eta_\nu(\mu)d\nu = \int_0^1 (\nu-\mu)\left[cP\,\frac{\nu^2}{\nu^2-\mu^2} + \lambda(\nu)\delta(\nu-\mu)\right]d\nu = c\int_0^1\frac{\nu^2}{\nu+\mu}\,d\nu.$$

$$(3.26b)$$

Using this observation, multiplying through by $I_0(R/\mu)$, and transposing terms, we complete the separation of Eq. (3.26a) into singular and non-singular parts as

$$\int_0^1 A'(\nu)\eta_\nu(\mu)d\nu = \Phi'(\mu) \qquad (3.27a)$$

where

$$\Phi'(\mu) = I_0(R/\mu)\left\{\frac{K_0(R/\mu)J_1(R/|\nu_0|)}{|\nu_0|}\right.$$

$$\left. - \frac{K_1(R/\mu)J_0(R/|\nu_0|)}{\mu}\right\}Ra_0\eta_0(\mu)$$

$$- c\int_0^1\frac{A'(\nu)H(\nu,\mu)\nu^2}{\nu+\mu}\,d\nu \qquad (3.27b)$$

and

$$A'(\nu) = A(\nu)I_0(R/\nu). \qquad (3.27c)$$

The discrete expansion coefficient, a_o, is chosen to correspond to some arbitrary power level and is thereby set equal to unity. The remaining problem is to find a solution for the continuum expansion coefficient, $A'(\nu)$. Eq. (3.27a) does not provide a closed form solution for $A'(\nu)$ because of the nondegenerate Fredholm term appearing in the definition of $\Phi'(\mu)$. However, an iterative solution for $A'(\nu)$ can be constructed, provided that a free expression for $A'(\nu)$ can be found. Now Eq. (3.27a) is the equivalent half-range form of Eq. (B.2a) in the proof of completeness for the pseudo eigenfunctions. Therefore, the desired free expression for $A'(\nu)$ corresponds to Eq. (B.15) which we write as

$$A'(\nu) = \frac{1}{N(\nu)} \int_0^1 \mu^2 \eta_\nu(\mu) \Phi'(\mu) d\mu \qquad (3.28)$$

where $N(\nu)$ is the normalization function for the continuum eigenfunctions, Eq. (A.31). The criticality condition is the auxiliary condition Eq. (B.11a) in the completeness proof, expressed over the half range as

$$c \int_0^1 \frac{\mu^2 \Phi'(\mu)}{\mu^2 + |\nu_o|^2} d\mu = 0 . \qquad (3.29)$$

Eqs. (3.27a, b, c), (3.28), and (3.29) form the solution for the bare critical cylinder. Successive approximations are constructed by the following scheme:

$$A_o'(\mu) = 0 \qquad (3.30a)$$

$$\Phi_o'(\mu) = I_o(R/\mu)R\eta_o(\mu)\left\{\frac{K_o(R/\mu)J_1(R/|\nu_o|)}{|\nu_o|} - \frac{K_1(R/\mu)J_o(R/|\nu_o|)}{\mu}\right\}(3.30b)$$

$$A'_{n+1}(\nu) = \frac{1}{N(\nu)} \int_0^1 \mu^2 \eta_\nu(\mu) \Phi'_n(\mu) d\mu \qquad (3.30c)$$

$$\Phi'_{n+1}(\mu) = \Phi'_0(\mu) - c \int_0^1 \frac{A'_{n+1}(\nu)H(\nu,\mu)\nu^2}{\nu + \mu} d\nu \qquad (3.30d)$$

$$c \int_0^1 \frac{\mu^2 \Phi'_{n+1}(\mu)}{\mu^2 + |\nu_0|^2} d\mu = 0. \qquad (3.30e)$$

The critical core radius is found by conducting a radius search to satisfy the criticality condition, Eq. (3.30e), for a convergent iterative sequence for $A'(\nu)$, Eqs. (3.30a through 3.30d). After the critical radius and converged expansion coefficients are obtained, the neutron density distribution can be calculated as

$$\rho(r) = a_0 J_0(r/|\nu_0|) + \int_0^1 A'(\nu) d\nu, \qquad (3.31)$$

which we have obtained by operating on Eq. (3.22) as in Eq. (3.8), substituting $A'(\nu)$ from Eq. (3.27c), and using the normalization, Eq. (3.16). Numerical results for the bare critical cylinder are presented in Chapter V.

CHAPTER IV

SOLUTION FOR THE REFLECTED CRITICAL CYLINDER

4.1 Formulation of the Equations

The solution for the two-region problem generally follows that of

the one-region problem. However, here we have the added complexity of

an intermediate boundary separating the core region $C_1 > 1$, and the

reflector region, $C_2 < 1$. We begin by rewriting Eq. (2.29), the mono-

energetic integral transport equation describing the neutron density

in an isotropically scattering medium as

$$\rho(\underline{r}) = \frac{1}{4\pi} \int_{\underline{r}'} \frac{c(\underline{r}')\rho(\underline{r}')e^{-|\underline{r}-\underline{r}'|}}{|\underline{r}-\underline{r}'|^2} d^3r' \qquad (4.1)$$

where $c(\underline{r}')$ denotes the mean number of neutron secondaries per collision

and distances are measured in mean free paths. By assuming a constant

neutron mean free path throughout, we are able to apply this equation to

the two region cylindrical geometry shown in Fig. 3. In Fig. 3 we have

represented $\underline{r}'$ by the cylindrical coordinates (t, α, z) and have located

$\underline{r}$ at (r, o, o). We observe from Fig. 3 that

$$|\underline{r}-\underline{r}'|^2 = x^2 + z^2 = r^2 + t^2 - 2rt\cos(\alpha) + z^2$$

Expressing the volume integral over $\underline{r}'$ in the cylindrical coordinates,

Eq. (4.1) becomes

$$\rho(r) = \frac{1}{4\pi} \int_0^{R_2} c(t)t\rho(t)dt \int_0^{2\pi} d\alpha \int_{-\infty}^{\infty} \frac{\exp\left[-\sqrt{x^2+z^2}\right]}{x^2+z^2} dz, \qquad (4.2)$$
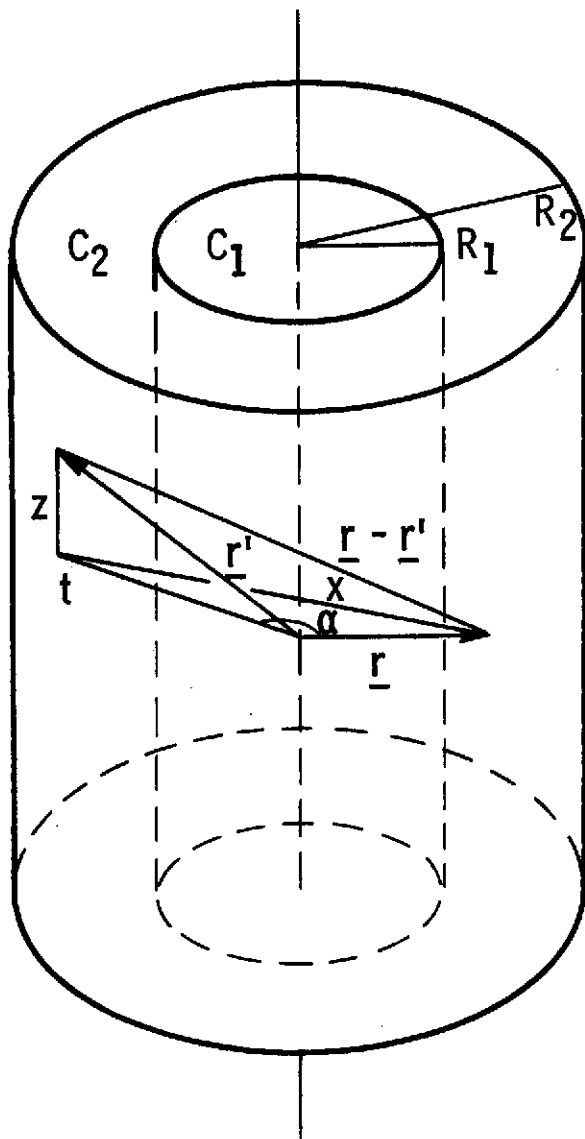
Figure 3. – Two region cylindrical geometry.

where $c(t) = C_1$, $0 \leq t \leq R_1$; $c(t) = C_2$, $R_1 \leq t \leq R_2$, and the limits on z correspond to the axially infinite cylinder.

The integral over z in Eq. (4.2) is reduced in the same manner as in Chapter III, Eqs. (3.4a through 3.4f). Under this procedure Eq. (4.2) becomes

$$\rho(r) = \frac{1}{2\pi} \int_0^{R_2} c(t)t\rho(t)dt \int_0^{2\pi} d\alpha \int_0^1 K_0\left(\frac{\sqrt{r^2 + t^2 - 2rt\cos(\alpha)}}{\mu}\right)\frac{d\mu}{\mu^2} \quad . \quad (4.3)$$

The integral over α in Eq. (4.3) is performed by applying the addition theorem for the modified Bessel function of the second kind,

$$K_0\left(\frac{\sqrt{r^2 + t^2 - 2rt\cos(\alpha)}}{\mu}\right) = \sum_{-\infty}^{\infty} e^{in\alpha} \begin{cases} K_n(r/\mu)I_n(t/\mu) & r \geq t \\ K_n(t/\mu)I_n(r/\mu) & r \leq t \end{cases} ,$$

and noting that

$$\int_0^{2\pi} e^{in\alpha}d\alpha = \begin{matrix} 2\pi, & n = 0 \\ 0, & n \neq 0 \end{matrix} \quad .$$

The result of this procedure is an integral equation for the neutron density in each region given by

$$\rho_1(r) = \int_0^1 \frac{d\mu}{\mu^2} \left\{ C_1 \int_0^r K_0(r/\mu)I_0(t/\mu)t\rho(t)dt \right.$$

$$0 \leq r \leq R_1$$

$$+ C_1 \int_r^{R_1} K_0(t/\mu)I_0(r/\mu)t\rho(t)dt$$

$$\left. + C_2 \int_{R_1}^{R_2} K_0(t/\mu)I_0(r/\mu)t\rho(t)dt \right\} \quad , \quad (4.4a)$$

$$\rho_2(r) = \int_0^1 \frac{d\mu}{\mu^2} \left\{ C_1 \int_0^{R_1} K_0(r/\mu) I_0(t/\mu) t\rho(t) dt \right.$$

$$R_1 \leqq r \leqq R_2$$

$$\left. + C_2 \int_{R_1}^r K_0(r/\mu) I_0(t/\mu) t\rho(t) dt + C_2 \int_r^{R_2} K_0(t/\mu) I_0(r/\mu) t\rho(t) dt \right\}.$$

$$(4.4b)$$

4.2 The Pseudo Neutron Distribution Functions

As in the bare core solution, we again adopt the nomenclature of Mitsis[2] by defining the kernels appearing in Eqs. (4.4a & b) as pseudo neutron distribution functions related to the neutron densities such that

$$\rho_1(r) = \int_0^1 \frac{\Phi_1(r,\mu)}{\mu^2} d\mu, \qquad (4.5a)$$

and

$$\rho_2(r) = \int_0^1 \frac{\Phi_2(r,\mu)}{\mu^2} d\mu, \qquad (4.5b)$$

where

$$\Phi_1(r,\mu) = C_1 \int_0^r K_0(r/\mu) I_0(t/\mu) t\rho(t) dt$$

$$o \leqq r \leqq R_1$$

$$+ C_1 \int_r^{R_1} K_0(t/\mu) I_0(r/\mu) t\rho(t) dt$$

$$+ C_2 \int_{R_1}^{R_2} K_0(t/\mu) I_0(r/\mu) t\rho(t) dt, \qquad (4.6a)$$

and

$$\Phi_2(r,\mu) = C_1 \int_0^{R_1} K_0(r/\mu) I_0(t/\mu) t\rho(t) dt$$

$$R_1 \leqq r \leqq R_2$$

$$+ C_2 \int_{R_1}^r K_0(r/\mu) I_0(t/\mu) t\rho(t) dt$$

$$+ C_2 \int_r^{R_2} K_0(t/\mu) I_0(r/\mu) t\rho(t) dt. \qquad (4.6b)$$

Next we wish to show that both $\Phi_1(r,\mu)$ and $\Phi_2(r,\mu)$ obey the same

integro-differential equation, Eq. (3.10d), obeyed by the pseudo neutron

distribution function in the bare core solution. Toward this end we

take the first derivative of $\Phi_1(r,\mu)$ and $\Phi_2(r,\mu)$ by using the relations

$K_0'(z) = -K_1(z)$ and $I_0'(z) = I_1(z)$, and Leibnitz's rule to obtain

$$\frac{\partial \Phi_1(r,\mu)}{\partial r} = - \frac{C_1}{\mu} \int_0^r K_1(r/\mu)I_0(t/\mu)t\rho(t)dt$$

$$+ \frac{C_1}{\mu} \int_r^{R_1} K_0(t/\mu)I_1(r/\mu)t\rho(t)dt$$

$$+ \frac{C_2}{\mu} \int_{R_1}^{R_2} K_0(t/\mu)I_1(r/\mu)t\rho(t)dt, \qquad (4.7a)$$

and

$$\frac{\partial \Phi_2(r,\mu)}{\partial r} = - \frac{C_1}{\mu} \int_0^{R_1} K_1(r/\mu)I_0(t/\mu)t\rho(t)dt$$

$$- \frac{C_2}{\mu} \int_{R_1}^r K_1(r/\mu)I_0(t/\mu)t\rho(t)dt$$

$$+ \frac{C_2}{\mu} \int_r^{R_2} K_0(t/\mu)I_1(r/\mu)t\rho(t)dt. \qquad (4.7b)$$

We find the second derivatives by continuing the above procedure,

using the additional relations

$$I_1'(z) = I_0(z) - \frac{1}{z} I_1(z), \quad K_1'(z) = - K_0(z) - \frac{1}{z} K_1(z)$$

and applying the Wronskin for the modified Bessel functions

$$K_0(z)I_1(z) + K_1(z)I_0(z) = 1/z$$

to obtain

$$\frac{\partial^2 \Phi_1(r,\mu)}{\partial r^2} = \frac{C_1}{\mu^2} \int_0^r \left[K_0(r/\mu) + \frac{\mu}{r} K_1(r/\mu) \right] I_0(t/\mu) t\rho(t) dt$$

$$+ \frac{C_1}{\mu^2} \int_r^{R_1} K_0(t/\mu) \left[I_0(r/\mu) - \frac{\mu}{r} I_1(r/\mu) \right] t\rho(t) dt$$

$$+ \frac{C_2}{\mu^2} \int_{R_1}^{R_2} K_0(t/\mu) \left[I_0(r/\mu) - \frac{\mu}{r} I_1(r/\mu) \right] t\rho(t) dt - C_1\rho_1(r)$$

$$(4.8a)$$

and

$$\frac{\partial^2 \Phi_2(r,\mu)}{\partial r^2} = \frac{C_1}{\mu^2} \int_0^{R_1} \left[K_0(r/\mu) + \frac{\mu}{r} K_1(r/\mu) \right] I_0(t/\mu) t\rho(t) dt$$

$$+ \frac{C_2}{\mu^2} \int_{R_1}^r \left[K_0(r/\mu) + \frac{\mu}{r} K_1(r/\mu) \right] I_0(t/\mu) t\rho(t) dt$$

$$+ \frac{C_2}{\mu^2} \int_r^{R_2} K_0(t/\mu) \left[I_0(r/\mu) - \frac{\mu}{r} I_1(r/\mu) \right] t\rho(t) dt - C_2\rho_2(r)$$

$$(4.8b)$$

Now substituting from Eqs. (4.6a), (4.7a), and (4.8a), we form the equation

$$\frac{\partial^2 \Phi_1(r,\mu)}{\partial r^2} + \frac{1}{r} \frac{\partial \Phi_1(r,\mu)}{\partial r} - \frac{1}{\mu^2} \Phi_1(r,\mu)$$

$$= \frac{C_1}{\mu^2} \int_0^r \left[K_0(r/\mu) + \frac{\mu}{r} K_1(r/\mu) \right] I_0(t/\mu) t\rho(t) dt + \frac{C_1}{\mu^2} \int_r^{R_1} K_0(t/\mu) \left[I_0(r/\mu) \right.$$

$$\left. - \frac{\mu}{r} I_1(r/\mu) \right] t\rho(t) dt + \frac{C_2}{\mu^2} \int_{R_1}^{R_2} K_0(t/\mu) \left[I_0(r/\mu) - \frac{\mu}{r} I_1(r/\mu) \right] t\rho(t) dt$$

$$- C_1\rho_1(r) - \frac{C_1}{r\mu} \int_0^r K_1(r/\mu) I_0(t/\mu) t\rho(t) dt + \frac{C_1}{r\mu} \int_r^{R_1} K_0(t/\mu) I_1(r/\mu) t\rho(t) dt$$

$$+ \frac{C_2}{r\mu} \int_{R_1}^{R_2} K_0(t/\mu) I_1(r/\mu) t\rho(t) dt - \frac{C_1}{\mu^2} \int_0^r K_0(r/\mu) I_0(t/\mu) t\rho(t) dt -$$

$$- \frac{C_1}{\mu^2} \int_r^{R_1} K_o(t/\mu) I_o(r/\mu) t\rho(t) dt$$

$$- \frac{C_2}{\mu^2} \int_{R_1}^{R_2} K_o(t/\mu) I_o(r/\mu) t\rho(t) dt. \tag{4.9a}$$

Upon cancellation of like terms in the right hand side of Eq. (4.9a) and the substitution of Eq. (4.5a) for $\rho_1(r)$, Eq. (4.9a) becomes

$$\frac{\partial^2 \Phi_1(r,\mu)}{\partial r^2} + \frac{1}{r} \frac{\partial \Phi_1(r,\mu)}{\partial r} - \frac{1}{\mu^2} \Phi_1(r,\mu) = -C_1 \int_0^1 \frac{\Phi_1(r,\mu')}{\mu'^2} d\mu, \tag{4.9b}$$

which is identical in form to Eq. (3.10d). Now substituting from Eqs. (4.6b), (4.7b), and (4.8b), we form the equation

$$\frac{\partial^2 \Phi_2(r,\mu)}{\partial r^2} + \frac{1}{r} \frac{\partial \Phi_2(r,\mu)}{\partial r} - \frac{1}{\mu^2} \Phi_2(r,\mu)$$

$$= \frac{C_1}{\mu^2} \int_0^{R_1} \left[K_o(r/\mu) + \frac{\mu}{r} K_1(r/\mu) \right] I_o(t/\mu) t\rho(t) dt + \frac{C_2}{\mu^2} \int_{R_1}^r \left[K_o(r/\mu) \right.$$

$$\left. + \frac{\mu}{r} K_1(r/\mu) \right] I_o(t/\mu) t\rho(t) dt + \frac{C_2}{\mu^2} \int_r^{R_2} K_o(t/\mu) \left[I_o(r/\mu) \right.$$

$$\left. - \frac{\mu}{r} I_1(r/\mu) \right] t\rho(t) dt - c_2 \rho_2(r) - \frac{C_1}{r\mu} \int_0^{R_1} K_1(r/\mu) I_o(t/\mu) t\rho(t) dt$$

$$- \frac{C_2}{r\mu} \int_{R_1}^r K_1(r/\mu) I_o(t/\mu) t\rho(t) dt + \frac{C_2}{r\mu} \int_r^{R_2} K_o(t/\mu) I_1(r/\mu) t\rho(t) dt$$

$$- \frac{C_1}{\mu^2} \int_0^{R_1} K_o(r/\mu) I_o(t/\mu) t\rho(t) dt - \frac{C_2}{\mu^2} \int_{R_1}^r K_o(r/\mu) I_o(t/\mu) t\rho(t) dt$$

$$- \frac{C_2}{\mu^2} \int_r^{R_2} K_o(t/\mu) I_o(r/\mu) t\rho(t) dt. \tag{4.10a}$$

Upon cancellation of like terms in the right hand side of Eq. (4.10a) and the substitution of Eq. (4.5b) for $\rho_2(r)$, Eq. (4.10a) becomes

$$\frac{\partial^2 \Phi_2(r,\mu)}{\partial r^2} + \frac{1}{r}\frac{\partial \Phi_2(r,\mu)}{\partial r} - \frac{1}{\mu^2}\Phi_2(r,\mu) = -C_2 \int_0^1 \frac{\Phi_2(r,\mu')}{\mu'^2}d\mu', \qquad (4.10b)$$

which is identical in form to Eqs. (4.9b) and (3.10d).

Having established that $\Phi_1(r,\mu)$ and $\Phi_2(r,\mu)$ obey the same integro-differential equation that arises for $\Phi(r,\mu)$ in the bare core solution, we now wish to determine the boundary conditions satisfied by $\Phi_1(r,\mu)$ and $\Phi_2(r,\mu)$. Inspection of $\Phi_1(r,\mu)$ as defined in Eq. (4.6a) at the core centerline, $r = 0$, with the consideration that $I_0(0) = 1$, and that the limit of $tK_0(t/\mu) = 0$ as $t \to 0$, establishes the boundary condition:

$$\Phi_1(0,\mu) \text{ finite.} \qquad (4.11)$$

Next we evaluate $\Phi_1(r,\mu)$ and $\Phi_2(r,\mu)$ as defined in Eqs. (4.6a,b) at the core-reflector interface, $r = R_1$, obtaining

$$\Phi_1(R_1,\mu) = C_1 \int_0^{R_1} K_0(R_1/\mu)I_0(t/\mu)t\rho(t)dt + C_2 \int_{R_1}^{R_2} K_0(t/\mu)I_0(R_1/\mu)t\rho(t)dt,$$

$$\qquad (4.12a)$$

and

$$\Phi_2(R_1,\mu) = C_1 \int_0^{R_1} K_0(R_1/\mu)I_0(t/\mu)t\rho(t)dt + C_2 \int_{R_1}^{R_2} K_0(t/\mu)I_0(R_1/\mu)t\rho(t)dt.$$

$$\qquad (4.12b)$$

Comparison of Eqs. (4.12 a and b) yields one interface boundary condition as

$$\Phi_1(R_1,\mu) = \Phi_2(R_1,\mu). \qquad (4.13)$$

A second interface boundary condition is established by evaluating the first derivative terms, Eqs. (4.7a and b) at $r = R_1$, obtaining

$$\frac{\delta \Phi_1(r,\mu)}{\delta r} \Bigg|_{r = R_1} = -\frac{C_1}{\mu} \int_0^{R_1} K_1(R_1/\mu) I_0(t/\mu) t \rho(t) dt + \frac{C_2}{\mu} \int_{R_1}^{R_2} K_0(t/\mu) I_1(R_1/\mu) t \rho(t) dt$$

(4.14a)

and

$$\frac{\delta \Phi_2(r,\mu)}{\delta r} \Bigg|_{r = R_1} = -\frac{C_1}{\mu} \int_0^{R_1} K_1(R_1/\mu) I_0(t/\mu) t \rho(t) dt + \frac{C_2}{\mu} \int_{R_1}^{R_2} K_0(t/\mu) I_1(R_1/\mu) t \rho(t) dt$$

(4.14b)

Comparison of Eqs. (4.14a & b) yields the second interface boundary condition as

$$\frac{\delta \Phi_1(r,\mu)}{\delta r} \Bigg|_{r = R_1} = \frac{\delta \Phi_2(r,\mu)}{\delta r} \Bigg|_{r = R_1}$$

(4.15)

It is interesting to note that the result of operating on boundary condition (4.13) by Eqs. (4.5a, b), thereby converting to the neutron density, is the familiar continuity of scalar flux across the interface boundary which is used in neutron diffusion theory solutions. The result of performing the same operation on boundary condition (4.15) is equivalent to the continuity of the neutron current. This equivalence is dependent on identical diffusion coefficients in each region which holds here due to the identical total cross sections and isotropic scattering in the postulated two-region model.

A fourth boundary condition is sought at the outer reflector boundary, $r = R_2$. First we evaluate $\Phi_2(r,\mu)$, Eq. (4.6b), and its first derivative, Eq. (4.7b), at the outer boundary, obtaining

$$\Phi_2(R_2,\mu) = C_1 \int_0^{R_1} K_0(R_2/\mu)I_0(t/\mu)t\rho(t)dt + C_2 \int_{R_1}^{R_2} K_0(R_2/\mu)I_0(t/\mu)t\rho(t)dt,$$

(4.16a)

and

$$\frac{\partial\Phi_2(r,\mu)}{\partial r}\bigg|_{r=R_2} = \frac{-C_1}{\mu} \int_0^{R_1} K_1(R_2/\mu)I_0(t/\mu)t\rho(t)dt - \frac{C_2}{\mu} \int_{R_1}^{R_2} K_1(R_2/\mu)I_0(t/\mu)t\rho(t)dt.$$

(4.16b)

Inspection of Eqs. (4.16a,b) as combined below establishes the outer

boundary condition as

$$K_0(R_2/\mu) \frac{\partial\Phi_2(r,\mu)}{\partial r}\bigg|_{r=R_2} + \frac{K_1(R_2/\mu)}{\mu} \Phi(R_2,\mu) = 0,$$

(4.17)

which corresponds to Eq. (3.11d) in the bare core solution.

In summary, we have developed two pseudo neutron distribution

functions given by Eqs. (4.6a,b) and have shown that they obey the

same integro-differential equation, Eqs. (4.9b), (4.10b). Also we

have established four boundary conditions, Eqs. (4.11), (4.13), (4.15),

(4.17), satisfied by the pseudo neutron distribution functions.

4.3 Singular Eigenfunction Expansion and Solution

Since it was shown in the previous section that both $\Phi_1(r,\mu)$

and $\Phi_2(r,\mu)$ obey integro-differential equations of the same form as

Eq. (3.10d) in the bare core solution, the general solution for

$\Phi_1(r,\mu)$ and $\Phi_2(r,\mu)$ corresponds to the form of Eq. (3.21) which we

write here as

$$\Phi_\ell(r,\mu) = \left[\alpha_{o\ell}I_0(r/\nu_{o\ell}) + \beta_{o\ell}K_0(r/\nu_{o\ell})\right]\mu^2\eta_{o\ell}(\mu)$$

$$\ell = 1,2$$

$$+ \int_0^1 \left[\alpha_{\ell\nu}I_0(r/\nu) + \beta_{\ell\nu}K_0(r/\nu)\right]\mu^2\eta_{\ell\nu}(\mu)d\nu$$

(4.18)

where $\eta_{o\ell}(\mu)$ and $\eta_{\ell\nu}(\mu)$ are given by Eqs. (3.19) and (3.20), respectively. Two additional aspects of the bare core solution are present here for the pseudo neutron distribution function in the core region. One is that ν_{o1} will again be imaginary, giving rise to regular Bessel functions, and the second is that the centerline boundary condition, Eq. (4.11), is identical to the bare core centerline boundary condition, Eq. (3.11a). Therefore, Eq. (4.18) for $\Phi_1(r,\mu)$ reduces to the form of Eq. (3.22) which we write here as

$$\Phi_1(r,\mu) = b_o J_o(r/|\nu_{o1}|)\mu^2\eta_{o1}(\mu) + \int_o^1 B(\nu)I_o(r/\nu)\mu^2\eta_{1\nu}(\mu)d\nu \ . \quad (4.19)$$

Adopting more specific symbols for the coefficients in the reflector region, we write Eq. (4.18) for $\Phi_2(r,\mu)$ as

$$\Phi_2(r,\mu) = \left[a_o I_o(r/\nu_{o2}) + d_o K_o(r/\nu_{o2})\right]\mu^2\eta_{o2}(\mu)$$

$$+ \int_o^1 \left[A(\nu)I_o(r/\nu) + D(\nu)K_o(r/\nu)\right]\mu^2\eta_{2\nu}(\mu)\,d\nu. \quad (4.20)$$

The coefficients in Eqs. (4.19) and (4.20) will be obtained from the following iterative procedure:

1. $B(\nu)$ is initially taken to be zero.

2. b_o is an arbitrary constant corresponding indirectly to the power level which we set equal to unity.

At the core-reflector interface we obtain

3. a_o as a function of discrete terms and $B(\nu)$.

4. d_o as a function of discrete terms, a_o, and $B(\nu)$.

5. $D(\nu)$ as a function of discrete terms and $B(\nu)$.

At the outer boundary we obtain

6. an inner iterative sequence for $A(\nu)$ depending

on a_o, d_o, and $D(\nu)$. This sequence provides

the criticality condition.

At the core-reflector interface we obtain

7. $B(\nu)$ as a function of a_o, d_o, $A(\nu)$, and $D(\nu)$,

completing the iterative sequence.

To effect steps 3 through 7 of the iterative solution, extensive use will be made of the orthogonality and normalization relations for the pseudo eigenfunctions developed in Appendix A. Another useful equation which relates the continuum eigenfunctions in different regions is written as

$$\eta_{j\nu}(\mu) = \frac{C_j}{C_i}\,\eta_{i\nu}(\mu) + \left(\frac{C_i - C_j}{C_i}\right)\delta(\nu - \mu). \tag{4.21a}$$

To verify Eq. (4.21a), we substitute Eq. (3.20) for $\eta_{i\nu}(\mu)$ obtaining

$$\eta_{j\nu}(\mu) = \frac{C_j}{C_i}\left\{C_i P\,\frac{\nu^2}{\nu^2 - \mu^2} + \left[1 - C_i P \int_0^1 \frac{\nu^2}{\nu^2 - \mu^2}\,d\mu\right]\delta(\nu - \mu)\right\}$$
$$+ \delta(\nu - \mu) - \frac{C_j}{C_i}\,\delta(\nu - \mu) \tag{4.21b}$$

where we have substituted Eq. (2.15) for $\lambda_i(\nu)$. Canceling the like terms on the right hand side of Eq. (4.21b) we have

$$\eta_{j\nu}(\mu) = C_j P\,\frac{\nu^2}{\nu^2 - \mu^2} + \lambda_j(\nu)\delta(\nu - \mu), \tag{4.21c}$$

which establishes Eq. (4.21a).

Proceeding with the solution, we substitute Eqs. (4.19) and (4.20) into the interface boundary condition Eq. (4.13), obtaining

$$b_o J_o(R_1/|\nu_{o1}|)\mu^2\eta_{o1}(\mu) + \int_0^1 B(\nu)I_o(R_1/\nu)\mu^2\eta_{1\nu}(\mu)d\nu$$

$$= \left[a_o I_o(R_1/\nu_{o2}) + d_o K_o(R_1/\nu_{o2})\right]\mu^2\eta_{o2}(\mu)$$

$$+ \int_0^1\left[A(\nu)I_o(R_1/\nu) + D(\nu)K_o(R_1/\nu)\right]\mu^2\eta_{2\nu}(\mu)d\nu. \tag{4.22}$$

Next we operate on Eq. (4.22) with the integral of $\eta_{o2}(\mu)$ over μ to yield

$$b_o J_o(R_1/|\nu_{o1}|)\int_0^1 \mu^2\eta_{o1}(\mu)\eta_{o2}(\mu)d\mu$$

$$+ \int_0^1 d\nu B(\nu)I_o(R_1/\nu)\int_0^1\left\{\frac{C_1}{C_2}\eta_{2\nu}(\mu) + \left(\frac{C_2-C_1}{C_2}\right)\delta(\nu-\mu)\right\}\mu^2\eta_{o2}(\mu)d\mu$$

$$= \left[a_o I_o(R_1/\nu_{o2}) + d_o K_o(R_1/\nu_{o2})\right]\int_0^1 \mu^2\eta_{o2}(\mu)\eta_{o2}(\mu)d\mu$$

$$+ \int_0^1 d\nu\left[A(\nu)I_o(R_1/\nu) + D(\nu)K_o(R_1/\nu)\right]\int_0^1 \mu^2\eta_{2\nu}(\mu)\eta_{o2}(\mu)d\mu, \tag{4.23}$$

where we have substituted Eq. (4.21a) for $\eta_{1\nu}(\mu)$. Now we apply the orthogonality and normalization relations, Eqs. (A.6), (A.7) and (A.12), to reduce Eq. (4.23) to the form:

$$b_o J_o(R_1/|\nu_{o1}|)N_{o12} + \int_0^1 d\nu B(\nu)I_o(R_1/\nu)\left(\frac{C_2-C_1}{C_2}\right)\nu^2\eta_{o2}(\nu)$$

$$= \left[a_o I_o(R_1/\nu_{o2}) + d_o K_o(R_1/\nu_{o2})\right]N_{o2}. \tag{4.24}$$

At this point we accomplish step 4 of the iterative procedure by solving Eq. (4.24) for d_o in terms of the other variables, resulting in

$$d_o = \frac{1}{K_o(R_1/\nu_{o2})N_{o2}} \left[b_o J_o(R_1/|\nu_{o1}|)N_{o12} - a_o I_o(R_1/\nu_{o2})N_{o2} \right.$$

$$\left. + \int_0^1 d\nu B(\nu) I_o(R_1/\nu)\left(\frac{C_2 - C_1}{C_2}\right)\nu^2 \eta_{o2}(\nu) \right]. \quad (4.25)$$

To obtain another equation so as to isolate a_o, we turn to the second interface boundary condition Eq. (4.15) and substitute Eqs. (4.19) and (4.20), obtaining

$$\frac{-b_o}{|\nu_{o1}|} J_1(R_1/|\nu_{o1}|)\mu^2 \eta_{o1}(\mu) + \int_0^1 \frac{B(\nu)}{\nu} I_1(R_1/\nu)\mu^2 \eta_{1\nu}(\mu)d\nu$$

$$= \left[\frac{a_o}{\nu_{o2}} I_1(R_1/\nu_{o2}) - \frac{d_o}{\nu_{o2}} K_1(R_1/\nu_{o2}) \right]\mu^2 \eta_{o2}(\mu)$$

$$+ \int_0^1 \left[\frac{A(\nu)}{\nu} I_1(R_1/\nu) - \frac{D(\nu)}{\nu} K_1(R_1/\nu) \right] \mu^2 \eta_{2\nu}(\mu)d\nu. \quad (4.26)$$

Next we operate on Eq. (4.26) with the integral of $\eta_{o2}(\mu)$ over μ to yield

$$\frac{-b_o}{|\nu_{o1}|} J_1(R_1/|\nu_{o1}|)\int_0^1 \mu^2 \eta_{o2}(\mu)\eta_{o1}(\mu)d\mu$$

$$+ \int_0^1 d\nu \frac{B(\nu)}{\nu} I_1(R_1/\nu) \int_0^1 \left\{ \frac{C_1}{C_2} \eta_{2\nu}(\mu) + \left(\frac{C_2 - C_1}{C_2}\right) \delta(\nu - \mu) \right\}\mu^2 \eta_{o2}(\mu)d\mu$$

$$= \left[\frac{a_o}{\nu_{o2}} I_1(R_1/\nu_{o2}) - \frac{d_o}{\nu_{o2}} K_1(R_1/\nu_{o2}) \right] \int_0^1 \mu^2 \eta_{o2}(\mu)\eta_{o2}(\mu)d\mu$$

$$+ \int_0^1 d\nu \left[\frac{A(\nu)}{\nu} I_1(R_1/\nu) - \frac{D(\nu)}{\nu} K_1(R_1/\nu) \right] \int_0^1 \mu^2 \eta_{2\nu}(\mu)\eta_{o2}(\mu)d\mu, \quad (4.27)$$

where we have substituted Eq. (4.21a) for $\eta_{1\nu}(\mu)$. Now we apply the orthogonality and normalization relations, Eqs. (A.6), (A.7), and (A.12), to reduce Eq. (4.27) to the form:

$$\frac{-b_o}{|\nu_{o1}|} J_1(R_1/|\nu_{o1}|)N_{o12} + \int_0^1 d\nu \frac{B(\nu)}{\nu} I_1(R_1/\nu)\left(\frac{C_2 - C_1}{C_2}\right)\nu^2\eta_{o2}(\nu)$$

$$= \left[\frac{a_o}{\nu_{o2}} I_1(R_1/\nu_{o2}) - \frac{d_o}{\nu_{o2}} K_1(R_1/\nu_{o2})\right]N_{o2}. \tag{4.28}$$

Now, with Eqs. (4.24) and (4.28), we algebraically eliminate d_o and, after substituting the Wronskian for the modified Bessel functions, obtain the equation for a_o required in step 3 as

$$a_o = \frac{R_1}{N_{o2}}\left\{b_o\left[\frac{J_o(R_1/|\nu_{o1}|)K_1(R_1/\nu_{o2})}{\nu_{o2}} - \frac{J_1(R_1/|\nu_{o1}|)K_o(R_1/\nu_{o2})}{|\nu_{o1}|}\right] N_{o12}\right.$$

$$\left. + \left(\frac{C_2 - C_1}{C_2}\right)\int_0^1 d\nu B(\nu)\left[\frac{I_o(R_1/\nu)K_1(R_1/\nu_{o2})}{\nu_{o2}} + \frac{I_1(R_1/\nu)K_o(R_1/\nu_{o2})}{\nu}\right]\nu^2\eta_{o2}(\nu)\right\}. \tag{4.29}$$

To develop the equation for $D(\nu)$ as required in step 5, we return to Eq. (4.22), operate with the integral of $\eta_{2\nu'}(\mu)$ over μ, and thereby obtain

$$b_o J_o(R_1/|\nu_{o1}|) \int_0^1 \mu^2\eta_{o1}(\mu)\left\{\frac{C_2}{C_1} \eta_{1\nu'}(\mu) + \left(\frac{C_1 - C_2}{C_1}\right) \delta(\nu' - \mu)\right\}d\mu$$

$$+ \int_0^1 d\nu B(\nu)I_o(R_1/\nu) \int_0^1 \mu^2\eta_{1\nu}(\mu)\left\{\frac{C_2}{C_1} \eta_{1\nu'}(\mu) + \left(\frac{C_1 - C_2}{C_1}\right) \delta(\nu' - \mu)\right\}d\mu$$

$$= \left[a_o I_o(R_1/\nu_{o2}) + d_o K_o(R_1/\nu_{o2})\right] \int_0^1 \mu^2\eta_{o2}(\mu)\eta_{2\nu'}(\mu)d\mu$$

$$+ \int_0^1 d\nu\left[A(\nu)I_o(R_1/\nu) + D(\nu)K_o(R_1/\nu)\right] \int_0^1 \mu^2\eta_{2\nu}(\mu)\eta_{2\nu'}(\mu)d\mu \tag{4.30}$$

where on the left hand side we have substituted Eq. (4.21a) for $\eta_{2\nu'}(\mu)$. Now we apply the orthogonality and normalization relations, Eqs. (A.6) and (A.21), to reduce Eq. (4.30) to the form:

$$b_o J_o(R_1/|\nu_{o1}|)\left(\frac{C_1 - C_2}{C_1}\right)\nu'^2 \eta_{o1}(\nu') + B(\nu')I_o(R_1/\nu')\frac{C_2}{C_1}N_1(\nu')$$

$$+ \int_0^1 d\nu B(\nu)I_o(R_1/\nu)\left(\frac{C_1 - C_2}{C_1}\right)\nu'^2 \eta_{1\nu}(\nu')$$

$$= \left[A(\nu')I_o(R_1/\nu') + D(\nu')K_o(R_1/\nu_1)\right]N_2(\nu'). \tag{4.31}$$

Now returning to Eq. (4.26), we again operate with the integral of $\eta_{2\nu'}(\mu)$ over μ to obtain

$$\frac{-b_o}{|\nu_{o1}|} J_1(R_1/|\nu_{o1}|)\int_0^1 \mu^2 \eta_{o1}(\mu)\left\{\frac{C_2}{C_1}\eta_{1\nu'}(\mu) + \left(\frac{C_1 - C_2}{C_1}\right)\delta(\nu' - \mu)\right\}d\mu$$

$$+ \int_0^1 d\nu \frac{B(\nu)}{\nu} I_1(R_1/\nu)\int_0^1 \mu^2 \eta_{1\nu}(\mu)\left\{\frac{C_2}{C_1}\eta_{1\nu}(\mu) + \left(\frac{C_1 - C_2}{C_1}\right)\delta(\nu' - \mu)\right\}d\mu$$

$$= \left[\frac{a_o}{\nu_{o2}}I_1(R_1/\nu_{o2}) - \frac{d_o}{\nu_{o2}}K_1(R_1/\nu_{o2})\right]\int_0^1 \mu^2 \eta_{o2}(\mu)\eta_{2\nu'}(\mu)d\mu$$

$$+ \int_0^1 d\nu\left[\frac{A(\nu)}{\nu}I_1(R_1/\nu) - \frac{D(\nu)}{\nu}K_1(R_1/\nu)\right]\int_0^1 \mu^2 \eta_{2\nu}(\mu)\eta_{2\nu'}(\mu)d\mu, \tag{4.32}$$

where on the left hand side we have substituted Eq. (4.21a) for $\eta_{2\nu'}(\mu)$. Now we apply the orthogonality and normalization relations, Eqs. (A.6) and (A.21) to reduce Eq. (4.32) to the form:

$$\frac{-b_o}{|\nu_{o1}|} \, J_1(R_1/|\nu_{o1}|)\left(\frac{C_1 - C_2}{C_1}\right)\nu'^2\eta_{o1}(\nu') + \frac{B(\nu')}{\nu} \, I_1(R_1/\nu') \, \frac{C_2}{C_1} \, N_1(\nu')$$

$$+ \int_0^1 d\nu \, \frac{B(\nu)}{\nu} \, I_1(R_1/\nu)\left(\frac{C_1 - C_2}{C_1}\right)\nu'^2\eta_{1\nu}(\nu')$$

$$= \left[\frac{A(\nu')}{\nu'} \, I_1(R_1/\nu') - \frac{D(\nu')}{\nu'} \, K_1(R_1/\nu')\right] N_2(\nu'). \tag{4.33}$$

Now, with Eqs. (4.31) and (4.33) we algebraically eliminate $A(\nu)$ and, after substituting the Wronskian for the modified Bessel functions, obtain the equation for $D(\nu)$ required in step 5 as

$$D(\nu') = \frac{R_1}{N_2(\nu')} \left\{ b_o\left(\frac{C_1 - C_2}{C_1}\right)\nu'^2\eta_{o1}(\nu')\left[\frac{J_o(R_1/|\nu_{o1}|)I_1(R_1/\nu')}{\nu'}\right.\right.$$

$$+ \left.\frac{J_1(R_1/|\nu_{o1}|)I_o(R_1/\nu')}{|\nu_{o1}|}\right] + \left(\frac{C_1 - C_2}{C_1}\right)\int_0^1 d\nu B(\nu)\nu'^2\eta_{1\nu}(\nu')\left[\frac{I_o(R_1/\nu)I_1(R_1/\nu')}{\nu'}\right.$$

$$- \left.\left.\frac{I_1(R_1/\nu)I_o(R_1/\nu')}{\nu}\right]\right\}. \tag{4.34}$$

Substituting Eq. (3.20) for $\eta_{1\nu}(\nu')$ in Eq. (4.34) and evaluating the delta function leaves the indeterminate form

$$F(\nu,\nu') = \frac{1}{\nu^2 - \nu'^2}\left[\frac{I_o(R_1/\nu)I_1(R_1/\nu')}{\nu'} - \frac{I_1(R_1/\nu)I_o(R_1/\nu')}{\nu}\right].$$

The function is evaluated by L'Hospital's rule to be

$$F(\nu,\nu) = \frac{R_1}{2\nu^4}\left[I_o(R_1/\nu)I_o(R_1/\nu) - I_1(R_1/\nu)I_1(R_1/\nu)\right]. \tag{4.36}$$

To accomplish step 6 of the iterative procedure, we turn to the outer boundary condition, Eq. (4.17), and substitute Eq. (4.20) along with its derivative for the pseudo neutron distribution function in the reflector to obtain

$$\left\{ \frac{K_0(R_2/\mu)I_1(R_2/\nu_{02})}{\nu_{02}} + \frac{K_1(R_2/\mu)I_0(R_2/\nu_{02})}{\mu} \right\} a_0 \mu^2 \eta_{02}(\mu)$$

$$+ \left\{ \frac{K_1(R_2/\mu)K_0(R_2/\nu_{02})}{\mu} - \frac{K_0(R_2/\mu)K_1(R_2/\nu_{02})}{\nu_{02}} \right\} d_0 \mu^2 \eta_{02}(\mu)$$

$$+ \int_0^1 \left\{ \frac{K_0(R_2/\mu)I_1(R_2/\nu)}{\nu} + \frac{K_1(R_2/\mu)I_0(R_2/\nu)}{\mu} \right\} A(\nu)\mu^2 \eta_{2\nu}(\mu)d\nu$$

$$+ \int_0^1 \left\{ \frac{K_1(R_2/\mu)K_0(R_2/\nu)}{\mu} - \frac{K_0(R_2/\mu)K_1(R_2/\nu)}{\nu} \right\} D(\nu)\mu^2 \eta_{2\nu}(\mu)d\nu = 0. \quad (4.36)$$

Separation of Eq. (4.36) into singular and nonsingular parts follows directly as in Eqs. (3.23) through (3.27c) in the bare core solution. The result of this procedure on Eq. (4.36) is

$$\int_0^1 A'(\nu)\eta_{2\nu}(\mu)d\nu = \Phi'(\mu), \quad (4.37)$$

where

$$\Phi'(\mu) = -R_2 I_0(R_2/\mu) \left\{ \left[\frac{K_0(R_2/\mu)I_1(R_2/\nu_{02})}{\nu_{02}} + \frac{K_1(R_2/\mu)I_0(R_2/\nu_{02})}{\mu} \right] a_0 \eta_{02}(\mu) \right.$$

$$+ \left[\frac{K_1(R_2/\mu)K_0(R_2/\nu_{02})}{\mu} - \frac{K_0(R_2/\mu)K_1(R_2/\nu_{02})}{\nu_{02}} \right] d_0 \eta_{02}(\mu)$$

$$\left. + \int_0^1 \left[\frac{K_1(R_2/\mu)K_0(R_2/\nu)}{\mu} - \frac{K_0(R_2/\mu)K_1(R_2/\nu)}{\nu} \right] D(\nu)\eta_{2\nu}(\mu)d\nu \right\}$$

$$- C_2 \int_0^1 \frac{A'(\nu)\nu^2 H(\nu,\mu)}{\nu+\mu} d\nu,$$

$A'(\nu) = A(\nu)I_o(R/\nu)$, and $H(\nu,\mu)$ is defined in Eq. (3.25b). To demonstrate that $\Phi'(\mu)$ is indeed nonsingular, we further reduce the integral containing $D(\nu)$ by substituting Eq. (3.20) for $\eta_{2\nu}(\mu)$ and immediately evaluate the delta function to obtain

$$\int_o^1 \left[\frac{K_1(R_2/\mu)K_0(R_2/\nu)}{\mu} - \frac{K_0(R_2/\mu)K_1(R_2/\nu)}{\nu}\right] \frac{D(\nu)C_2}{\nu^2-\mu^2} \nu^2 d\nu.$$

Next we extract the indeterminate portion of the above integral and define it as

$$F(\nu,\mu) = \frac{1}{\nu^2-\mu^2} \left[\frac{K_1(R_2/\mu)K_0(R_2/\nu)}{\nu} - \frac{K_0(R_2/\mu)K_1(R_2/\mu)}{\nu}\right]. \qquad (4.38)$$

Finally, we apply L'Hospital's rule to Eq. (4.38) for $F(\nu,\mu)$ to obtain

$$F(\nu,\nu) = \frac{R_2}{2\nu^4} \left[K_1(R_2/\nu)K_1(R_2/\nu) - K_0(R_2/\nu)K_0(R_2/\nu)\right]. \qquad (4.39)$$

With the above demonstration and recalling that $H(\nu,\nu)$, Eq. (3.25c), is a bounded finite function, we have successfully demonstrated that $\Phi'(\mu)$, as defined above, is a nonsingular function.

Now the inner iterative sequence for $A'(\nu)$ required in step 6 can be constructed in a manner closely analogous to that of the bare core solution, Eqs. (3.27a) through (3.29). The associated discussion concerning the completeness theorem proof giving rise to a free expression for $A'(\nu)$ and the criticality condition carries over directly. Successive approximations for $A'(\nu)$ are constructed by the following iteration scheme:

$$A_o'(\nu) = 0 \qquad (4.40a)$$

$$\Phi_o'(\mu) = -R_2 I_o(R_2/\mu)\left\{\left[\frac{K_o(R_2/\mu)I_1(R_2/\nu_{o2})}{\nu_{o2}} + \frac{K_1(R_2/\mu)I_o(R_2/\nu_{o2})}{\mu}\right] a_o \eta_{o2}(\mu)\right.$$

$$+ \left[\frac{K_1(R_2/\mu)K_o(R_2/\nu_{o2})}{\mu} - \frac{K_o(R_2/\mu)K_1(R_2/\nu_{o2})}{\nu_{o2}}\right] d_o \eta_{o2}(\mu)$$

$$\left. + \int_o^1 \left[\frac{K_1(R_2/\mu)K_o(R_2/\nu)}{\mu} - \frac{K_o(R_2/\mu)K_1(R_2/\nu)}{\nu}\right] D(\nu)\eta_{2\nu}(\mu)d\nu\right\} \qquad (4.40b)$$

$$A_{n+1}'(\nu) = \frac{1}{N_2(\nu)} \int_o^1 \mu^2 \eta_{2\nu}(\mu)\Phi_n'(\mu)d\mu \qquad (4.40c)$$

$$\Phi_{n+1}'(\mu) = \Phi_o'(\mu) - C_2 \int_o^1 \frac{A_{n+1}'(\nu)H(\nu,\mu)\nu^2}{\nu+\mu} d\nu \qquad (4.40d)$$

$$C_2 \int_o^1 \frac{\mu^2 \Phi'(\mu)}{\mu^2 - \nu_{o2}^2} d\mu = 0 \qquad (4.40e)$$

Eqs. (4.40a) through (4.40d) represent the inner iterative sequence for $A'(\nu)$. The criticality condition, Eq. (4.40e), is checked after convergence of the outer iterative sequence for a_o, d_o, $D(\nu)$ and $B(\nu)$ and after a simultaneous convergence of the inner iterative sequence for $A(\nu)$. Among the solutions for two-region problems, this solution is unusual in that the criticality condition is developed at the outer reflector boundary.

The remaining portion of the solution is to develop the equation for $B(\nu)$ as required in step 7. Toward this end, we return to Eq. (4.22) and operate with the integral of $\eta_{1\nu'}(\mu)$ over μ to obtain

$$b_o J_o(R_1/|\nu_{o1}|) \int_o^1 \mu^2 \eta_{o1}(\mu) \eta_{1\nu'}(\mu) d\mu + \int_o^1 d\nu B(\nu) I_o(R_1/\nu) \int_o^1 \mu^2 \eta_{1\nu}(\mu) \eta_{1\nu'}(\mu) d\mu$$

$$= \left[a_o I_o(R_1/\nu_{o2}) + d_o K_o(R_1/\nu_{o2}) \right] \int_o^1 \mu^2 \eta_{o2}(\mu) \left\{ \frac{C_1}{C_2} \eta_{2\nu'}(\mu) + \left(\frac{C_2 - C_1}{C_2} \right) \delta(\nu' - \mu) \right\} d\mu$$

$$+ \int_o^1 d\nu \left[A(\nu) I_o(R_1/\nu) + D(\nu) K_o(R_1/\nu) \right] \int_o^1 \mu^2 \eta_{2\nu}(\mu) \left\{ \frac{C_1}{C_2} \eta_{2\nu'}(\mu) + \left(\frac{C_2 - C_1}{C_2} \right) \delta(\nu' - \mu) \right\} d\mu$$

$$\tag{4.41}$$

where we have substituted Eq. (4.21a) for $\eta_{1\nu'}(\mu)$ on the right hand
side of Eq. (4.41). Now we apply the orthogonality and normalization
relations, Eqs. (A.6) and (A.21) to reduce Eq. (4.31) to the form:

$$B(\nu') I_o(R_1/\nu') N_1(\nu') = \left[a_o I_o(R_1/\nu_{o2}) + d_o K_o(R_1/\nu_{o2}) \right] \left(\frac{C_2 - C_1}{C_2} \right) \nu'^2 \eta_{o2}(\nu')$$

$$+ \left[A(\nu') I_o(R_1/\nu') + D(\nu') K_o(R_1/\nu') \right] \frac{C_1}{C_2} N_2(\nu')$$

$$+ \int_o^1 d\nu \left[A(\nu) I_o(R_1/\nu) + D(\nu) K_o(R_1/\nu) \right] \left(\frac{C_2 - C_1}{C_2} \right) \nu'^2 \eta_{2\nu}(\nu'). \tag{4.42}$$

Rearrangement of Eq. (4.42) yields the required equation for $B(\nu)$ as

$$B(\nu') = \frac{1}{I_o(R_1/\nu') N_1(\nu')} \left\{ \left[a_o I_o(R_1/\nu_{o2}) + d_o K_o(R_1/\nu_{o2}) \right] \left(\frac{C_2 - C_1}{C_2} \right) \nu'^2 \eta_{o2}(\nu') \right.$$

$$+ \left[A(\nu') I_o(R_1/\nu') + D(\nu') K_o(R_1/\nu') \right] \frac{C_1}{C_2} N_2(\nu')$$

$$+ \left. \int_o^1 d\nu \left[A(\nu) I_o(R_1/\nu) + D(\nu) K_o(R_1/\nu) \right] \left(\frac{C_2 - C_1}{C_2} \right) \nu'^2 \eta_{2\nu}(\nu') \right\}. \tag{4.43}$$

We note that the integral term in Eq. (4.43) leads to a singularity.
The numerical evaluation of such singular integrals is discussed in
Chapter V.

Finally, we identify the various equations which appear in the iterative solution for the two-region problem previously outlined.

1. $B(\nu)$ is initially taken to be zero.

2. b_o is set equal to unity.

3. a_o from Eq. (4.29).

4. d_o from Eq. (4.25).

5. $D(\nu)$ from Eq. (4.34).

6. Inner iterative sequence for $A(\nu)$, Eqs. (4.40a) through (4.40d), criticality condition Eq. (4.40e).

7. $B(\nu)$ from Eq. (4.43).

Upon finding the critical core radius for given values of C_1, C_2, and the reflector thickness, the expansion coefficients can be used to calculate the neutron density distribution in each region from the equations:

$$\rho_1(r) = b_o J_o(r/|\nu_{o1}|) + \int_o^1 B(\nu)I_o(r/\nu)d\nu \qquad (4.45)$$

$$o \leq r \leq R_1$$

$$\rho_2(r) = a_o I_o(r/\nu_{o2}) + d_o K_o(r/\nu_{o2}) + \int_o^1 \left[A'(\nu) + D(\nu)K_o(r/\nu)\right]d\nu, \qquad (4.46)$$

$$R_1 \leq r \leq R_2$$

which we have obtained by operating on Eqs. (4.19) and (4.20) as indicated in Eqs. (4.5a and b) and applying the normalization of the pseudo eigenfunctions as in Eq. (3.16).

This completes the solution for the radially reflected critical cylinder. Numerical results are presented in Chapter V.

CHAPTER V

NUMERICAL METHODS AND RESULTS

5.1 Numerical Methods

In obtaining numerical results from the iterative solutions developed in Chapters III and IV, various parameters, functions, and operations appearing in the solutions were evaluated by the following methods:

1. The dispersion function for the discrete eigenvalues, which is the transcendental equation, Eq. (2.13), was solved by Newton's method.

2. The regular Bessel functions were calculated with a recurrence relationship.

3. The modified Bessel functions were calculated with a series expansion for the smaller arguments and by an asymptotic series for the larger arguments.

4. Singular integrals were treated by subtracting out the singularity, evaluating the resulting integral term by Gauss-Legendre quadrature and evaluating the derivative term by Lagrange interpolation.

5. Nonsingular integrals were evaluated by Gauss-Legendre quadrature.

Although these methods are generally well-known, for completeness we shall give a brief description of each method and make appropriate references.

For $c > 1$ the discrete eigenvalue as given by Eq. (2.13) is purely imaginary. The solutions developed in Chapters III and IV are formulated in terms of the magnitude of this imaginary eigenvalue. Therefore, we

use Newton's iteration scheme as

$$|\nu|_{i+1} = |\nu|_i - \frac{\Lambda(|\nu|_i)}{\Lambda'(|\nu|_i)},$$ (5.1)

(i=0,1,2,...)

where $\Lambda(|\nu|) = 1 - c|\nu| \tan^{-1}(1/|\nu|)$

and $\Lambda'(|\nu|) = c\left[|\nu|/(|\nu|^2+1) - \tan^{-1}(1/|\nu|)\right]$.

For $c < 1$ the discrete eigenvalue is real and we apply Newton's method as

$$\nu_{i+1} = \nu_i - \frac{\Lambda(\nu_i)}{\Lambda'(\nu_i)},$$ (5.2)

(i=0,1,2,...)

where $\Lambda(\nu) = 1 - \frac{c\nu}{2} \ln\left(\frac{\nu+1}{\nu-1}\right)$

and $\Lambda'(\nu) = \frac{c}{2}\left[2\nu/(\nu^2-1) - \ln\left(\frac{\nu+1}{\nu-1}\right)\right]$.

Initial estimates for $|\nu_0|$ are taken from Fig. 4. The iterative sequences, Eqs. (5.1) and (5.2), were run until the error in $|\nu_0|$ was less than 10^{-9}.

The recurrence relation used to calculate the regular Bessel functions is taken from Goldstein and Thaler.[13] The recurrence relation is

$$F_{n+1}(x) + F_{n-1}(x) = \left(\frac{2n}{x}\right) F_n(x).$$ (5.3)

The desired Bessel function is

$$J_n(x) = \frac{F_n(x)}{\alpha},$$ (5.4)

where $\alpha = F_0(x) + 2 \sum_{m=1}^{M-2} F_{2m}(x)$ (5.5)

and M is initialized at M_0.

M_0 is the greater of M_A and M_B where

$$M_A = \begin{cases} [x+6] & \text{if } x < 5 \\ [1.4x + 60/x] & \text{if } x \geq 5 \end{cases}$$ (5.6a)

and

$$M_B = [n + x/4 + 2]$$ (5.6b)
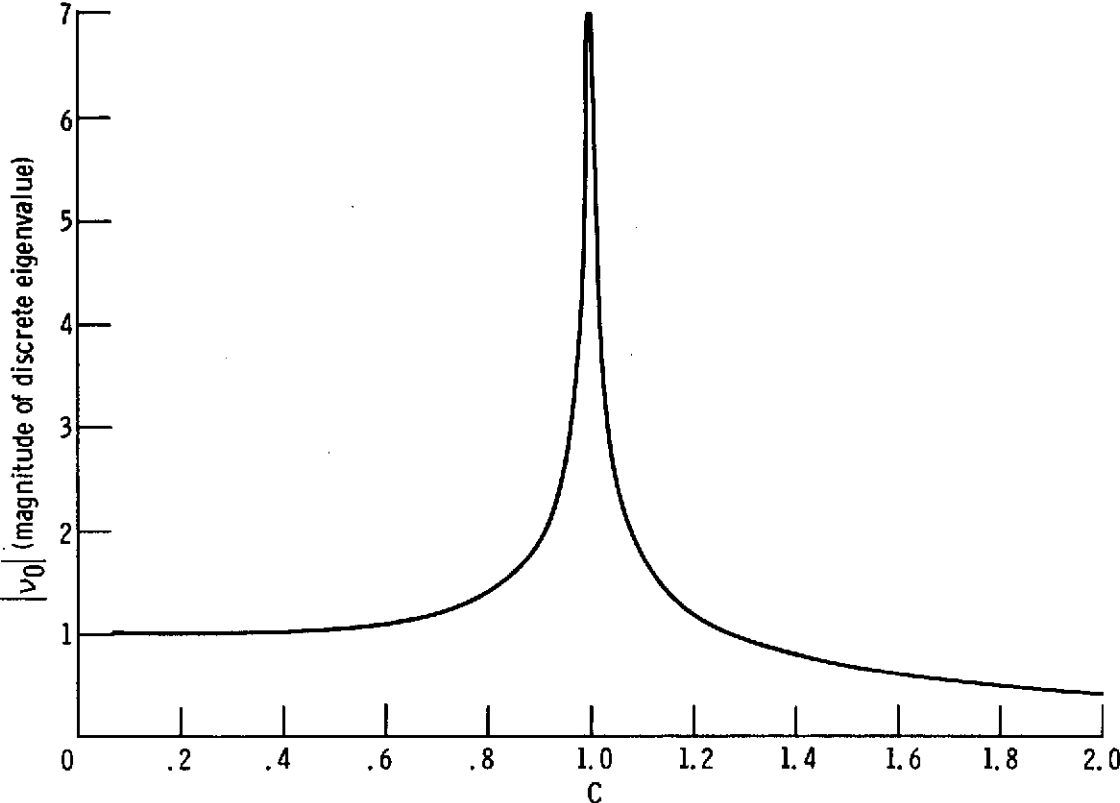
Figure 4. - Variation of the discrete eigenvalue for $0 \leq c \leq 2$. (Mean number of second-aries per collision).

Sequential values F_{M-2}, F_{M-3}, . . ., F_2, F_1, F_0 are evaluated using Eq. (5.3) with $F_M = 0$ and $F_{M-1} = 10^{-30}$. Values of α and $J_n(x)$ are then computed using Eqs. (5.5) and (5.4), respectively. The computation is repeated for $M + 3$ and the values of $J_n(x)$ for M and $M + 3$ are compared. If these values differ by less than 10^{-9}, the value of $J_n(x)$ is accepted. If the test fails, the computation is continued by adding 3 to M and using this as a new value of M.

The methods for calculating the modified Bessel functions are taken from Abramowitz and Stegun.[12] For values of the argument less than 8.5, we use the ascending series:

$$I_0(z) = 1 + \frac{\frac{1}{4} z^2}{(1!)^2} + \frac{(\frac{1}{4} z^2)^2}{(2!)^2} + \frac{(\frac{1}{4} z^2)^3}{(3!)^3} + \ldots, \tag{5.7}$$

and

$$K_0(z) = -[\ln(\tfrac{1}{2}z) + \gamma] \, I_0(z) + \frac{\frac{1}{4} z^2}{(1!)}$$
$$+ (1+\tfrac{1}{2}) \, \frac{(\frac{1}{4} z^2)^2}{(2!)^2} + (1+\tfrac{1}{2}+\tfrac{1}{3}) \, \frac{(\frac{1}{4} z^2)^3}{(3!)^3} + \ldots, \tag{5.8}$$

where γ is Euler's constant. The first order modified Bessel functions are calculated from the differentiated forms of Eqs. (5.7) and (5.8) according to

$$I_1(z) = I_0'(z), \tag{5.9a}$$

and

$$K_1(z) = -K_0'(z). \tag{5.9b}$$

The expansions were carried out to thirty terms or until a major under flow results from the calculation. For values of the argument greater than 8.5, we use the asymptotic series

$$I_n(z) \cong \frac{e^z}{\sqrt{2\pi z}} \left\{ 1 - \frac{\mu-1}{8z} + \frac{(\mu-1)(\mu-9)}{2!} \frac{}{(8z)^2} \right.$$

$$\left. - \frac{(\mu-1)(\mu-9)(\mu-25)}{3!} \frac{}{(8z)^3} + \ldots \right\}, \tag{5.10}$$

and

$$K_n(z) \cong \sqrt{\frac{\pi}{2z}} \; e^{-z} \left\{ 1 + \frac{\mu-1}{8z} + \frac{(\mu-1)(\mu-9)}{2!} \frac{}{(8z)^2} \right.$$

where $\mu = 4n^2$. $\qquad \left. + \frac{(\mu-1)(\mu-9)(\mu-25)}{3!} \frac{}{(8z)^3} + \ldots \right\}, \tag{5.11}$

The series were carried out to thirty-two terms.

Principal value integrals were treated by subtracting out the singularity as shown in Metcalf and Zweifel,[14]

$$P\int_0^1 \frac{F(\mu')d\mu'}{\mu'-\mu} = \int_0^1 \frac{[F(\mu') - F(\mu)] \, d\mu'}{\mu' - \mu} + F(\mu) \, \ell n\left(\frac{1-\mu}{\mu}\right), \tag{5.12}$$

and approximating the principal value by

$$P\int_0^1 \frac{F(\mu')d\mu'}{\mu'-\mu} \cong \sum_{\substack{j=1 \\ j\neq i}}^{M} W_j \left[\frac{F(\mu_j)-F(\mu_i)}{\mu_j-\mu_i} \right] + \frac{W_i \, dF(\mu)}{d\mu}\bigg|_{\mu=\mu_i} + F(\mu_i)\ell n\left(\frac{1-\mu_i}{\mu_i}\right), \tag{5.13}$$

where the singularity is at μ_i and the W's and μ's are the weight factors and abscissas of Gauss-Legendre quadrature adjusted to the half-range as shown below. The derivative term in Eq. (5.13) is evaluated by Lagrange's differentiation formula:

$$F'(\mu_i) = \sum_{k=0}^{M} \ell_k'(\mu_i)F(\mu_k) + R_M'(\mu_i), \tag{5.14}$$

where $\quad \ell_k'(\mu_i) = \sum_{\substack{j=0 \\ j\neq k}}^{M} \frac{\displaystyle\prod_{n=0}^{M}(\mu_i-\mu_n)}{(\mu_i-\mu_k)(\mu_i-\mu_j)\displaystyle\prod_{\substack{n=0 \\ n\neq k}}^{M}(\mu_k-\mu_n)}, \tag{5.15a}$

and $\quad R'_M (\mu_i) = \prod_{\substack{n=o \\ n \neq i}}^{M} (\mu_i - \mu_n) \; \frac{1}{(M+1)!} \; \left. \frac{d^{M+1}F(\mu)}{d\mu^{M+1}} \right|_{\mu=\xi, \; \mu_O \leq \xi \leq \mu_M}$. $\qquad$ (5.15b)

Using M Gauss-Legendre quadrature points, the error in calculating $F'(\mu_i)$ by Eq. (5.14) is proportional to the (M+1)th order derivative of the function as shown by Eq. (5.15b). At the beginning of the computer program, the coefficients $\ell'_k (\mu_i)$ are calculated by Eq. (5.15a) and stored. This procedure significantly simplifies the subsequent numerical evaluation of the principal value integrals in the iterative solutions.

Nonsingular integrals were evaluated by Gauss-Legendre quadrature over the half-range as

$$\int_o^1 F(\mu) \, d\mu = \sum_{i=1}^{M} w_i \, F(\mu_i),$$ $\qquad$ (5.16)

where $\quad \mu_i = (X_i + 1)/2,$

and $\quad w_i = W_i/2,$

X_i and W_i being the full-range Gauss-Legendre abscissas and weight factors listed in Abramowitz and Stegun.[12]

5.2 Numerical Precision

The objective in seeking numerical results from the iterative solutions of Chapters III and IV was to obtain critical dimensions accurate to a minimum of six significant figures. Results of this high precision can be used as input data for evaluating design analysis programs as is demonstrated in Chapter VI. Therefore, the computer programs used to obtain these results were written entirely in double precision. The calculations were performed on IBM-7094-II and CDC-6600 computers. A minimum of twelve significant figures were carried in

performing the calculations.

Where possible, comparisons were made between the results of methods described in section 5.1 and tabulated values in the literature. The discrete eigenvalues agreed with the seven-significant-figure values of Kowalska.[15] Sample values of the Bessel functions agreed with the tabulated values in Abramowitz and Stegun[12] to at least nine significant figures.

The bare and reflected core calculations were done over Gauss-Legendre quadratures of twenty-four and forty points respectively. The variation of the critical core radius with the number of Gauss-Legendre points is shown in Table I. It indicates that twenty-four Gauss-Legendre points are sufficient for seven significant accuracy in the bare core radii. The use of forty Gauss-Legendre points provides seven significant figure accuracy for the large reflected cores and six significant figure accuracy for the smaller configurations. This reflects the increasing importance of the continuum contribution and its integrated quantities in the solution for the smaller configurations.

At each trial value in the critical radii searches, the iterated quantities in the solutions were converged to nine significant figures before the criticality conditions were evaluated. The criticality conditions, Eqs. (3.29) and (4.40e), were considered satisfied when the value of the integral was less than 10^{-9}.

5.3 Bare Core Results

Critical radii calculated with the one-region cylinder solution of Chapter III, along with results of other analytic solutions found in the literature, are listed in Table II. Using the results of the present

TABLE I. -VARIATION OF CRITICAL CORE RADIUS WITH
THE NUMBER OF GAUSS-LEGENDRE QUADRATURE POINTS

Case Description			Number of Gauss-Legendre Points			
c_1	c_2	$R_2 - R_1$	8	24	40	96
1.02	Bare	----	9.0432542	9.0432547	9.0432547	--------
2.0	Bare	----	.66862087	.66861281	.66861285	--------
1.1	0.9	10.0	2.795180	2.795122	2.795120	2.795120
1.4	.85	1.0	1.141910	1.141755	1.141750	1.141748

TABLE II. - CRITICAL RADII IN MEAN FREE PATHS FOR BARE CYLINDERS

c	Present Solution	Carlson-Bell[16]	Hendry[17] F_3G_8	Hembd[18] IT_4
1.02	9.043255	9.0433	-----	9.04458
1.05	5.411288	5.4118	5.414	5.41152
1.1	3.577391	3.5783	-----	3.57744
1.2	2.287209	2.2884	-----	2.28724
1.4	1.396979	1.3973	-----	1.39699
1.6	1.020839	1.0209	-----	1.02085
1.8	0.807427	0.8067	-----	0.80743
2.0	0.668613	0.6673	0.670	0.66862

work as reference values, we see that the values of Carlson and Bell[16] are most accurate for the largest system (c = 1.02) and least accurate for the smallest system (c = 2.0). Carlson and Bell used the extrapolated endpoint method for the larger systems, R > 1.5. For the smaller systems, they interpolated between values calculated with the extrapolated endpoint and variational methods. The values of Hendry[17] were obtained by Fourier expansion of the neutron distribution function in one of the angular variables and solution of the resulting equations using integration by Gauss quadrature. The IT_n method of Hembd[18] is based upon a Fourier transformation of the integral equation. It appears to be particularly effective, especially for the smaller systems. The reduced accuracy of the IT_n method for the larger systems is recognized by the author.[18]

The neutron density or total flux was calculated from Eq. (3.31). Table III lists the neutron density relative to the centerline value. It is seen that the radial drop-off in the neutron density decreases with a reduction in the size of the system. Figure 5 shows the neutron density distribution for the smallest case, c = 2.0, calculated by the method presented here and by various order discrete ordinate calculations. The discrete ordinate calculations were performed with the TDSN program[19] using a moment modified quadrature. The neutron density distribution from the S_{16} calculation agrees very closely with the exact distribution. However, the excess system multiplication calculated by discrete ordinates indicates the increasing importance of the error in the neutron density distribution as the discrete quadrature order is reduced.

The first term of the neutron density, Eq. (3.31), is the asymptotic density arising from the discrete mode. The asymptotic density

TABLE III. - NEUTRON DENSITY AS A FUNCTION OF POSITION

r/R_c	c							
	1.02	1.05	1.1	1.2	1.4	1.6	1.8	2.0
0.0	1.0000	1.0000	1.0000	1.0000	1.0000	1.0000	1.0000	1.0000
0.25	0.9236	0.9299	0.9361	0.9433	0.9508	0.9550	0.9578	0.9598
0.50	0.7118	0.7340	0.7561	0.7819	0.8093	0.8248	0.8352	0.8426
0.75	0.4124	0.4522	0.4922	0.5399	0.5918	0.6218	0.6421	0.6570
0.85	0.2821	0.3267	0.3718	0.4263	0.4868	0.5223	0.5466	0.5644
0.91	0.2033	0.2492	0.2960	0.3535	0.4181	0.4566	0.4830	0.5026
0.95	0.1502	0.1958	0.2430	0.3016	0.3686	0.4088	0.4366	0.4572
0.98	0.1086	0.1531	0.1999	0.2589	0.3273	0.3688	0.3976	0.4190
1.0	0.0747	0.1179	0.1641	0.2233	0.2926	0.3351	0.3646	0.3867
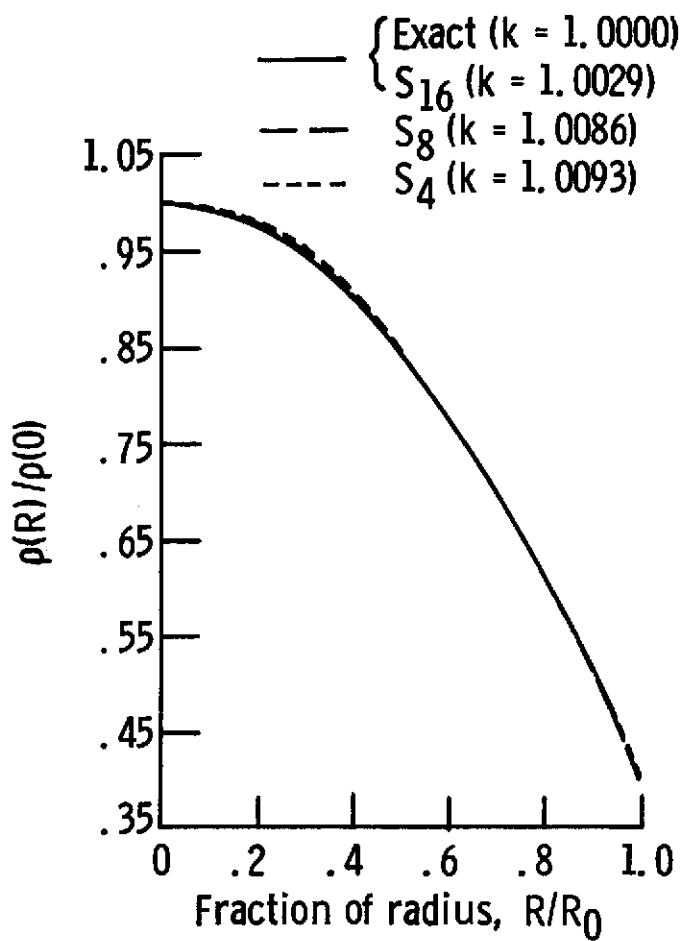
Figure 5. - Neutron density distribution (C = 2.0).

corresponds to the diffusion theory solution based on the exact diffusion coefficient. Table IV lists the ratio of the asymptotic to total neutron density as a function of position. The value of this ratio at the outer boundary for the case c = 1.02 agrees with the corresponding value for the Milne problem[3] with c = 1.0. As anticipated, the error in the asymptotic density is most severe on the boundary of the smallest system.

5.4 Reflected Core Results

Critical core radii as a function of core and reflector multiplying properties and reflector thickness are presented in Table V. We note the anticipated increase in critical core radius with a decrease in either reflector multiplication or reflector thickness.

The critical dimensions of two widely varying cases in Table V were used in one-dimensional discrete-ordinates and diffusion theory analyses. The results of these analyses are given in Table VI. The discrete-ordinates calculations were performed with the TDSN program[19] using a moment modified quadrature. For both types of calculations it is seen that the variation of the effective multiplication factor from critical is strongly dependent on the amount of neutron absorption in the core. Thus it appears that in evaluating numerical methods by comparison with exact analyses, one should include a realistic amount of absorption in choosing the cross sections. A relatively high order of angular quadrature is required for good discrete-ordinates analysis of the small system. Diffusion theory is adequate for analyzing the large system which more closely corresponds to power reactors.

TABLE IV. - ASYMPTOTIC RELATIVE TO TOTAL NEUTRON DENSITY

r/R_c	c							
	1.02	1.05	1.1	1.2	1.4	1.6	1.8	2.0
0.0	1.0000	1.0000	1.0004	1.0024	1.0087	1.0153	1.0214	1.0266
0.25	1.0000	1.0001	1.0006	1.0030	1.0102	1.0174	1.0239	1.0294
0.50	1.0000	1.0004	1.0018	1.0062	1.0164	1.0258	1.0337	1.0403
0.75	1.0006	1.0034	1.0092	1.0205	1.0391	1.0532	1.0641	1.0728
0.85	1.0033	1.0110	1.0226	1.0406	1.0652	1.0821	1.0946	1.1043
0.91	1.0109	1.0263	1.0443	1.0680	1.0965	1.1146	1.1277	1.1376
0.95	1.0294	1.0539	1.0773	1.1041	1.1335	1.1513	1.1639	1.1734
0.98	1.0775	1.1084	1.1326	1.1571	1.1824	1.1976	1.2084	1.2165
1.0	1.2318	1.2337	1.2368	1.2424	1.2522	1.2601	1.2664	1.2716

TABLE V -CRITICAL CORE RADII IN MEAN FREE PATHS FOR REFLECTED CYLINDERS

Case		Reflector Thickness (MFP)				
c_1	c_2	1	3	6	10	20
1.02	0.99	8.160095	6.981947	6.220461	5.914592	5.814384
1.02	.95	8.286641	7.621081	7.431634	7.410246	7.409152
1.02	.90	8.411027	8.036229	7.981761	7.979325	7.979288
1.02	.85	8.508960	8.276755	.8.255960	8.255474	8.255471
1.05	0.99	4.618945	3.772231	3.325398	3.159486	3.105828
1.05	.95	4.724733	4.203900	4.068247	4.053117	4.052340
1.05	.90	4.831448	4.520869	4.477548	4.475609	4.475579
1.05	.85	4.917318	4.718400	4.700988	4.700581	4.700578
1.1	0.99	2.899832	2.323758	2.057837	1.961971	1.930929
1.1	.95	2.982381	2.602577	2.511010	2.500863	2.500339
1.1	.90	2.068188	2.828581	2.796556	2.795120	2.795098
1.1	.85	3.13909	2.97985	2.96628	2.96596	2.96596
1.2	0.99	1.76189	1.41589	1.26942	1.21684	1.19964
1.2	.95	1.81837	1.57685	1.52221	1.51616	1.51585
1.2	.90	1.87916	1.71823	1.69762	1.69670	1.69668
1.2	.85	1.93105	1.81967	1.81047	1.81025	1.81025
1.4	0.99	1.03831	.853831	.778234	.750720	.741640
1.4	.95	1.07179	.938396	.909237	.905989	.905820
1.4	.90	1.10898	1.01652	1.00504	1.00452	1.00451
1.4	.85	1.14175	1.07560	1.07028	1.07015	1.07015

TABLE VI -NUMERICAL ANALYSES OF CRITICAL CONFIGURATIONS

Case Description				
c_1	1.02	1.02	1.4	1.4
c_2	.99	.99	.85	.85
R_2-R_1	20.0	20.0	1.0	1.0
Σ_{a1}	.0	.25	.0	.25
Effective Multiplication Factor*				
Discrete Ordinates				
S_4	1.00695	1.00051	1.02280	1.01391
S_8	1.00288	1.00021	1.00753	1.00462
S_{16}	1.00224	1.00016	1.00217	1.00134
S_{32}	-------	-------	1.00074	1.00045
S_{64}	-------	-------	1.00035	1.00021
Diffusion Theory				
	0.98310	0.99873	0.80653	0.87137

*To be compared with $k_{eff} = 1$.

The neutron density distribution as calculated by the present solution and by discrete ordinates is presented in Fig. 6. The distribution from the S_{64} calculation agrees with the exact values to at least three significant figures at all points. The tendency of the distribution as calculated by discrete ordinates to peak away from the core centerline is most pronounced for the S_4 calculation but persists even into the S_{32} calculation. Here again, the excess multiplication calculated by discrete ordinates indicates the increasing importance of the error in the neutron density distribution as the discrete quadrature order is reduced.

The values of tabulated neutron density distributions for a number of cases, as supplementary to the critical dimensions given in Table V when applied as analytic standards, are given in Appendix C.
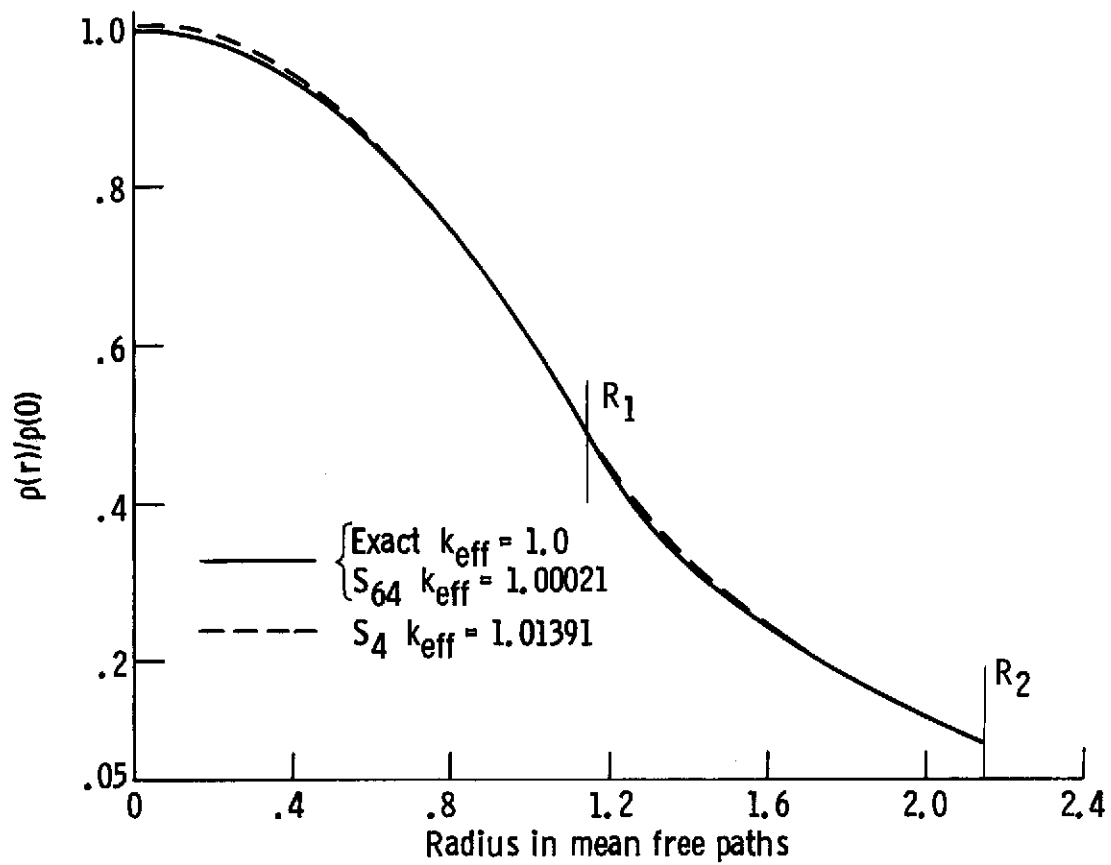
Figure 6. - Neutron density distribution. C_1, 1.4; C_2, 0.85; reflector thickness, 1 MFP

CHAPTER VI

APPLICATIONS AS AN ANALYTIC STANDARD

6.1 The Analytical Model

For this study, a model was chosen which, in the context of the two-region solution developed in Chapter IV, most closely approximates the Advanced Power Reactor concept described by Whitmarsh[10] and shown in Fig. 7. The operational requirements for this space power reactor concept are that it provide 2.17 thermal megawatts for 50,000 hours with a coolant outlet temperature of $1222°K$ to a Brayton-cycle power conversion system. The design requirements of compact size, long core lifetime, and high operating temperature dictate the materials appearing in the system and therefore its neutronic characteristics. The concept employs highly-enriched uranium nitride fuel, tantalum-based alloy clad and structural material, lithium coolant, and molybdenum reflectors. This material composition leads to a very hard spectrum, fast reactor with a median neutron energy of 0.44 MeV.

Two major problem areas arise in the neutronic analysis of this design. The first problem area concerns the adequacy of the neutron cross sections for these relatively little-used materials. Estimates of the reactivity biases due to the cross sections have been obtained from the analysis of small, fast-spectrum critical assemblies[20] containing these materials and are reported in Mayo and Lantz.[21] Unfortunately, it is not possible to separate the error in the reactivity due to the cross sections from that which arises from the approximations inherent in the method of analysis. This difficulty brings us to the second major problem area, the analytical bias. Since the analyses leading to

Outlet-end, control-
drum drive nozzles

T-111 Pressure vessel

Core fuel elements

TZM outlet-end
reflector

Honeycomb core
support structure

Control-drum
assembly

Drum fuel elements

TZM control-
drum reflector

TZM side reflector

T-111 control-
drum poison

TZM inlet-end
reflector

Inlet-end, control
drum bearing

CD-10889-22
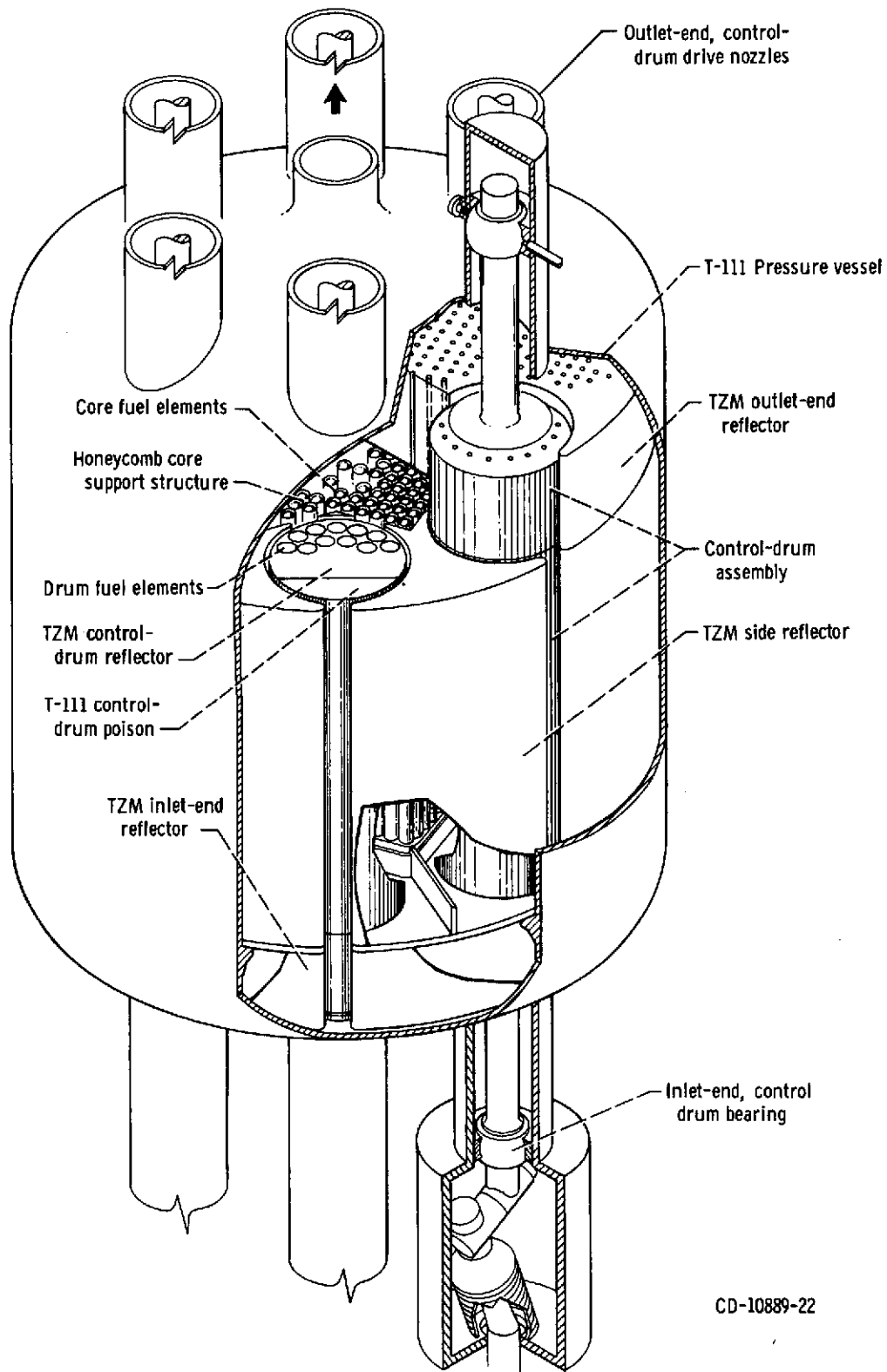
Figure 7. - Advanced power reactor concept.

the critical dimensions presented in Chapter V are based on hypothetical c values, these dimensions are particularly suitable for use in studying various contributions to the analytical bias in the design methods.

At the high neutron energies present in this reactor, the cross sections are much smaller than those associated with thermal reactors. Thus the average neutron mean free path is of the same order of magnitude as the physical dimensions of the system. The resulting relative proximity of any position in the system to the core and reflector boundaries precludes the use of neutron diffusion theory in performing design analysis. Consequently, the design analysis has been performed with the discrete-ordinates transport theory programs TDSN,[19] ANISN,[22] and DOT-IIW.[23]

The azimuthal asymmetry of this drum-controlled concept necessitates two-dimensional calculations in the analysis of quantities such as control swings and radial power distributions. With these large spatial descriptions, computer running time and storage considerations have restricted the analytical model to the S_4 angular quadrature approximation. The first investigation of the present study concerns the effects of quadrature order and quadrature type upon the reactivity. The second investigation is concerned with a consistent discrepancy between the multiplication factors for a single configuration calculated with x-y and R-θ geometry descriptions. Each of these investigations employs the analytical model described in Table VII. The neutron cross sections are approximate one group values. They have been derived from spatial and energy group flux-averaged reaction rates taken from a multigroup discrete-ordinates calculation of the Advanced Power Reactor concept.

Table VII

The Analytical Model

Cross Sections	Core, $c_1 = 1.1$ $R_1 = 2.6025766 \text{MFP}$	Reflector, $C_2 = 0.95$ $R_2 - R_1 = 3\text{MFP}$
Σ_a	0.105	0.05
$\nu\Sigma_f$	0.205	0.00
Σ_t	1.000	1.00
Σ_s	0.895	0.95

Although the cross sections only approximately represent the actual system, in the context of the one group model they accurately produce the core and reflector c values. That is, neutron absorption and secondary neutron production are conserved. To meet the criterion of identical neutron mean free paths in the core and reflector regions, the cross sections are adjusted to a normalized total macroscopic cross section of one cm^{-1} in each region. The core and reflector dimensions in mean free paths closely correspond to the one-group average values of the actual configuration. These dimensions, along with the c values, represent one of the cases in Table V.

6.2 Discrete-Ordinates Quadrature Study

This study is concerned with the effects of quadrature type and quadrature order as used in calculating the analytical model in R-θ geometry with the DOT-IIW discrete-ordinates transport program.[23] The interest in R-θ geometry arises from the sixty degree azimuthal symmetry present in Advanced Power Reactor configuration. The effects of quadrature type are studied in the S_4 approximation corresponding to the approximation level employed in the design analysis.

In addition to the even moment quadrature set ordinarily used with the DOT-IIW program, seven other quadrature sets are included in the study. The various prescriptions under which the quadrature points were selected are described in the literature. The even moment, odd moment, level moment, and $P_3 T_4$ quadrature sets are from Lathrop and Carlson.[24] The projection invariant sets A and B are from Carlson.[25] The DP_1 quadrature set is from Carlson and Lee.[26] And the moment modified quadrature set is from Carlson.[27]

The quadrature sets are presented in Tables VIII through XV. The points are located on the surface of the unit sphere an octant of which is shown in Fig. 8. The tabulated values include eight positive values of the direction cosine η followed by eight negative values. Thus the values include the entire upper half of the surface of the unit sphere. The points are located along fixed values of the direction cosine ξ. It should be noted that these R-θ quadrature sets are orthogonal to the more familiar X-Y and R-Z quadrature sets which are based upon fixed values of the direction cosine called η in our convention.

The R-θ geometry used to describe the analytical model in the DOT-IIW calculations is shown in Fig. 9. The largest radial mesh intervals are 0.26 cm (MFP) in the core and 0.3 cm in the reflector. Much smaller mesh intervals are grouped near the center and at the boundaries. The angular mesh interval is one degree. Perfect reflection boundary conditions were applied at the top, center, and bottom boundaries. A vacuum boundary condition was applied at the outer boundary. The cross sections used appear in Table VII.

The results of this study are given in Table XVI. From the viewpoint of quadrature type, it is reassuring to observe that the even moment set which is ordinarily used in DOT-IIW and the moment modified set which is ordinarily used in TDSN give the best results.

From the viewpoint of quadrature order, it is somewhat disturbing to observe the 0.6% $\Delta k/k$ reactivity bias associated with the results given by the standard S_4 design analysis approximation. However, this information can be used to obtain an estimate of the reactivity bias associated with the design analysis of the actual configuration.

Table VIII

Even Moment, S_4, R-θ Quadrature Set

i	ω_i	$|\eta|_{i,i+8}$*	$\mu_{i,i+8}$
1	0.0	0.00000001	-0.93674178
2	0.08333333	0.35002120	-0.86889028
3	0.08333333	0.86889028	-0.35002120
4	0.08333333	0.86889028	0.35002120
5	0.08333333	0.35002120	0.86889028
6	0.0	0.00000001	-0.49500473
7	0.08333333	0.35002120	-0.35002120
8	0.08333333	0.35002120	0.35002120

*The sequence listed here corresponds to the input sequence used in the DOT-IIW code. The negative values of η in the second quadrant are positioned in the same order as the first quadrant values shown in Fig. 8.

Table IX

Level Moment, S_4, R-θ Quadrature Set

i	ω_1	$\lceil\eta\rceil_{1,1+8}$	$\mu_{1,1+8}$
1	0.0	0.00000001	-0.95006840
2	0.08333333	0.31276157	-0.89711210
3	0.08333333	0.89736271	-0.31204180
4	0.08333333	0.89736271	0.31204180
5	0.08333333	0.31276157	0.89711210
6	0.0	0.00000001	-0.44180300
7	0.08333333	0.31276157	-0.31204180
8	0.08333333	0.31276157	0.31204180

Table X

Moment Modified, S_4, R-θ Quadrature Set

i	ω_i	$\eta_{i,i+8}$	$\mu_{i,i+8}$
1	0.0	0.00000001	-0.93743690
2	0.08333333	0.35874166	-0.86607870
3	0.08333333	0.86607872	-0.35874166
4	0.08333333	0.86607872	0.35874166
5	0.08333333	0.35874166	0.86607170
6	0.0	0.08650678	-0.49236600
7	0.08333333	0.35874166	-0.34815530
8	0.83333333	0.35874166	0.34815530

Table XI

Odd Moment, S_4, R-θ Quadrature Set

i	ω_i	$|\eta|_{i,i+8}$	$\mu_{i,i+8}$
1	0.0	0.00000001	-0.95522640
2	0.08333333	0.29587580	-0.90824830
3	0.08333333	0.90824826	-0.29587590
4	0.08333333	0.90824826	0.29587590
5	0.08333333	0.29587580	0.90824830
6	0.0	0.00000001	-0.41843159
7	0.08333333	0.29587580	-0.29587590
8	0.08333333	0.29587580	0.29587590

Table XII

P_3T_4, S_4, R-θ Quadrature Set

i	ω_i	$|\eta|_{i,i+8}$	$\mu_{i,i+8}$
1	0.0	0.11676916	-0.94043230
2	0.08151814	0.34041838	-0.86884590
3	0.08151814	0.86096378	-0.35988780
4	0.08151814	0.86096378	0.35988780
5	0.08151814	0.34041838	0.86884590
6	0.0	0.11548774	-0.50837410
7	0.08696369	0.34041838	-0.35947480
8	0.08696369	0.34041838	0.35947480

Table XIII

DP_1, S_4, R-θ Quadrature Set

i	ω_1	$|\eta|_{1,i+8}$	$\mu_{1,i+8}$
1	0.0	0.00000001	-0.97741590
2	0.125	0.57735032	-0.78867510
3	0.0625	0.95429742	-0.21132490
4	0.0625	0.95429742	0.21132490
5	0.125	0.57735032	0.78867510
6	0.0	0.00000001	-0.61481020
7	0.0625	0.57735032	-0.21132490
8	0.0625	0.57735032	0.21132490

Table XIV

Projection Invariant Set A, S_4, R-θ Quadrature Set

i	ω_i	$|\eta|_{i,i+8}$	$\mu_{i,i+8}$
1	0.0	0.00000001	-0.94280904
2	0.08333333	0.33333333	-0.88191710
3	0.08333333	0.88191710	-0.33333333
4	0.08333333	0.88191710	0.33333333
5	0.08333333	0.33333333	0.88191710
6	0.0	0.00000001	-0.47140452
7	0.08333333	0.33333333	-0.33333333
8	0.08333333	0.33333333	0.33333333

Table XV

Projection Invariant Set B, S_4, R-θ Quadrature Set

i	ω_i	$|\eta|_{i,i+8}$	$\mu_{i,i+8}$
1	0.0	0.00000001	-0.71007688
2	0.08333333	0.09175171	-0.70412415
3	0.08333333	0.70412415	-0.09175171
4	0.08333333	0.70412415	0.09175171
5	0.08333333	0.09175171	0.70412415
6	0.0	0.00000001	-0.99578192
7	0.08333333	0.70412415	-0.70412415
8	0.08333333	0.70412415	0.70412415
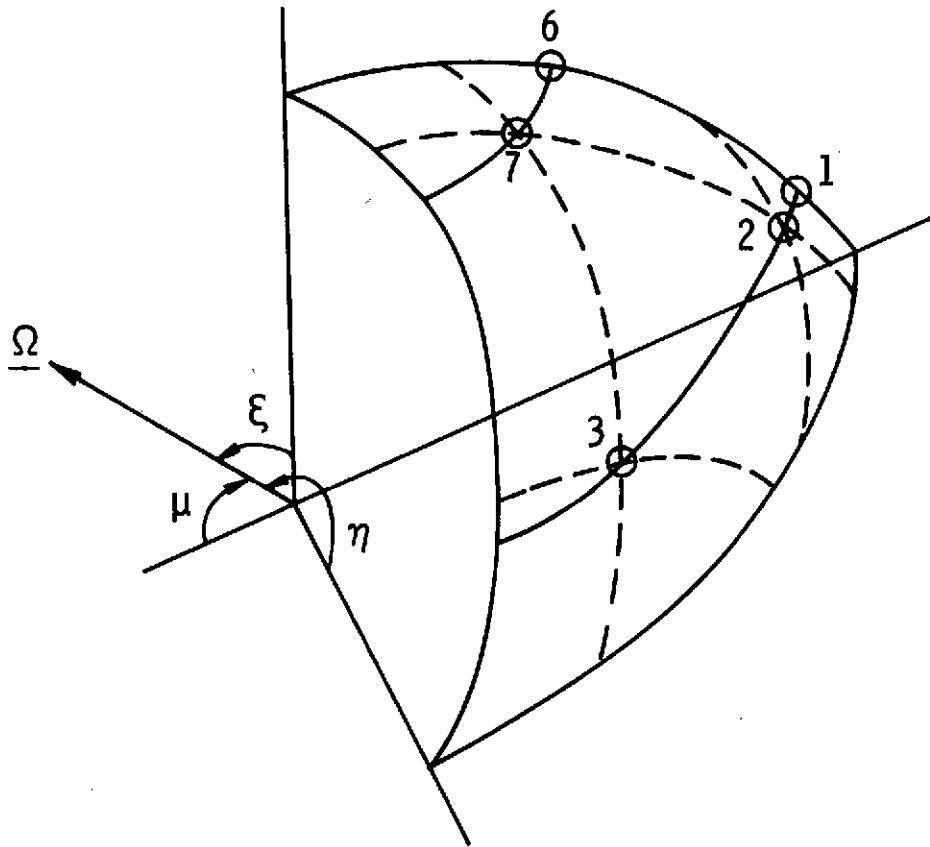
Figure 8. - Direction mesh for S_4 quadrature.

Core-reflector boundary
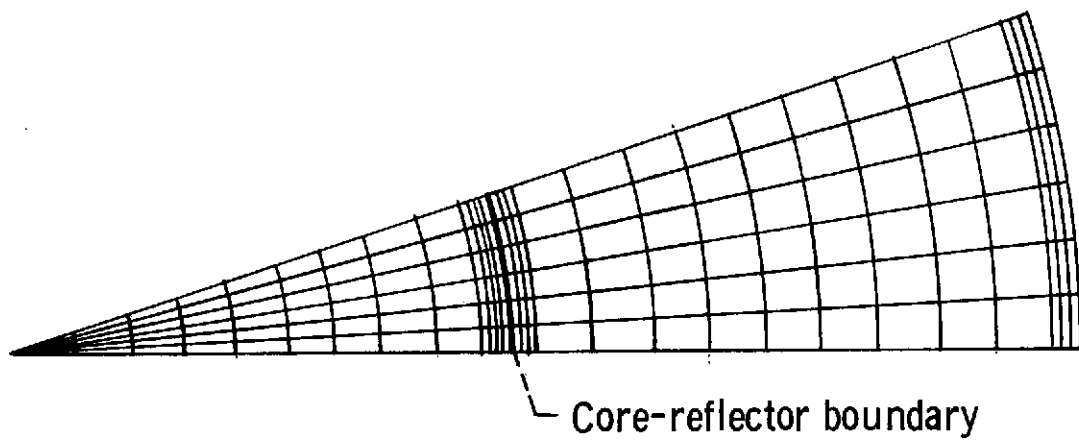
Figure 9. - R-θ description of the analytical model.

Table XVI

APR Model Quadrature Study[1]

Quadrature Type	Quadrature Order	k_{eff}*
DP_1	4	1.0081
P_3T_4	4	1.0065
Level Moment	4	1.0095
Even Moment[2]	4	1.0062
Even Moment	8	1.0016
Odd Moment	4	1.0112
Moment Modified[3]	4	1.0064
Proj. Inv. Set A	4	1.0074
Proj. Inv. Set B	4	1.0211

[1] All calculations performed with the DOT-IIW program in R-θ geometry using the diamond difference model.

[2] Normally used with DOT-IIW.

[3] Normally used with TDSN.

* To be compared with $k_{eff} = 1$.

The difference between the multiplication factors given by the S_4 and S_8 calculations in Table XVI is 0.46% $\Delta k/k$. The corresponding value given by the analysis of the actual configuration is 0.3% $\Delta k/k$. The larger value given by the analysis of the analytical model reflects the greater importance of the radial leakage in the axially infinite model. By scaling the 0.6% $\Delta k/k$ reactivity bias by the ratio of these differences, we obtain an approximate value of 0.4% $\Delta k/k$ reactivity bias to be used with the standard S_4, R-θ design approximation. This value is significant when compared to the 0.32% $\Delta k/k$ total reactivity requirement for the first 10,000 hours of operation as calculated by Whitmarsh.[10]

6.3 X-Y Boundary Approximation Study

The motivation for this study is the observation that, for the type of fast reactors under design consideration, an R-θ calculation of the multiplication factor consistently produces a higher value than does an X-Y calculation of the same parameter. This phenomenon was noted by Mayo and Lantz[21] in their pre-critical analyses. In the neutronic design analysis of the Advanced Power Reactor concept by Whitmarsh,[10] this discrepancy is determined to be worth 0.65% $\Delta k/k$ in reactivity.

An X-Y representation of a circular boundary is done in a stepwise manner. This results in an outward displacement of the core material into the reflector region accompanied by an inward displacement of the reflector material into the core region. Also the length of a stepwise boundary is a factor of 4/π greater than the actual boundary. The combined effects of having the fuel material in a lower importance

region and having a higher probability of neutron leakage from the core will result in a negative reactivity effect. This will be somewhat offset by the positive reactivity due to the possible unrealistic first-flight neutron reentry into the core.

On the other hand, an R-θ geometry is capable of describing circular boundaries exactly. Therefore it might be assumed that the lower multiplication factors calculated in X-Y geometry are in error due to the effects discussed above. However, without an absolute standard it is not possible to assess the accuracy of either geometrical representation. This demonstrates the usefulness of applying the highly precise analytic values of Chapter V in resolving this discrepancy.

The approach taken in performing the study was to calculate the analytical model in systematically finer X-Y geometrical representations and note the improvement in the multiplication factor due to the reduction of the effects discussed above. A computer program was written to determine the X-Y boundaries and provide the input for the discrete-ordinates program, DOT-IIW.

The program selects the X-Y boundaries according to three criteria.

1. The areas of the core and reflector regions are preserved.

2. Each of the interstitial areas formed by the X-Y and circular boundaries is no greater than a maximum input value.

3. Paired sets of successive interstitial areas exterior and interior to the circular boundary are the same size.

These criteria are effected in the following manner. First, we consider two successive interstitial areas as shown on the next page:
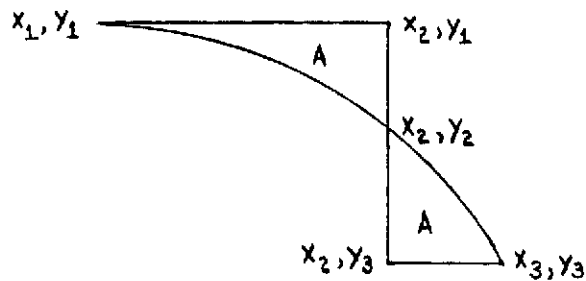
Here we have assumed that the point, x_1,y_1, is known and A corresponds

to the input value of the maximum interstitial area. The value of x_2

is found by integration of

$$A = \int_{x_1}^{x_2} \left(y_1 - \sqrt{R^2-x^2} \right) dx, \tag{6.1a}$$

obtaining

$$A = y_1 x_2 - \frac{x_2}{2} (R^2-x_2^2)^{\frac{1}{2}} - \frac{R^2}{2} \sin^{-1}\left(\frac{x_2}{R}\right)$$

$$- y_1 x_1 + \frac{x_2}{2} (R^2-x_1^2)^{\frac{1}{2}} + \frac{R^2}{2} \sin^{-1}\left(\frac{x_1}{R}\right) , \tag{6.1b}$$

and solving the transcendental Eq. (6.1b) for x_2 by Newton's method.

Having found x_2, we determine y_2 by $y_2 = \sqrt{R^2-x_2^2}$.

Next, the value of y_3 is found by integration of

$$A = \int_{y_3}^{y_2} \left(\sqrt{R^2-y^2} - x_2 \right) dy, \tag{6.2a}$$

obtaining

$$A = \frac{y_2}{2} (R^2-y_2^2)^{\frac{1}{2}} + \frac{R^2}{2} \sin^{-1}\left(\frac{y_2}{R}\right) - x_2 y_2$$

$$- \frac{y_3}{2} (R^2-y_3^2)^{\frac{1}{2}} - \frac{R^2}{2} \sin^{-1}\left(\frac{y_3}{R}\right) + x_2 y_3, \tag{6.2b}$$

and solving the transcendental Eq. (6.2b) for y_3 by Newton's method.

This procedure is repeated until the unknown x is found to be greater than $R/\sqrt{2}$ or the unknown y is found to be less than $R/\sqrt{2}$. The point, $x = y = R/\sqrt{2}$, corresponds to where the forty-five degree line drawn from the center intersects the circle. The symmetry about this line allows us to reflect the boundaries found for the upper octant of the circle into the lower octant. That is, $x_n = y_1$, $y_n = x_1$, $x_{n-1} = y_2$, $y_{n-1} = x_2$, etc. The only problem remaining is the approach to the interface point. If this point is passed on an x search, x_2 is determined by

$$x_2 = \frac{R^2}{2(x_1 - y_1)} \left[2 \sin^{-1} \frac{x_1}{R} - \pi/2 \right], \tag{6.3}$$

which is found by solving Eqs. (6.1b) and (6.2b) simultaneously and substituting

$$x_1 = y_3 \text{ and } \sqrt{R^2 - x^2} = y_2.$$

A similar procedure cannot be used upon passing the interface point on a y search, since criterion 1 could then not be satisfied. In this instance, the previous x search calculation is re-performed on successively finer values of the interstitial area until the subsequent y search produces a value greater than $R/\sqrt{2}$. Then the final value of x_2 is found by Eq. (6.3).

Two of the four x-y descriptions of the analytical model which have been determined by the above procedure are shown in Figures 10 and 11. The input criterion for the maximum interstitial area was 0.04 MFP squared for the coarsest mesh. This value was successively halved to a value of 0.005 MFP squared for the finest mesh.
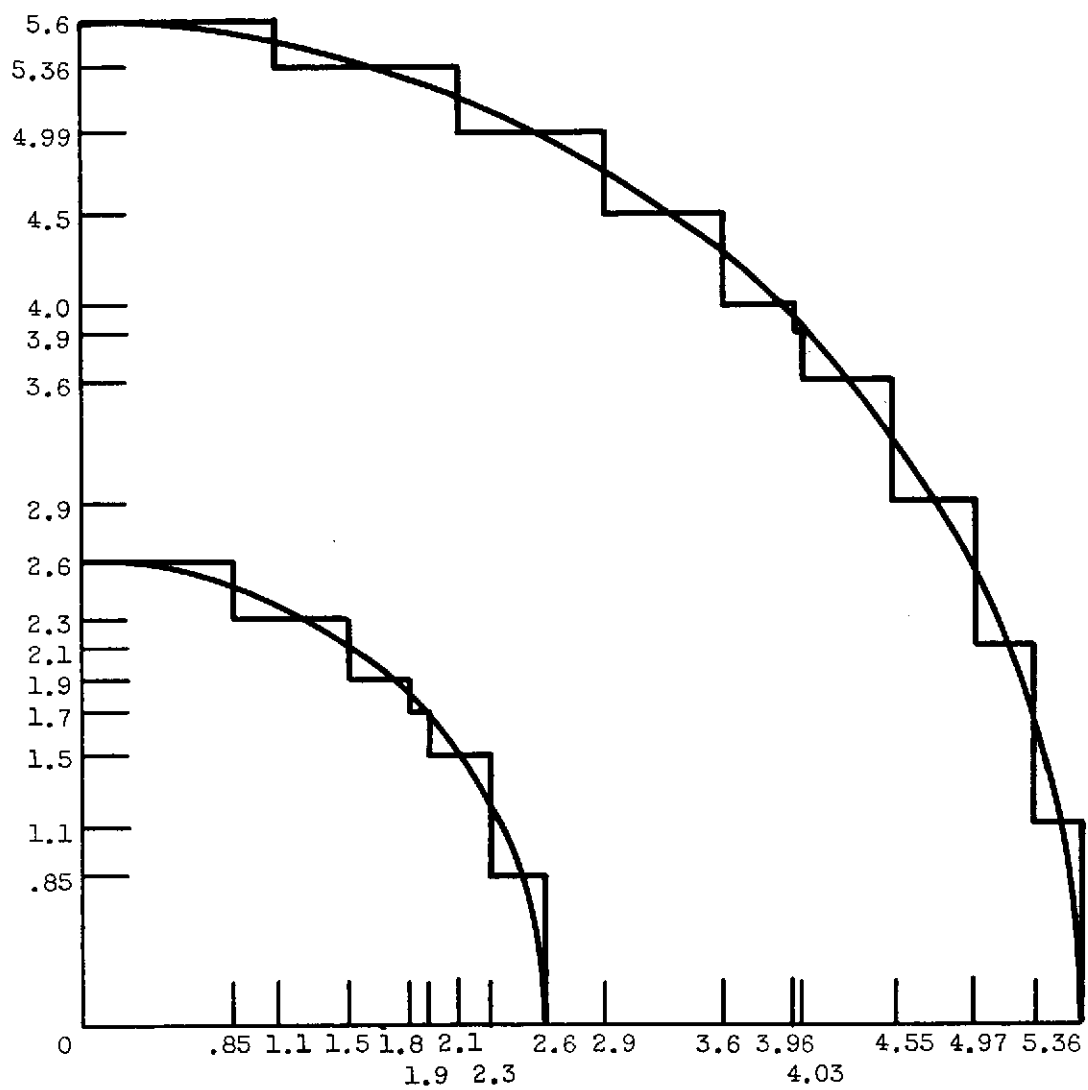
Figure 10. - X-Y description of the analytical model, 16 x 16 mesh.
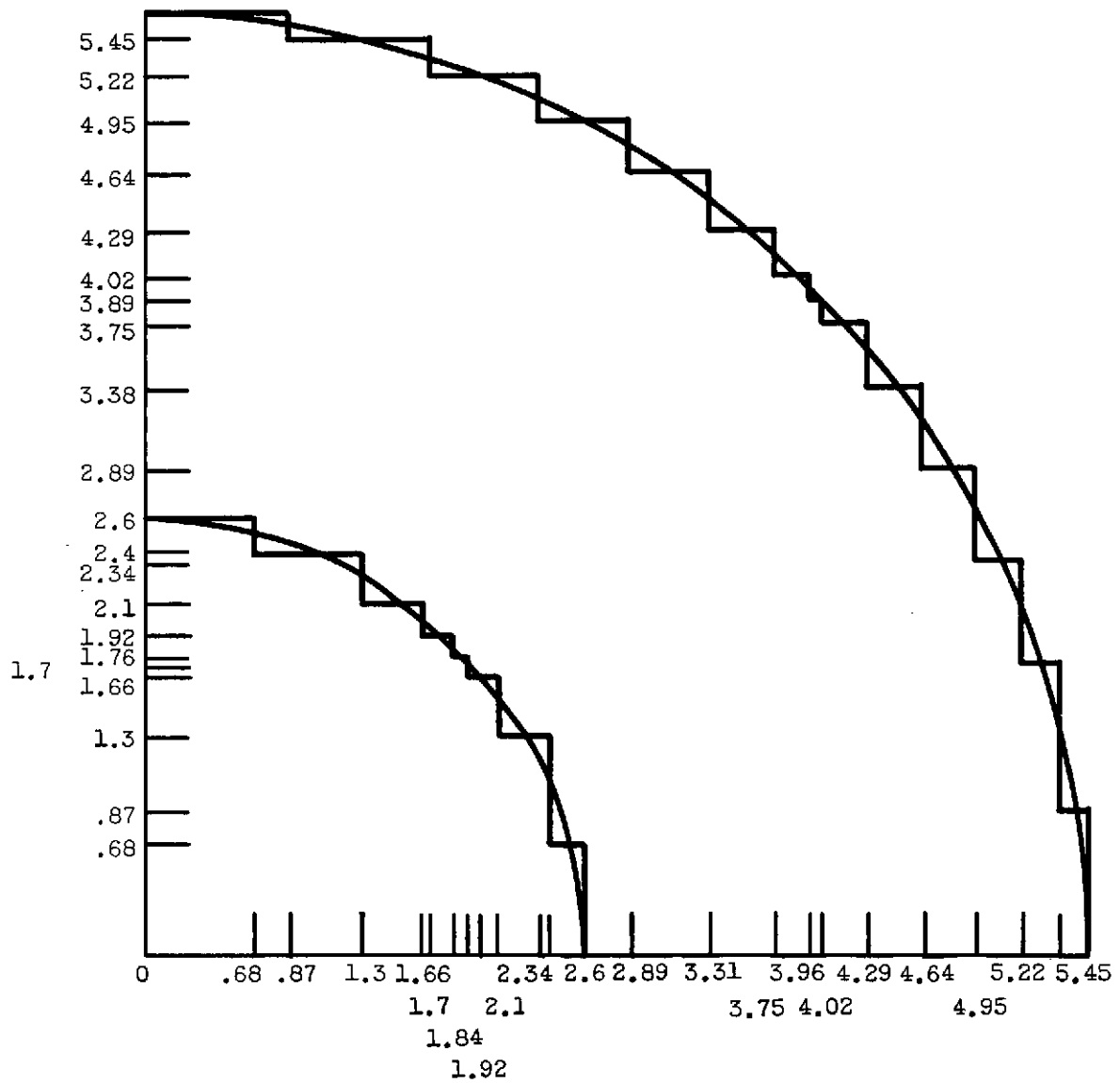
Figure 11. - X-Y description of the analytical model, 22 x 22 mesh.

The calculations were performed with the DOT-IIW discrete-ordinates program using the diamond difference model and the even moment, S_4, quadrature. Thus, these calculations differ from the even moment, S_4, R-θ calculation of Table XVI only in the geometry description.

The results of the x-y calculations are given in Table XVII. As anticipated, the calculated value of the multiplication factor is low and it improves as the x-y mesh is refined. However, it was unanticipated that even the least accurate x-y calculation yields a better value of the multiplication factor than that given by the R-θ calculation. Furthermore, the results of the finer x-y mesh calculations appear to be approaching 0.1% Δk/k below critical. This value is better than that given by the S_8, R-θ calculation. The general conclusion of this study is that the source of the discrepancy between the results of x-y and R-θ calculations lies in the inaccuracy of the R-θ calculation. Therefore, it is recommended that design calculations from which highly precise values of the multiplication factor are required, be done in the x-y geometry. It is noted that it was not possible to resolve the source of this discrepancy without the highly precise results of the analytical solution presented in Chapter IV.

As shown in Chapter V, both the error in the multiplication factor and the error in the neutron density distribution from R-θ calculations are quadrature dependent. Therefore, it is reasonable to assume that these errors are related and that possible methods to eliminate the "centerline dip" and improve the neutron density distribution as calculated by low quadrature order, discrete-ordinates calculations in R-θ geometry would be a worthwhile subject for further research.

Table XVII

X-Y Step Boundary Approximation Study[1]

Interstitial Area $(MFP)^2$	Mesh Size	k_{eff} *
0.04	16 X 16	0.99539
0.02	22 X 22	0.99718
0.01	28 X 28	0.99832
0.005	38 X 38	0.99895

[1] All calculations performed with the DOT-IIW program using an even moment, S_4 quadrature and the diamond-difference model.

*To be compared with k_{eff} = 1.

CHAPTER VII

CONCLUSIONS AND RECOMMENDATIONS

7.1 Conclusions

The conclusions drawn from this study fall into two general categories. The first category concerns the successful development of the singular eigenfunction solution for the reflected critical cylinder through the use of new relations for the singular eigenfunctions. The second category concerns the application of the highly precise numerical results obtained from this solution in assessing the accuracy of more approximate methods of transport analysis.

In evaluating the singular eigenfunction solution for the bare critical cylinder by Mitsis, it was found that his solution contained an unbounded function. This function was reformulated and the continuum expansion coefficient was redefined to obtain a converging solution. Furthermore, it was shown that the procedure taken by Mitsis in decomposing the singular eigenfunctions into the sum of the Case plane geometry eigenfunctions was unneccessary and that it introduced additional numerical complexity into the solution. This procedure was avoided through the use of a completeness proof for the singular eigenfunctions which naturally arise in the solution of the transformed integral transport equation in cylindrical geometry.

In developing the singular eigenfunction solution for the reflected critical cylinder, application was made of the reformulated function and the completeness proof mentioned above. Also, extensive use was made of orthogonality and normalization relations found for the singular eigenfunctions. The solution is in the form of two coupled iterative

sequences with which the expansion coefficients and ultimately the critical dimensions can be found to any desired degree of accuracy.

Critical core radii accurate to seven significant figures are presented for bare cylinders and compared with the results of other analytic methods. It was found that for small systems, $C > 1.6$, values that had previously served as analytic standards are accurate to only three significant figures.

Highly precise values of critical core radii as a function of core and reflector multiplying properties and reflector thickness are presented. Comparison of these results for two widely varying systems with the results of numerical solutions demonstrates the relative accuracy of various design approximations. High order discrete-ordinates calculations gave good results for both systems while the diffusion theory was inadequate for analyzing the smaller system. It was shown that errors in the multiplication factor and the neutron density distribution as calculated by discrete ordinates are dependent on the order of angular quadrature used. Also, it was shown that the introduction of a realistic amount of neutron absorption in making-up the core c values significantly improved the results of the numerical calculations.

Additional conclusions were reached in a study of design analysis methods using the highly precise results of the present solution as analytic standards. These analytic standards are particularly effective because of their lack of dependence upon measured values of neutron cross sections. Three conclusions concerning the neutronic design analysis of the fast reactor concept under consideration were made.

First, of eight different types of angular quadrature sets studied, the even moment set ordinarily used in the DOT-IIW discrete-ordinates program is as effective as any of the other sets studied when applied in the S_4 approximation in R-θ geometry. Second, using this level of design analysis introduces an estimated analytical bias in the multiplication factor of +0.4% Δk/k. Third, for the same level of quadrature order, an x-y geometry representation can be used to obtain a much more accurate value of the multiplication factor than can be obtained in R-θ geometry.

7.2 Recommendations

Since this work represents the first successful singular eigenfunction solution of the transport equation for critical cylinders, the opportunity exists for much worthwhile additional work in this area. For example, a two energy group solution would be very useful for the analysis of hydrogen moderated systems. Also, a solution including anisotropic scattering could be used to analyze systems in which this phenomenon is important. These features have been successfully incorporated into singular eigenfunction solutions[29,30,31] of the Boltzmann equation in critical slab geometry. How these features might be incorporated into the present solution, which is based on the transformed integral transport equation, has not been investigated. However, it appears to be relatively straightforward to apply the techniques developed in the present work to obtain solutions for multiregion problems. The results from such solutions could be used as analytic standards for methods used to analyze radially fuel-zoned cores or deep radiation penetration into multilayered shield configurations.

From the results of Chapter VI, it is recommended that further design analysis of the Advanced Power Reactor concept using the DOT-IIW discrete-ordinates transport program in the S_4 approximation and in R-θ geometry include a reactivity bias of -0.4% $\Delta k/k$ applied to the calculated multiplication factor. It is also recommended that x-y rather than R-θ geometry be used in analysis requiring high precision in the multiplication factor.

Finally, the results of Chapters V and VI have shown a serious deficiency of low quadrature order discrete-ordinates transport analysis in R-θ geometry. Investigation into the source of this problem would be a worthwhile area for further research.

REFERENCES

1. Case, K. M., "Elementary Solutions of the Transport Equation and Their Applications," Ann. Phys., 9, 1 (1960).

2. Mitsis, G. J., "Transport Solutions to the Monoenergetic Critical Problems," ANL-6787, Argonne National Laboratory (1963).

3. Case, K. M. and P. F. Zweifel, Linear Transport Theory, Addison-Wesley Publ. Co., Reading, Mass. (1967).

4. Gibbs, A. G., J. Math. Phys., 10, 875 (1969).

5. Lathrop, K. D. and A. Leonard, Nucl. Sci. Eng., 22, 115 (1965).

6. Hendry, W. L., K. D. Lathrop, S. Vandervoort, and J. Wooten, "Bibliography on Neutral Particle Transport Theory," LA-4287-MS, Los Alamos Scientific Laboratory (1970).

7. Smith, O. J., and C. E. Siewert, J. Nucl. Energy, 22, 579 (1968).

8. Leuthäuser, K. D., Atomkernenergie, 14, 254 (1969).

9. Smith, O. J., "Radiation Transport in Plane and Spherical Media," Ph.D. Thesis, North Carolina State University (1969).

10. Whitmarsh, C. L., "Neutronic Design for a Lithium-Cooled Reactor for Space Applications," NASA TN D-6169, Lewis Research Center (1971).

11. Bell, G. I. and S. Glasstone, Nuclear Reactor Theory, Van Nostrand Reinhold Co., New York (1970).

12. Abramowitz, M. and I. A. Stegun, Eds., Handbook of Mathematical Functions, Appl. Math. Ser. 55, National Bureau of Standards, Washington, D.C. (1964).

13. Goldstein, M. and R. M. Thaler, Math. Tables and Other Aids to Comp., 13, 102 (1959).

14. Metcalf, D. R., and P. F. Zweifel, Nucl. Sci. Eng., 33, 318 (1968).

15. Kowalska, K., "Tables of the Functions $X(c,-\nu)$ and $X^{\pm}(c_1,c_2)$," Rep. No. 630/IX A/PR, Institute of Nuclear Research, Warsaw (1965).

16. Carlson, B. G., and G. I. Bell, "Solution of the Transport Equation by the S_n Method," Proc. Second Int. Conf. Peaceful Uses Atomic Energy, 16, 541 (1958).

17. Hendry, W. L., _Nucl. Sci. Eng._, 34, 134 (1968).

18. Hembd, H., _Nucl. Sci. Eng._, 40, 224 (1970).

19. Barber, C. E., "A Fortran IV Two-Dimensional Discrete Angular Segmentation Transport Program," NASA TN D-3573, Lewis Research Center (1966).

20. Paxton, H. C., "Los Alamos Critical Mass Data" LAMS-3067, Los Alamos Scientific Laboratory (1964).

21. Mayo, W. and E. Lantz, "Analysis of Fuel Loading Requirements and Neutron Energy Spectrum of a Fast Spectrum, Molybdenum-Reflected, Critical Assembly," NASA TM X-52762, Lewis Research Center (1970).

22. Engle, W. W., Jr., "A User's Manual for ANISN, A One-Dimensional Discrete Ordinates Transport Code with Anisotropic Scattering," USAEC Report K-1693, (1967).

23. Soltez, R. G., R. K. Disney, and G. Collier, "Users Manual for the DOT-IIW Discrete Ordinates Transport Computer Program," WANL-TME-1982, Westinghouse Electric Corporation (1969).

24. Lathrop, K. D., and B. G. Carlson, "Discrete Ordinates Angular Quadrature of the Neutron Transport Equation," LA-3186, Los Alamos Scientific Laboratory, (1965).

25. Carlson, B. G., "The Numerical Theory of Neutron Transport", Statistical Physics, _Vol. 1 of Methods in Computational Physics_, B. Adler, S. Fernbach and M. Rotenberg, Eds., Academic Press, New York (1963).

26. Carlson, B. G. and C. E. Lee, "Mechanical Quadrature and the Transport Equation," LAMS-2573, Los Alamos Scientific Laboratory (1961).

27. Carlson, B. G., "Numerical Solution of Transient and Steady-State Neutron Transport Problems," LA-2260, Los Alamos Scientific Laboratory (1959).

28. Muskhelishvili, N. I., _Singular Integral Equations_, Nordhoff, Groningen, Holland (1953).

29. Forster, R. A., "Two Group Tansport Solutions to the One-Dimensional Critical Slab Problem," Ph.D. Thesis, University of Virginia (1970).

30. Bosler, G. E., "Critical Slab Solution to the Two-Group Neutron Transport Equation for Linearly Anisotropic Scattering," Ph.D. Thesis, University of Virginia (1972).

31. Stewart, J. E., III, "Two-Media Solutions to the Neutron Transport Equation," Ph.D. Thesis, University of Virginia (1974).

APPENDICES

APPENDIX A

ORTHOGONALITY AND NORMALIZATION RELATIONS
FOR THE PSEUDO EIGENFUNCTIONS

The purpose of this appendix is to present the development of an orthogonality relation for the pseudo eigenfunctions found in Chapter III and the development of normalization relations for their discrete and continuum modes.

To demonstrate the orthogonality properties, we begin by substituting Eq. (3.18) for $\eta_\nu(\mu)$ into the Eq. (3.16), obtaining

$$\int_0^1 \eta_\nu(\mu)d\mu = 1. \tag{A.1}$$

Making the same substitution into Eq. (3.17), we have

$$(\nu^2 - \mu^2)\eta_\nu(\mu) = c\nu^2. \tag{A.2}$$

Next we rewrite Eq. (A.2) for two eigenvalues, ν and ν', in the form:

$$\left(1 - \frac{\mu^2}{\nu^2}\right)\eta_\nu(\mu) = c, \tag{A.3a}$$

and

$$\left(1 - \frac{\mu^2}{\nu'^2}\right)\eta_{\nu'}(\mu) = c. \tag{A.3b}$$

Now we operate on Eq. (A.3a) with the integral of $\eta_{\nu'}(\mu)$ over μ and operate on Eq. (A.3b) with the integral of $\eta_\nu(\mu)$ over μ, obtaining

$$\int_0^1 \left(1 - \frac{\mu^2}{\nu^2}\right)\eta_\nu(\mu)\eta_{\nu'}(\mu)d\mu = c\int_0^1 \eta_{\nu'}(\mu)d\mu, \tag{A.4a}$$

and

$$\int_0^1 \left(1 - \frac{\mu^2}{\nu'^2}\right)\eta_{\nu'}(\mu)\eta_\nu(\mu)d\mu = c\int_0^1 \eta_\nu(\mu)d\mu. \tag{A.4b}$$

We observe from Eq. (A.1) that the right hand sides of Eqs. (A.4a,b) are just equal to c. With this observation, we subtract Eq.(A.4b) from Eq. (A.4a) to obtain

$$\left(\frac{1}{\nu'^2} - \frac{1}{\nu^2} \right) \int_0^1 \mu^2 \eta_\nu(\mu) \eta_{\nu'}(\mu) = 0. \tag{A.5}$$

Eq. (A.5) implies the orthogonality relation

$$\int_0^1 \mu^2 \eta_\nu(\mu) \eta_{\nu'}(\mu) d\mu = 0, \quad \nu' \neq \nu. \tag{A.6}$$

Next we wish to develop the normalization integral for the discrete modes, defined by

$$N_o = \int_0^1 \mu^2 \eta_o(\mu) \eta_o(\mu) d\mu. \tag{A.7}$$

Substituting Eq. (3.19) for $\eta_o(\mu)$ into Eq. (A.7) we have

$$N_o = \int_0^1 \mu^2 \frac{c\nu_o^2}{\nu_o^2 - \mu^2} \frac{c\nu_o^2}{\nu_o^2 - \mu^2} d\mu. \tag{A.8}$$

By partial fraction expansion Eq. (A.8) can be shown to be equivalent to

$$N_o = \frac{c^2 \nu_o^3}{4} \int_0^1 \left[\frac{\mu}{(\nu_o - \mu)^2} - \frac{\mu}{(\nu_o + \mu)^2} \right] d\mu. \tag{A.9}$$

Performing the integral over the terms in Eq. (A.9) we obtain

$$N_o = \frac{c^2 \nu_o^3}{4} \left[\ln|\nu_o - \mu| + \frac{\nu_o}{\nu_o - \mu} - \ln|\nu_o + \mu| - \frac{\nu_o}{\nu_o + \mu} \right]_0^1, \tag{A.10}$$

which is evaluated at the limits to yield

$$N_o = \frac{c\nu_o^4}{2} \left[\frac{c}{\nu_o^2 - 1} - \frac{1}{\nu_o^2} \right]. \tag{A.11}$$

Anticipating the requirement for a discrete normalization integral to apply in solving the two-region problem of Chapter IV, we next seek the relation

$$N_{o12} = \int_0^1 \mu^2 \eta_{b1}(\mu)\eta_{b2}(\mu)d\mu, \tag{A.12}$$

where $c_1 > 1$, ν_{o1} imaginary; $c_2 < 1$, ν_{o2} real. Substituting the discrete mode eigenfunctions into Eq. (A.12) we have

$$N_{o12} = \int_0^1 \mu^2 \frac{c_1|\nu_{o1}|^2}{|\nu_{o1}|^2 + \mu^2} \frac{c_2\nu_{o2}^2}{\nu_{o2}^2 - \mu^2} d\mu. \tag{A.13}$$

Upon partial fraction expansion Eq. (A.13) becomes

$$N_{o12} = \frac{c_1 c_2 |\nu_{o1}|^2 \nu_{o2}^2}{|\nu_{o1}|^2 + \nu_{o2}^2} \int_0^1 \left[\frac{\nu_{o2}^2}{\nu_{o2}^2 - \mu^2} - \frac{|\nu_{o1}|^2}{|\nu_{o1}|^2 + \mu^2} \right] d\mu. \tag{A.14}$$

Performing the integral over the terms in Eq. (A.14), we obtain

$$N_{o12} = \frac{c_1 c_2 |\nu_{o1}|^2 \nu_{o2}^2}{|\nu_{o1}|^2 + \nu_{o2}^2} \left[\frac{\nu_{o2}\ell n}{2} \left| \frac{\nu_{o2} + \mu}{\nu_{o2} - \mu} \right| - \frac{|\nu_{o1}|\ell n}{2i} \left| \frac{|\nu_{o1}| + i\mu}{|\nu_{o1}| - i\mu} \right| \right]_0^1 \tag{A.15}$$

which is evaluated at the limits to yield

$$N_{o12} = \frac{c_1 c_2 |\nu_{o1}|^2 \nu_{o2}^2}{|\nu_{o1}|^2 + \nu_{o2}^2} \left[\frac{1}{c_2} - \frac{1}{c_1} \right]. \tag{A.16}$$

Finally, we wish to obtain the normalization function for the continuum modes, defined by

$$N(\nu) = \int_0^1 \mu^2 \eta_\nu(\mu)\eta_{\nu'}(\mu)d\mu, \quad \nu' = \nu. \tag{A.17}$$

This function is to be used in the evaluation of coefficients, $A(\nu')$, appearing in the expansion of an arbitrary function, $f(\mu)$ in the

following manner:

$$f(\mu) = \int_0^1 A(\nu') \, \eta_{\nu'}(\mu) d\nu'. \tag{A.18}$$

Operating on Eq. (A.18) by the integral of $\mu^2 \eta_\nu(\mu)$ over μ, we obtain

$$\int_0^1 \mu^2 \eta_\nu(\mu) f(\mu) d\mu = \int_0^1 \mu^2 \eta_\nu(\mu) d\mu \int_0^1 A(\nu') \eta_{\nu'}(\mu) d\nu' \tag{A.19}$$

Initially we define the normalization function, $N(\nu)$, such that

$$A(\nu)N(\nu) = \int_0^1 \mu^2 \eta_\nu(\mu) f(\mu) d\mu \tag{A.20}$$

Now, substituting Eq. (A.20) into Eq. (A.19), we obtain

$$N(\nu) = \frac{1}{A(\nu)} \int_0^1 \mu^2 \eta_\nu(\mu) d\mu \int_0^1 A(\nu') \eta_{\nu'}(\mu) d\nu'. \tag{A.21}$$

Recognizing that the order of integration over singular functions is not directly interchangeable, we evaluate Eq. (A.21) by considering

$$\overline{N}(\nu) = \frac{1}{A(\nu)} \int_0^1 d\nu' A(\nu') \int_0^1 \mu^2 \eta_{\nu'}(\mu) \eta_\nu(\mu) d\mu. \tag{A.22}$$

Upon substitution of Eq. (3.20) for $\eta_\nu(\mu)$ and $\eta_{\nu'}(\mu)$, Eq. (A.22) becomes

$$A(\nu)\overline{N}(\nu) = \int_0^1 d\nu' A(\nu') \int_0^1 \mu^2 d\mu \left\{ \lambda(\nu)\delta(\nu-\mu)\lambda(\nu')\delta(\nu'-\mu) \right.$$
$$+ \lambda(\nu')\delta(\nu'-\mu)cP \frac{\nu^2}{\nu^2 - \mu^2}$$
$$+ \lambda(\nu)\delta(\nu-\mu)cP \frac{\nu'^2}{\nu'^2 - \mu^2}$$
$$\left. + cP \frac{\nu^2}{\nu^2 - \mu^2} \quad cP \frac{\nu'^2}{\nu'^2 - \mu^2} \right\}. \tag{A.23}$$

Evaluating the terms in Eq. (A.23) which contain delta functions we have

$$A(\nu)\bar{N}(\nu) = A(\nu)\nu^2\lambda^2(\nu) + \nu^2 cP\int_0^1 d\nu' A(\nu') \frac{\nu'^2\lambda(\nu')}{\nu^2 - \nu'^2}$$

$$+ \nu^2\lambda(\nu)cP\int_0^1 d\nu' A(\nu') \frac{\nu'^2}{\nu'^2 - \nu^2}$$

$$+ c^2\nu^2\int_0^1 d\nu' A(\nu')\nu'^2\int_0^1 \mu^2 \frac{P}{\nu^2 - \mu^2} \frac{P}{\nu'^2 - \mu^2} d\mu. \qquad (A.24)$$

The last term in Eq. (A.24) is expanded by partial fractions to yield

$$c^2\nu^2\int_0^1 d\nu' A(\nu') \frac{\nu'^2}{\nu'^2 - \nu^2}\int_0^1 \left\{ P\frac{\nu^2}{\nu^2 - \mu^2} - P\frac{\nu'^2}{\nu'^2 - \mu^2} \right\} d\mu.$$

Next we use the function, $\lambda(\nu)$, in the form obtained by integrating Eq. (3.20) over μ,

$$\lambda(\nu) = 1 - cP\int_0^1 \frac{\nu^2}{\nu^2 - \mu^2} d\mu,$$

to write this term as

$$c\nu^2\int_0^1 d\nu' A(\nu') \frac{\nu'^2}{\nu'^2 - \nu^2} [\lambda(\nu') - \lambda(\nu)].$$

The term as written above identically cancels the second and third terms of Eq. (A.24), leaving

$$A(\nu)\bar{N}(\nu) = A(\nu)\nu^2\lambda^2(\nu). \qquad (A.25)$$

Now returning to the evaluation of Eq. (A.21) we insert the eigenfunctions to obtain

$$A(\nu)N(\nu) = \int_0^1 d\mu\mu^2 \left\{ cP\frac{\nu^2}{\nu^2-\mu^2} + \lambda(\nu)\delta(\nu-\mu)\right\} \int_0^1 d\nu' A(\nu')\left\{ cP\frac{\nu'^2}{\nu'^2-\mu^2} \right.$$

$$\left. + \lambda(\nu')\delta(\nu'-\mu) \right\}. \qquad (A.26)$$

After performing the integrals over the terms containing delta functions in Eq. (A.26) we have

$$A(\nu)N(\nu) = A(\nu)\nu^2\lambda^2(\nu) + c\nu^2\int_0^1 d\nu' A(\nu') P \frac{\nu'^2}{\nu^2 - \nu'^2} \lambda(\nu')$$

$$+ c\nu^2\lambda(\nu)\int_0^1 d\nu' A(\nu') P \frac{\nu'^2}{\nu'^2-\nu^2}$$

$$+ \int_0^1 cP \frac{\nu^2\mu^2}{\nu^2-\mu^2} d\mu \int_0^1 d\nu' A(\nu') cP \frac{\nu'^2}{\nu'^2-\mu^2} \tag{A.27}$$

We note that the first three terms of Eq. (A.27) are identical to those of Eq. (A.24). The fourth terms differ by the order of integration. We evaluate the fourth term of Eq. (A.27) by putting it in the form of the Poincare'-Bertrand formula[28] as follows:

$$c^2 P\int_0^1 \frac{\mu^2\nu^2}{\nu^2-\mu^2} d\mu P\int_0^1 A(\nu') \frac{\nu'^2}{\nu'^2-\mu^2} d\nu'$$

$$= -c^2\nu^2 P\int_0^1 \frac{d\mu}{\mu-\nu} P\int_0^1 \frac{g(\nu',\mu)}{\nu'-\mu} d\nu' \tag{A.28}$$

where $g(\nu',\mu) = A(\nu')\nu'^2\mu^2/(\nu+\mu)(\nu'+\mu)$.

The Poincare'-Bertrand formula is

$$P\int_0^1 \frac{d\mu}{\mu-\nu} P\int_0^1 \frac{g(\nu',\mu)}{\nu'-\mu} d\nu'$$

$$= -\pi^2 g(\nu,\nu) + \int_0^1 d\nu' \int_0^1 P \frac{1}{\nu-\mu} P \frac{1}{\nu'-\mu} g(\nu',\mu) d\mu. \tag{A.29}$$

Now, comparison of Eqs. (A.28),(A.29) and the fourth term of Eq. (A.24) shows that the difference of the two fourth terms is the additional term, $c^2\nu^2\pi^2 g(\nu,\nu)$, arising from Eq. (A.29). With this observation, we cancel the identical terms of Eq. (A.27) as before and write Eq.(A.27) as

$$A(\nu)N(\nu) = A(\nu)\nu^2\lambda^2(\nu) + c^2\nu^2\pi^2 g(\nu,\nu). \tag{A.30}$$

Finally, substituting Eq. (A.28) for $g(\nu,\nu)$ into Eq. (A.30) and canceling like terms we obtain

$$N(\nu) = \nu^2 \lambda^2(\nu) + \frac{c^2 \pi^2 \nu^4}{4} \tag{A.31}$$

as the normalization function for the continuum modes of the pseudo eigenfunctions.

APPENDIX B

PSEUDO EIGENFUNCTION COMPLETENESS

Theorem: The functions $\eta_b(\mu)$ and $\eta_\nu(\mu)$ form a complete set in the sense that any arbitrary known even function $\Phi(\mu)$ can be expanded in terms of these eigenfunctions for $-1 \leq \mu \leq 1$. Proof: We write the expansion

$$\Phi(\mu) = a_o \eta_b(\mu) + \int_{-1}^{1} \frac{A(\nu)}{2} \eta_\nu(\mu)d\nu, \quad -1 \leq \mu \leq 1 \tag{B.1}$$

and the task is to show that we can solve for the expansion coefficients a_o, $A(\nu)$, in terms of the known function $\Phi(\mu)$.

In the proof we make use of the boundary values of the dispersion function, $\Lambda(z)$, where

$$\Lambda^{\pm}(\nu) = 2 + c\nu^2 \; P\int_{-1}^{1} \frac{d\mu}{\mu^2 - \nu^2} \pm \pi i c \nu,$$

or

$$\Lambda^{\pm}(\nu) = \lambda(\nu) \pm \pi i c \nu,$$

are obtained from the Plemelj formulas[28]

$$F^{\pm}(y) = P\int_{a}^{b} \frac{f(x)}{x-y} dx \pm \pi i f(y).$$

We note that $\Lambda(\nu)$ and $\lambda(\nu)$ are twice as large as the functions defined in Eqs. (2.13) and (2.15). This difference is consistent with the half range normalization to unity, Eq. (3.16). First we write from Eq. (B.1)

$$\Phi'(\mu) = \int_{-1}^{1} \frac{A(\nu)}{2} \eta_\nu(\mu)d\nu \tag{B.2a}$$

where

$$\Phi'(\mu) = \Phi(\mu) - a_o \eta_b(\mu). \tag{B.2b}$$

Inserting Eq. (3.20) for $\eta_\nu(\mu)$ into Eq. (B.2a) we have

$$\Phi'(\mu) = \frac{\lambda(\mu)A(\mu)}{2} + \frac{c}{2} P \int_{-1}^{1} \frac{A(\nu)\nu^2}{\nu^2 - \mu^2} \, d\nu, \tag{B.3a}$$

or

$$\Phi'(\mu) = \frac{1}{4} \left(\Lambda^+(\mu) + \Lambda^-(\mu) \right) A(\mu) + \frac{c}{2} P \int_{-1}^{1} \frac{A(\nu)\nu^2}{\nu^2 - \mu^2} \, d\nu, \tag{B.3b}$$

where we have substituted the sum of the boundary values of the dispersion function for $\lambda(\mu)$.

Next we introduce the function $N(z)$ defined by

$$N(z) = \frac{1}{4\pi i} \int_{-1}^{1} \frac{c\nu^2 A(\nu)}{\nu^2 - z^2} \, d\nu \,. \tag{B.4}$$

We note that $N(z) \in A$ in the complex plane cut from -1 to 1 along the real axis and $N(z) \sim 1/z^2$ as $z \to \infty$. Adding and subtracting the boundary values of $N(z)$ as given by the Plemelj formulas, we obtain

$$\frac{c}{2} P \int_{-1}^{1} \frac{A(\nu)\nu^2}{\nu^2 - \mu^2} \, d\nu = \pi i \left(N^+(\mu) + N^-(\mu) \right), \tag{B.5a}$$

and

$$A(\mu) = \frac{2}{c\mu} \left(N^+(\mu) - N^-(\mu) \right). \tag{B.5b}$$

Substitution of Eqs. (B.5a,b) into Eq. (B.3b) yields

$$\Phi'(\mu) = \frac{1}{2c\mu} \left\{ \left(\Lambda^+(\mu) + \Lambda^-(\mu) \right) \left(N^+(\mu) - N^-(\mu) \right) \right.$$
$$\left. + 2\pi i c\mu \left(N^+(\mu) + N^-(\mu) \right) \right\}. \tag{B.6}$$

Now, inserting the difference of the dispersion function boundary values for $2\pi i c\mu$, multiplying through and canceling like terms, Eq. (B.6) becomes

$$c\mu\Phi'(\mu) = \Lambda^+(\mu)N^+(\mu) - \Lambda^-(\mu)N^-(\mu). \tag{B.7}$$

Next we seek a function, $N(z)\Lambda(z)$, whose boundary values on the cut satisfy equation (B.7). Thus we define the function $J(z)$ as

$$J(z) = N(z)\Lambda(z) - \frac{c}{2\pi i} \int_{-1}^{1} \frac{\mu^2 \Phi'(\mu)}{\mu^2 - z^2} \, d\mu, \tag{B.8}$$

with boundary values such that

$$J^+(\mu) - J^-(\mu) = N^+(\mu)\Lambda^+(\mu) - N^-(\mu)\Lambda^-(\mu) - c\mu\Phi'(\mu). \tag{B.9}$$

Comparison of Eq. (B.9) and Eq. (B.7) shows that the difference of the J(z) function boundary values is zero. With no discontinuity across the cut, J(z) is a bounded entire function which, by Liouville's theorem, must be a constant. Furthermore, since $J(z)\to 0$ as $z^2\to\infty$, $J(z)$ is everywhere equal to zero. With this result we rewrite Eq. (B.8) as

$$N(z) = \frac{c}{2\pi i \Lambda(z)} \int_{-1}^{1} \frac{\mu^2 \Phi'(\mu)}{\mu^2 - z^2} \, d\mu, \quad |z| \geq 0. \tag{B.10}$$

Now since $\pm \nu_o$ are the roots of the dispersion function, in order for N(z) as defined in Eq. (B.10) to be analytic at $\pm \nu_o$, we must require

$$\int_{-1}^{1} \frac{c\mu^2 \Phi'(\mu)}{\mu^2 - \nu_o^2} \, d\mu = 0. \tag{B.11a}$$

To obtain the solution for the discrete coefficient a_o, we insert Eq. (B.2b) into Eq. (B.11a), yielding

$$\int_{-1}^{1} \frac{c\mu^2}{\mu^2 - \nu_o^2} \left(\Phi(\mu) - a_o \eta_o(\mu) \right) \, d\mu = 0. \tag{B.11b}$$

Substituting the definition of $\eta_o(\mu)$, Eq. (3.19), which is valid for the full range of ν and μ, we rewrite Eq. (B.11b) as

$$\frac{-1}{\nu_o^2} \int_{-1}^{1} \mu^2 \eta_o(\mu) \left(\Phi(\mu) - a_o \eta_o(\mu) \right) \, d\mu = 0. \tag{B.11c}$$

Now use of the normalization relation Eq. (A.7) yields the desired expression for a_o, namely

$$a_o = \frac{1}{2N_o} \int_{-1}^{1} \mu^2 \eta_o(\mu)\Phi(\mu)d\mu. \tag{B.12}$$

To obtain the similar expression for the continuum coefficient $A(\nu)$, we insert the boundary values of $N(\nu)$ as defined from Eq. (B.10) into (B.5b) to give

$$A(\mu) = \frac{2}{c\mu} \Bigg\} \frac{c}{2\pi i} \left[\frac{1}{\Lambda^+(\mu)} - \frac{1}{\Lambda^-(\mu)} \right] P \int_{-1}^{1} \frac{\mu'^2\Phi'(\mu')}{\mu'^2 - \mu^2} \, d\mu'$$
$$+ \left[\frac{1}{\Lambda^+(\mu)} + \frac{1}{\Lambda^-(\mu)} \right] \frac{c\mu\Phi'(\mu)}{2} \Bigg\{ \quad . \tag{B.13a}$$

Upon substitution of the sum and difference of the dispersion function boundary values Eq. (B.13a) becomes

$$A(\mu) = \frac{2}{\Lambda^+(\mu)\Lambda^-(\mu)} \left\{ P \int_{-1}^{1} \frac{c\mu'^2\Phi'(\mu')}{\mu^2 - \mu'^2} \, d\mu' + \Phi'(\mu)\lambda(\mu) \right\} . \tag{B.13b}$$

Now letting $\mu = \nu$ and $\mu' = \mu$ we have

$$A(\nu) = \frac{2}{\nu^2\Lambda^+(\nu)\Lambda^-(\nu)} \left\{ P \int_{-1}^{1} \frac{c\nu^2\Phi'(\mu)\mu^2}{\nu^2 - \mu^2} \, d\mu + \int_{-1}^{1} \nu^2\lambda(\nu)\Phi'(\nu)\delta(\nu-\mu)d\mu \right\} . \tag{B.13c}$$

The two terms of the continuum eigenfunction as defined by Eq. (3.20) appear in Eq. (B.13c), allowing us to write

$$A(\nu) = \frac{2}{\nu^2\Lambda^+(\nu)\Lambda^-(\nu)} \int_{-1}^{1} \mu^2 \eta_\nu(\mu)\Phi'(\mu)d\mu. \tag{B.13d}$$

Now inserting Eq. (B.2b) for $\Phi'(\mu)$ into Eq. (B.13d) we obtain

$$A(\nu) = \frac{2}{\nu^2\Lambda^+(\nu)\Lambda^-(\nu)} \int_{-1}^{1} \mu^2 \eta_\nu(\mu) \Big(\Phi'(\mu) - a_o\eta_o(\mu) \Big) d\mu. \tag{B.13e}$$

Applying the orthogonality relation, Eq. (A.6), and substituting the normalization constant $N(\nu)$, Eq. (A.31), we have the solution for $A(\nu)$ as

$$A(\nu) = \frac{1}{2N(\nu)} \int_{-1}^{1} \mu^2 \eta_\nu(\mu) \Phi(\mu) d\mu. \tag{B.14}$$

This completes the proof for the full range case.

An immediate extension can be made to the half range case if we note from Eqs. (3.17) and (3.18) that

$$\eta_\nu(-\mu) = \eta_\nu(\mu)$$

and from the theorem, $\Phi(-\mu) = \Phi(\mu)$.

Thus we can write the solution for $A(\nu)$ as

$$A(\nu) = \frac{1}{N(\nu)} \int_{0}^{1} \mu^2 \eta_\nu(\mu) \Phi(\mu) d\mu, \tag{B.15}$$

and the expansion given by Eq. (B.1) as

$$\Phi(\mu) = a_0 \eta_0(\mu) + \int_{0}^{1} A(\nu) \eta_\nu(\mu) d\nu, \tag{B.16}$$

where, again from Eq. (3.17) and (3.18), we have used

$\eta_{-\nu}(\mu) = \eta_\nu(\mu)$ and we have assumed, because of the evenness of all functions involved, that $A(-\nu) = A(\nu)$.

APPENDIX C

NEUTRON DENSITY DISTRIBUTIONS FOR REFLECTED CYLINDERS

Neutron density distributions corresponding to several of the cases for which the critical dimensions are given in Table V are presented here for the use of interested researchers. Since the numerical results of all one hundred cases calculated would be rather voluminous, we have selected combinations of cases which provide various parametric ranges. First, we present the largest and the smallest cases calculated. Then follows a variety of cases from which the effects of the independent variation of core c value, reflector c value and reflector thickness can be drawn.

$r_1 = r/R_1$ or $r_2 = \dfrac{r-R_1}{R_2-R_1}$	$c_1=1.02,\ c_2=0.99$ $R_2 - R_1 = 20$ MFP		$c_1=1.4,\ c_2=0.85$ $R_2 - R_1 = 1$ MFP	
	$\rho(r_1)/\rho(o)$	$\rho(r_2)/\rho(o)$	$\rho(r_1)/\rho(o)$	$\rho(r_2)/\rho(o)$
0.0	1.0000	0.5415	1.0000	0.4906
0.01	0.9999	0.5126	0.9999	0.4788
0.02	0.9998	0.4871	0.9998	0.4691
0.1	0.9949	0.3327	0.9946	0.4082
0.2	0.9795	0.2124	0.9785	0.3506
0.3	0.9542	0.1378	0.9520	0.3037
0.4	0.9192	0.0902	0.9153	0.2640
0.5	0.8752	0.0593	0.8688	0.2294
0.6	0.8228	0.0387	0.8131	0.1987
0.7	0.7628	0.0247	0.7485	0.1710
0.8	0.6959	0.0149	0.6753	0.1455
0.9	0.6228	0.0076	0.5927	0.1212
0.95	0.5838	0.0046	0.5464	0.1089
0.98	0.5592	0.0029	0.5155	0.1010
0.99	0.5507	0.0022	0.5041	0.0981
1.00	0.5415	0.0015	0.4906	0.0948

$r_1=r/R_1$ or $r_2=\dfrac{r-R_1}{R_2-R_1}$	$c_1=1.02$, $c_2=0.95$ $R_2 - R_1 = 3$ MFP		$c_1=1.02$, $c_2=0.95$ $R_2 - R_1 = 10$ MFP	
	$\rho(r_1)/\rho(o)$	$\rho(r_2)/\rho(o)$	$\rho(r_1)/\rho(o)$	$\rho(r_2)/\rho(o)$
0.0	1.0000	0.2858	1.0000	0.3153
0.01	0.9999	0.2806	0.9999	0.2990
0.02	0.9996	0.2758	0.9997	0.2847
0.1	0.9912	0.2423	0.9916	0.1977
0.2	0.9649	0.2068	0.9668	0.1277
0.3	0.9219	0.1761	0.9261	0.0830
0.4	0.8633	0.1490	0.8705	0.0542
0.5	0.7906	0.1249	0.8014	0.0354
0.6	0.7058	0.1031	0.7206	0.0230
0.7	0.6110	0.0834	0.6300	0.0147
0.8	0.5085	0.0651	0.5316	0.0090
0.9	0.4006	0.0476	0.4274	0.0050
0.95	0.3450	0.0387	0.3733	0.0033
0.98	0.3106	0.0330	0.3397	0.0024
0.99	0.2987	0.0309	0.3280	0.0020
1.0	0.2858	0.0283	0.3153	0.0016

$r_1=r/R_1$ or $r_2=\dfrac{r-R_1}{R_2-R_1}$	$c_1=1.05,\ c_2=0.95$ $R_2-R_1=3$ MFP		$c_1=1.05,\ c_2=0.95$ $R_2-R_1=10$ MFP	
	$\rho(r_1)/\rho(o)$	$\rho(r_2)/\rho(o)$	$\rho(r_1)/\rho(o)$	$\rho(r_2)/\rho(o)$
0.0	1.0000	0.4076	1.0000	0.4404
0.01	0.9999	0.3989	0.9999	0.4141
0.02	0.9997	0.3912	0.9997	0.3918
0.1	0.9931	0.3386	0.9936	0.2622
0.2	0.9726	0.2848	0.9745	0.1641
0.3	0.9388	0.2394	0.9431	0.1042
0.4	0.8926	0.2003	0.8999	0.0668
0.5	0.8347	0.1662	0.8458	0.0429
0.6	0.7663	0.1361	0.7816	0.0275
0.7	0.6887	0.1091	0.7086	0.0174
0.8	0.6032	0.0845	0.6278	0.0106
0.9	0.5108	0.0613	0.5399	0.0058
0.95	0.4617	0.0497	0.4928	0.0039
0.98	0.4307	0.0423	0.4628	0.0027
0.99	0.4197	0.0395	0.4522	0.0023
1.0	0.4076	0.0362	0.4404	0.0019

$r_1 = r/R_1$ or $r_2 = \dfrac{r-R_1}{R_2-R_1}$	$c_1 = 1.05,\ c_2 = 0.85$ $R_2 - R_1 = 3$ MFP		$c_1 = 1.05,\ c_2 = 0.85$ $R_2 - R_1 = 10$ MFP	
	$\rho(r_1)/\rho(o)$	$\rho(r_2)/\rho(o)$	$\rho(r_1)/\rho(o)$	$\rho(r_2)/\rho(o)$
0.0	1.0000	0.2859	1.0000	0.2897
0.01	0.9999	0.2765	0.9999	0.2624
0.02	0.9997	0.2685	0.9997	0.2405
0.1	0.9913	0.2177	0.9914	0.1291
0.2	0.9655	0.1708	0.9658	0.0625
0.3	0.9233	0.1349	0.9239	0.0309
0.4	0.8657	0.1067	0.8667	0.0155
0.5	0.7942	0.0842	0.7956	0.0078
0.6	0.7105	0.0660	0.7125	0.0040
0.7	0.6167	0.0510	0.6192	0.0020
0.8	0.5148	0.0384	0.5179	0.0010
0.9	0.4064	0.0275	0.4100	0.0005
0.95	0.3494	0.0223	0.3531	0.0003
0.98	0.3133	0.0190	0.3171	0.00021
0.99	0.3004	0.0178	0.3042	0.00018
1.0	0.2859	0.0164	0.2897	0.00015

$r_1=r/R_1$ or $r_2=\dfrac{r-R_1}{R_2-R_1}$	$c_1=1.1,\ c_2=0.95$ $R_2 - R_1 = 3$ MFP		$c_1=1.1,\ c_2=0.95$ $R_2 - R_1 = 10$ MFP	
	$\rho(r_1)/\rho(o)$	$\rho(r_2)/\rho(o)$	$\rho(r_1)/\rho(o)$	$\rho(r_2)/\rho(o)$
0.0	1.0000	0.4992	1.0000	0.5293
0.01	0.9999	0.4864	0.9999	0.4916
0.02	0.9998	0.4753	0.9998	0.4611
0.1	0.9945	0.4031	0.9949	0.2953
0.2	0.9780	0.3329	0.9796	0.1789
0.3	0.9508	0.2758	0.9545	0.1113
0.4	0.9134	0.2280	0.9197	0.0702
0.5	0.8662	0.1871	0.8758	0.0446
0.6	0.8099	0.1518	0.8233	0.0284
0.7	0.7452	0.1206	0.7628	0.0178
0.8	0.6728	0.0927	0.6947	0.0108
0.9	0.5927	0.0669	0.6189	0.0059
0.95	0.5491	0.0541	0.5773	0.0039
0.98	0.5208	0.0459	0.5502	0.0028
0.99	0.5106	0.0429	0.5404	0.0024
1.0	0.4992	0.0392	0.5293	0.0019

$r_1 = r/R_1$ or $r_2 = \dfrac{r-R_1}{R_2-R_1}$	$c_1=1.2$, $c_2=0.95$ $R_2 - R_1 = 3$ MFP		$c_1=1.2$, $c_2=0.85$ $R_2 - R_1 = 3$ MFP	
	$\rho(r_1)/\rho(o)$	$\rho(r_2)/\rho(o)$	$\rho(r_1)/\rho(o)$	$\rho(r_2)/\rho(o)$
0.0	1.0000	0.5732	1.0000	0.4639
0.01	0.9999	0.5539	0.9999	0.4266
0.02	0.9998	0.5380	0.9998	0.3976
0.1	0.9956	0.4413	0.9942	0.2483
0.2	0.9823	0.3546	0.9768	0.1487
0.3	0.9602	0.2879	0.9482	0.0922
0.4	0.9297	0.2342	0.9087	0.0582
0.5	0.8910	0.1898	0.8589	0.0371
0.6	0.8445	0.1523	0.7995	0.0237
0.7	0.7903	0.1199	0.7310	0.0151
0.8	0.7286	0.0915	0.6540	0.0094
0.9	0.6587	0.0655	0.5680	0.0055
0.95	0.6196	0.0528	0.5204	0.0040
0.98	0.5937	0.0447	0.4889	0.0031
0.99	0.5842	0.0417	0.4774	0.0027
1.0	0.5732	0.0382	0.4639	0.0024

$r_1 = r/R_1$ or $r_2 = \dfrac{r-R_1}{R_2-R_1}$	$c_1 = 1.4,\ c_2 = 0.95$ $R_2 - R_1 = 3$ MFP		$c_1 = 1.4,\ c_2 = 0.95$ $R_2 - R_1 = 10$ MFP	
	$\rho(r_1)/\rho(o)$	$\rho(r_2)/\rho(o)$	$\rho(r_1)/\rho(o)$	$\rho(r_2)/\rho(o)$
0.0	1.0000	0.4992	1.0000	0.6384
0.01	0.9999	0.4864	0.99996	0.5597
0.02	0.9998	0.4753	0.99985	0.5057
0.1	0.9945	0.4031	0.9965	0.2790
0.2	0.9780	0.3329	0.9859	0.1564
0.3	0.9508	0.2758	0.9683	0.0933
0.4	0.9134	0.2280	0.9438	0.0573
0.5	0.8662	0.1871	0.9128	0.0357
0.6	0.8099	0.1518	0.8744	0.0224
0.7	0.7452	0.1206	0.8275	0.0139
0.8	0.6728	0.0927	0.7774	0.0084
0.9	0.5927	0.0669	0.7168	0.0045
0.95	0.5490	0.0541	0.6819	0.0030
0.98	0.5208	0.0459	0.6581	0.0021
0.99	0.5106	0.0429	0.6491	0.0018
1.0	0.4992	0.0392	0.6384	0.0014